SOLID STATE ELECTRONIC DEVICES

SIXTH EDITION

Eastern Economy Edition

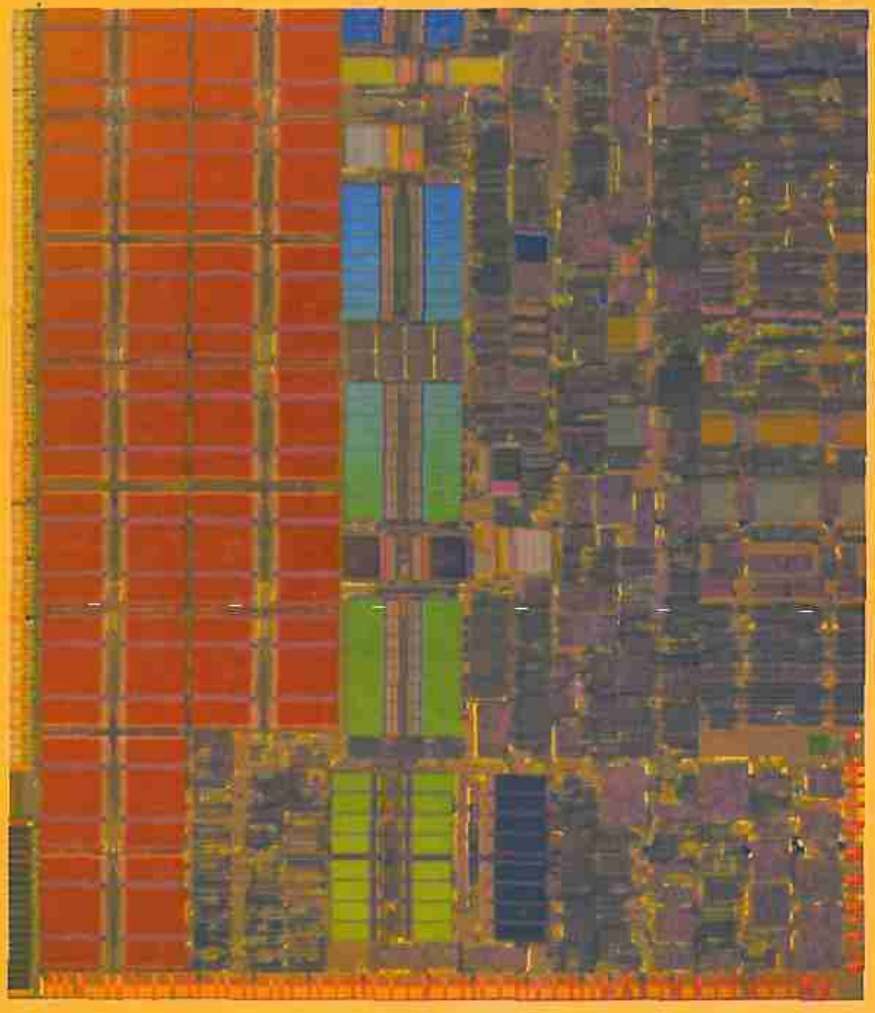

BEN G. STREETMAN • SANJAY KUMAR BANERJEE

PHI

PHI Learning

SIXTH EDITION

Solid State Electronic Devices

BEN G. STREETMAN AND SANJAY KUMAR BANERJEE

Microelectronics Research Center
Department of Electrical and Computer Engineering
The University of Texas at Austin

PHI Learning Private Limited
New Delhi-110001
2009

This Indian Reprint—Rs. 295.00
(Original U.S. Edition—Rs. 5695.00)

SOLID STATE ELECTRONIC DEVICES, 6th Ed.
by Ben G. Streetman and Sanjay Kumar Banerjee

© 2006 by Prentice-Hall, Inc. (now known as Pearson Education Inc.).Upper Saddle River, New Jersey 07458, U.S.A. All rights reserved. No part of this book may be reproduced in any form, by mimeograph or any other means, without permission in writing from the publisher.

The author and publisher of this book have used their best efforts in preparing this book. These efforts include the development, research, and testing of the theories and programs to determine their effectiveness. The author and publisher shall not be liable in any event for incidental or consequential damages with, or arising out of, the furnishing, performance, or use of these programs.

ISBN-978-81-203-3020-7

Published by Asoke K. Ghosh, PHI Learning Private Limited, M-97, Connaught Circus, New Delhi-110001 and Printed by Mohan Makhijani at Rekha Printers Private Limited, New Delhi-110020.

Solid State Electronic Devices

CONTENTS

PREFACE XIII

ABOUT THE AUTHORS XVII

1 CRYSTAL PROPERTIES AND GROWTH OF SEMICONDUCTORS 1

1.1 Semiconductor Materials 1
1.2 Crystal Lattices 3
1.2.1 Periodic Structures 3
1.2.2 Cubic Lattices 5
1.2.3 Planes and Directions 7
1.2.4 The Diamond Lattice 10
1.3 Bulk Crystal Growth 12
1.3.1 Starting Materials 13
1.3.2 Growth of Single-Crystal Ingots 13
1.3.3 Wafers 15
1.3.4 Doping 16
1.4 Epitaxial Growth 18
1.4.1 Lattice-Matching in Epitaxial Growth 18
1.4.2 Vapor-Phase Epitaxy 21
1.4.3 Molecular Beam Epitaxy 23

2 ATOMS AND ELECTRONS 31

2.1 Introduction to Physical Models 32
2.2 Experimental Observations 33
2.2.1 The Photoelectric Effect 33
2.2.2 Atomic Spectra 35
2.3 The Bohr Model 36
2.4 Quantum Mechanics 39
2.4.1 Probability and the Uncertainty Principle 40
2.4.2 The Schrödinger Wave Equation 41
2.4.3 Potential Well Problem 44
2.4.4 Tunneling 46
2.5 Atomic Structure and the Periodic Table 47
2.5.1 The Hydrogen Atom 47
2.5.2 The Periodic Table 50

Petitioner Canadian Solar (USA) Inc., Ex. 1030, p. v

3 ENERGY BANDS AND CHARGE CARRIERS IN SEMICONDUCTORS 61

3.1 Bonding Forces and Energy Bands in Solids 61
3.1.1 Bonding Forces in Solids 62
3.1.2 Energy Bands 64
3.1.3 Metals, Semiconductors, and Insulators 67
3.1.4 Direct and Indirect Semiconductors 68
3.1.5 Variation of Energy Bands with Alloy Composition 71
3.2 Charge Carriers in Semiconductors 71
3.2.1 Electrons and Holes 73
3.2.2 Effective Mass 76
3.2.3 Intrinsic Material 80
3.2.4 Extrinsic Material 81
3.2.5 Electrons and Holes in Quantum Wells 85
3.3 Carrier Concentrations 86
3.3.1 The Fermi Level 86
3.3.2 Electron and Hole Concentrations at Equilibrium 89
3.3.3 Temperature Dependence of Carrier Concentrations 94
3.3.4 Compensation and Space Charge Neutrality 96
3.4 Drift of Carriers in Electric and Magnetic Fields 98
3.4.1 Conductivity and Mobility 98
3.4.2 Drift and Resistance 102
3.4.3 Effects of Temperature and Doping on Mobility 103
3.4.4 High-Field Effects 105
3.4.5 The Hall Effect 106
3.5 Invariance of the Fermi Level at Equilibrium 108

4 EXCESS CARRIERS IN SEMICONDUCTORS 118

4.1 Optical Absorption 118
4.2 Luminescence 121
4.2.1 Photoluminescence 122
4.2.2 Electroluminescence 124
4.3 Carrier Lifetime and Photoconductivity 124
4.3.1 Direct Recombination of Electrons and Holes 125
4.3.2 Indirect Recombination; Trapping 127
4.3.3 Steady State Carrier Generation; Quasi-Fermi Levels 130
4.3.4 Photoconductive Devices 132
4.4 Diffusion of Carriers 134
4.4.1 Diffusion Processes 134
4.4.2 Diffusion and Drift of Carriers; Built-in Fields 137

4.4.3 Diffusion and Recombination; The Continuity Equation 140
4.4.4 Steady State Carrier Injection; Diffusion Length 141
4.4.5 The Haynes–Shockley Experiment 144
4.4.6 Grodients in the Quasi-Fermi Levels 147

5 JUNCTIONS 154

5.1 Fabrication of p-n Junctions 154
5.1.1 Thermal Oxidation 155
5.1.2 Diffusion 156
5.1.3 Rapid Thermal Processing 158
5.1.4 Ion Implantation 159
5.1.5 Chemical Vapor Deposition (CVD) 162
5.1.6 Photolithography 162
5.1.7 Etching 166
5.1.8 Metallization 167
5.2 Equilibrium Conditions 168
5.2.1 The Contact Potential 170
5.2.2 Equilibrium Fermi Levels 174
5.2.3 Space Charge at a Junction 175
5.3 Forward- and Reverse-Biased Junctions; Steady State Conditions 180
5.3.1 Qualitative Description of Current Flow at a Junction 180
5.3.2 Carrier Injection 184
5.3.3 Reverse Bias 193
5.4 Reverse-Bias Breakdown 196
5.4.1 Zener Breakdown 197
5.4.2 Avalanche Breakdown 198
5.4.3 Rectifiers 200
5.4.4 The Breakdown Diode 204
5.5 Transient and A-C Conditions 205
5.5.1 Time Variation of Stored Charge 205
5.5.2 Reverse Recovery Transient 208
5.5.3 Switching Diodes 211
5.5.4 Capacitance of p-n junctions 212
5.5.5 The Varactor Diode 217
5.6 Deviations from the Simple Theory 218
5.6.1 Effects of Contact Potential on Carrier Injection 219
5.6.2 Recombination and Generation in the Transition Region 221
5.6.3 Ohmic Losses 223
5.6.4 Graded Junctions 224

5.7 Metal–Semiconductor Junctions 227
5.7.1 Schottky Barriers 227
5.7.2 Rectifying Contacts 229
5.7.3 Ohmic Contacts 231
5.7.4 Typical Schottky Barriers 233
5.8 Heterojunctions 234

6 FIELD-EFFECT TRANSISTORS 251
6.1 Transistor Operation 252
6.1.1 The Load Line 252
6.1.2 Amplification and Switching 254
6.2 The Junction FET 254
6.2.1 Pinch-off and Saturation 255
6.2.2 Gate Control 257
6.2.3 Current–Voltage Characteristics 259
6.3 The Metal–Semiconductor FET 261
6.3.1 The GaAs MESFET 261
6.3.2 The High Electron Mobility Transistor (HEMT) 262
6.3.3 Short Channel Effects 264
6.4 The Metal–Insulator–Semiconductor FET 265
6.4.1 Basic Operation and Fabrication 266
6.4.2 The Ideal MOS Capacitor 270
6.4.3 Effects of Real Surfaces 281
6.4.4 Threshold Voltage 284
6.4.5 MOS Capacitance–Voltage Analysis 286
6.4.6 Time-Dependent Capacitance Measurements 290
6.4.7 Current–Voltage Characteristics of MOS Gate Oxides 291
6.5 The MOS Field-Effect Transistor 294
6.5.1 Output Characteristics 295
6.5.2 Transfer Characteristics 297
6.5.3 Mobility Models 300
6.5.4 Short Channel MOSFET I–V Characteristics 302
6.5.5 Control of Threshold Voltage 303
6.5.6 Substrate Bias Effects 309
6.5.7 Subthreshold Characteristics 311
6.5.8 Equivalent Circuit for the MOSFET 313
6.5.9 MOSFET Scaling and Hot Electron Effects 315
6.5.10 Drain-Induced Barrier Lowering 320
6.5.11 Short Channel Effect and Narrow Width Effect 322
6.5.12 Gate-Induced Drain Leakage 323

7 BIPOLAR JUNCTION TRANSISTORS 336
7.1 Fundamentals of BJT Operation 336
7.2 Amplification with BJTs 340
7.3 BJT Fabrication 343
7.4 Minority Carrier Distributions and Terminal Currents 346
7.4.1 Solution of the Diffusion Equation in the Base Region 347
7.4.2 Evaluation of the Terminal Currents 349
7.4.3 Approximations of the Terminal Currents 352
7.4.4 Current Transfer Ratio 354
7.5 Generalized Biasing 355
7.5.1 The Coupled-Diode Model 356
7.5.2 Charge Control Analysis 361
7.6 Switching 363
7.6.1 Cutoff 364
7.6.2 Saturation 365
7.6.3 The Switching Cycle 366
7.6.4 Specifications for Switching Transistors 368
7.7 Other Important Effects 368
7.7.1 Drift in the Base Region 369
7.7.2 Base Narrowing 370
7.7.3 Avalanche Breakdown 372
7.7.4 Injection Level; Thermal Effects 373
7.7.5 Base Resistance and Emitter Crowding 374
7.7.6 Gummel–Poon Model 376
7.7.7 Kirk Effect 380
7.8 Frequency Limitations of Transistors 382
7.8.1 Capacitance and Charging Times 382
7.8.2 Transit Time Effects 385
7.8.3 Webster Effect 386
7.8.4 High-Frequency Transistors 386
7.9 Heterojunction Bipolar Transistors 388

8 OPTOELECTRONIC DEVICES 398
8.1 Photodiodes 398
8.1.1 Current and Voltage in an Illuminated Junction 399
8.1.2 Solar Cells 402
8.1.3 Photodetectors 405
8.1.4 Gain, Bandwidth, and Signal-to-Noise Ratio of Photodetectors 407

8.2 Light-Emitting Diodes 411
8.2.1 Light-Emitting Materials 411
8.2.2 Fiber-Optic Communications 414
8.3 Lasers 417
8.4 Semiconductor Lasers 422
8.4.1 Population Inversion at a Junction 422
8.4.2 Emission Spectra for p-n Junction Lasers 424
8.4.3 The Basic Semiconductor Laser 426
8.4.4 Heterojunction Lasers 426
8.4.5 Materials for Semiconductor Lasers 430

9 INTEGRATED CIRCUITS 437

9.1 Background 438
9.1.1 Advantages of Integration 438
9.1.2 Types of Integrated Circuits 440
9.2 Evolution of Integrated Circuits 441
9.3 Monolithic Device Elements 444
9.3.1 CMOS Process Integration 444
9.3.2 Silicon-on-Insulator (SOI) 459
9.3.3 Integration of Other Circuit Elements 461
9.4 Charge Transfer Devices 466
9.4.1 Dynamic Effects in MOS Capacitors 466
9.4.2 The Basic CCD 468
9.4.3 Improvements on the Basic Structure 469
9.4.4 Applications of CCDs 470
9.5 Ultra Large-Scale Integration (ULSI) 470
9.5.1 Logic Devices 474
9.5.2 Semiconductor Memories 483
9.6 Testing, Bonding, and Packaging 496
9.6.1 Testing 497
9.6.2 Wire Bonding 497
9.6.3 Flip-Chip Techniques 501
9.6.4 Packaging 502

10 HIGH-FREQUENCY AND HIGH-POWER DEVICES 508

10.1 Tunnel Diodes 508
10.1.1 Degenerate Semiconductors 509
10.2 The IMPATT Diode 512
10.3 The Gunn Diode 515
10.3.1 The Transferred-Electron Mechanism 515
10.3.2 Formation and Drift of Space Charge Domains 518

10.4 The p-n-p-n Diode 520
10.4.1 Basic Structure 520
10.4.2 The Two-Transistor Analogy 521
10.4.3 Variation of α with Injection 522
10.4.4 Forward-Blocking State 523
10.4.5 Conducting State 524
10.4.6 Triggering Mechanisms 525
10.5 The Semiconductor-Controlled Rectifier 526
10.5.1 Turning off the SCR 527
10.6 Insulated-Gate Bipolar Transistor 528

APPENDICES

I. Definitions of Commonly Used Symbols 535
II. Physical Constants and Conversion Factors 539
III. Properties of Semiconductor Materials 540
IV. Derivation of the Density of States in the Conduction Band 541
V. Derivation of Fermi–Dirac Statistics 546
VI. Dry and Wet Thermal Oxide Thickness Grown on Si (100) as a Function of Time and Temperature 550
VII. Solid Solubilities of Impurities in Si 552
VIII. Diffusivities of Dopants in Si and SiO_2 554
IX. Projected Range and Straggle as Function of Implant Energy in Si 556

ANSWERS TO SELECTED SELF QUIZ QUESTIONS 559

INDEX 563

PREFACE

This book is an introduction to semiconductor devices for undergraduate electrical engineers, other interested students, and practicing engineers and scientists whose understanding of modern electronics needs updating. The book is organized to bring students with a background in sophomore physics to a level of understanding which will allow them to read much of the current literature on new devices and applications.

GOALS

An undergraduate course in electronic devices has two basic purposes: (1) to provide students with a sound understanding of existing devices, so that their studies of electronic circuits and systems will be meaningful; and (2) to develop the basic tools with which they can later learn about newly developed devices and applications. Perhaps the second of these objectives is the more important in the long run; it is clear that engineers and scientists who deal with electronics will continually be called upon to learn about new devices and processes in the future. For this reason, we have tried to incorporate the basics of semiconductor materials and conduction processes in solids, which arise repeatedly in the literature when new devices are explained. Some of these concepts are often omitted in introductory courses, with the view that they are unnecessary for understanding the fundamentals of junctions and transistors. We believe this view neglects the important goal of equipping students for the task of understanding a new device by reading the current literature. Therefore, in this text most of the commonly used semiconductor terms and concepts are introduced and related to a broad range of devices.

READING LISTS

As a further aid in developing techniques for independent study, the reading list at the end of each chapter includes a few articles which students can read comfortably as they study this book. We do not expect that students will read all articles recommended in the reading lists; nevertheless, some exposure to periodicals is useful in laying the foundation for a career of constant updating and self-education. We have also added a summary of the key concepts at the end of each chater.

PROBLEMS

One of the keys to success in understanding this material is to work problems that exercise the concepts. The problems at the end of each chapter are designed to facilitate learning the material. Very few are simple "plug-in" problems. Instead, they are chosen to reinforce or extend the material presented in the chapter. In

Petitioner Canadian Solar (USA) Inc., Ex. 1030, p. xiii

addition, we have added "self quiz" problems which test the conceptual understanding on the part of the students.

UNITS In keeping with the goals described above, examples and problems are stated in terms of units commonly used in the semiconductor literature. The basic system of units is rationalized MKS, although cm is often used as a convenient unit of length. Similarly, electron volts (eV) are often used rather than joules (J) to measure the energy of electrons. Units for various quantities are given in Appendices I and II.

PRESENTATION In presenting this material at the undergraduate level, one must anticipate a few instances which call for a phrase such as "It can be shown . . ." This is always disappointing; on the other hand, the alternative is to delay study of solid state devices until the graduate level, where statistical mechanics, quantum theory, and other advanced background can be freely invoked. Such a delay would result in a more elegant treatment of certain subjects, but it would prevent undergraduate students from enjoying the study of some very exciting devices.

The discussion includes both silicon and compound semiconductors, to reflect the continuing growth in importance for compounds in optoelectronic and high-speed device applications. Topics such as heterojunctions, lattice-matching using ternary and quaternary alloys, variation of band gap with alloy composition, and properties of quantum wells add up to the breadth of the discussion. Not to be outdone by the compounds, silicon-based devices have continued their dramatic record of advancement. The discussion of FET structures and Si integrated circuits reflects these advancements. Our objective is not to cover all the latest devices, which can only be done in the journal and conference literature. Instead, we have chosen devices to discuss which are broadly illustrative of important principles.

The first four chapters of the book provide background on the nature of semiconductors and conduction processes in solids. Included is a brief introduction to quantum concepts (Chapter 2) for those students who do not already have this background from other courses. Chapter 5 describes the p-n junction and some of its applications. Chapters 6 and 7 deal with the principles of transistor operation. Chapter 8 covers optoelectronics and Chapter 9 discusses integrated circuits. Chapters 10 applies the theory of junctions and conduction processes to microwave and power devices. All of the devices covered are important in today's electronics; furthermore, learning about these devices should be an enjoyable and rewarding experience. We hope this book provides that kind of experience for its readers.

ACKNOWLEDGMENTS

The sixth edition benefits greatly from comments and suggestions provided by students and teachers of the first five editions. The book's readers have generously provided comments which have been invaluable in developing the present version. We remain indebted to those persons mentioned in the Preface of the first five editions, who contributed so much to the development of the book. In particular, Nick Holonyak has been a source of continuing information and inspiration for all six editions. Additional thanks go to our colleagues at UT–Austin who have provided special assistance, particularly Joe Campbell, Leonard Frank Register, Ray Chen, Archie Holmes, Dim-Lee Kwong, Jack Lee, and Dean Neikirk. Lisa Weltzer provided useful assistance with the typing of the homework solutions. We thank the many companies and organizations cited in the figure captions for generously providing photographs and illustrations of devices and fabrication processes. Bill Dunnigan, Naras Iyengar, and Pradipto Mukherjee at Freescale, Peter Rickert and Puneet Kohli at TI, Chandra Mouli and Dan Spangler at Micron, Majeed Foad at Applied Materials, and Tim Sater at MEMC deserve special mention for the new pictures in this edition. Finally, we recall with gratitude many years of association with the late Al Tasch, a valued colleague and friend.

Ben G. Streetman
Sanjay Kumar Banerjee

PRENTICE HALL SERIES
IN SOLID STATE PHYSICAL ELECTRONICS
Nick Holonyak Jr., Editor

Cheo FIBER OPTICS: DEVICES AND SYSTEMS SECOND EDITION
Haus WAVES AND FIELDS IN OPTOELECTRONICS
Kroemer QUANTUM MECHANICS FOR ENGINEERING, MATERIALS SCIENCE, AND APPLIED PHYSICS
Nussbaum CONTEMPORARY OPTICS FOR SCIENTISTS AND ENGINEERS
Peyghambarian/Koch/Mysyrowicz INTRODUCTION TO SEMICONDUCTOR OPTICS
Shur PHYSICS OF SEMICONDUCTOR DEVICES
Soclof DESIGN AND APPLICATIONS OF ANALOG INTEGRATED CIRCUITS
Streetman SOLID STATE ELECTRONIC DEVICES SIXTH EDITION
Verdeyen LASER ELECTRONICS THIRD EDITION
Wolfe/Holonyak/Stillman PHYSICAL PROPERTIES OF SEMICONDUCTORS

Sanjay Kumar Banerjee is the Cockrell Chair Professor of Electrical and Computer Engineering, and Director of the Microelectronics Research Center at The University of Texas at Austin. He has more than 500 archival refereed publications and conference papers, has 25 U.S. patents, and has supervised 35 Ph.D. students. His honors include the NSF Presidential Young Investigator Award (1988), the Texas Atomic Energy Centennial Fellowship (1990–1997), Cullen Professorship (1997–2001), Distinguished National Lecturer for the IEEE Electron Devices Society (1997–), Fellow of the IEEE (1996), and ECS Callinan Award (2003).

ABOUT THE AUTHORS

Ben G. Streetman is Dean of the College of Engineering at The University of Texas at Austin and holds the Dula D. Cockrell Centennial Chair in Engineering. He is a Professor of Electrical and Computer Engineering and was the founding Director of the Microelectronics Research Center (1984-96). His teaching and research interests involve semiconductor materials and devices. After receiving a Ph.D. from The University of Texas at Austin (1966) he was on the faculty (1966-1982) of the University of Illinois at Urbana-Champaign. He returned to The University of Texas at Austin in 1982. His honors include the Education Medal of the Institute of Electrical and Electronics Engineers (IEEE), the Frederick Emmons Terman Medal of the American Society for Engineering Education (ASEE), and the Heinrich Welker Medal from the International Conference on Compound Semiconductors. He is a member of the National Academy of Engineering. He is a Fellow of the IEEE and the Electrochemical Society. He has been honored as a Distinguished Ahimnus of The University of Texas at Austin and as a Distinguished Graduate of the UT College of Engineering. He has received the General Dynamics Award for Excellence in Engineering Teaching, and was honored by the Parents' Association as a Teaching Fellow for outstanding teaching of undergraduates. He has served on numerous panels and committees in industry and government, and several corporate boards. He has published more than 270 articles in the technical literature. Thirty-three students of Electrical Engineering, Materials Science, and Physics have received their Ph.D.s under his direction.

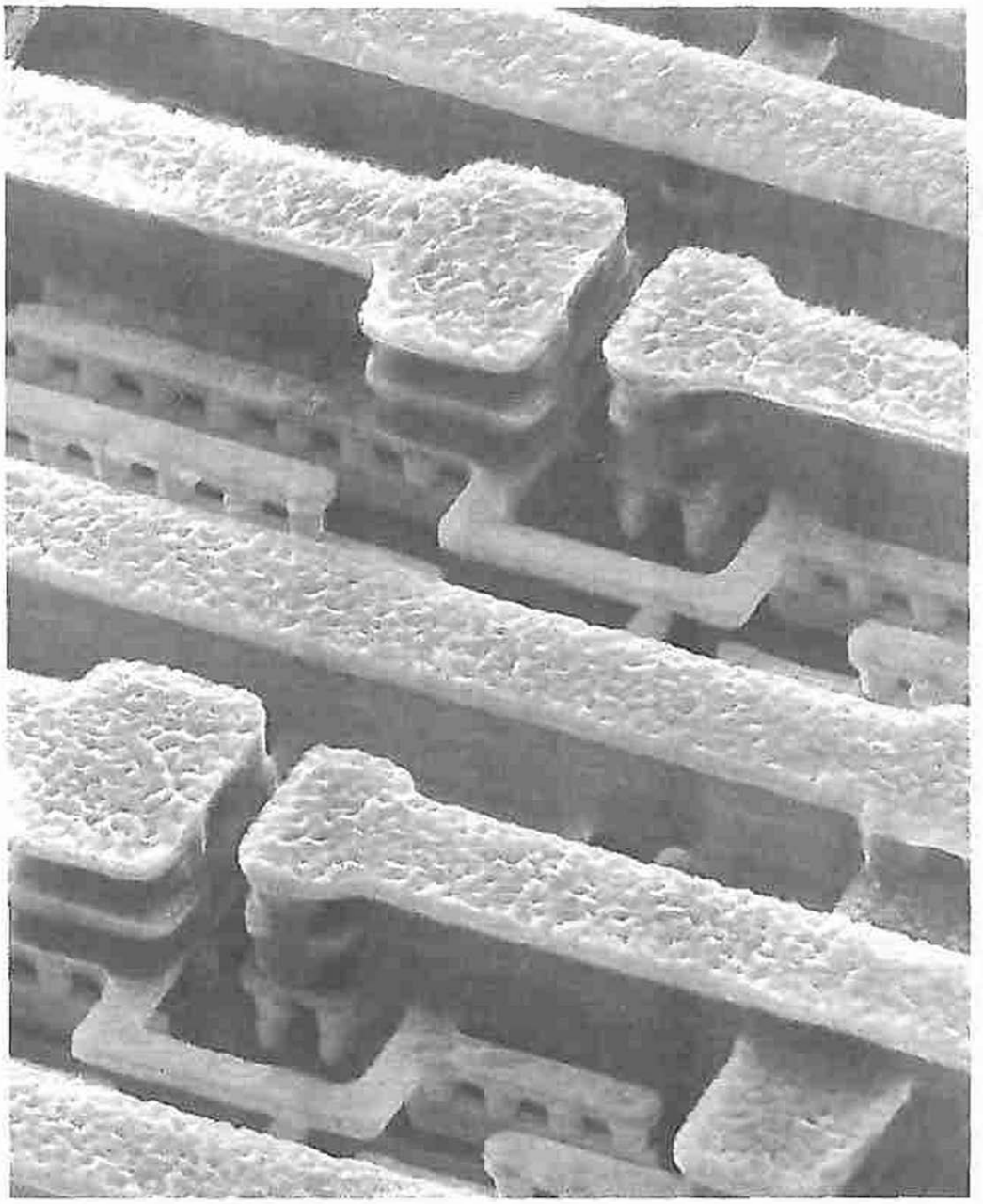

Multilevel copper metallization of a complementary metal oxide semiconductor (CMOS) chip. This scanning electron micrograph (scale: 1 cm = 3.5 microns) of a CMOS integrated circuit shows six levels of copper metallization that are used to carry electrical signals on the chip. The Inter-metal dielectric insulators have been chemically etched away here to reveal the copper interconnects. (Photograph courtesy of IBM.)

Chapter 1

Crystal Properties and Growth of Semiconductors

OBJECTIVES

1. Describe what a semiconductor is
2. Perform simple calculations about crystals
3. Understand what is involved in bulk Czochralski and thin-film epitaxial crystal growth
4. Learn about crystal defects

In studying solid state electronic devices we are interested primarily in the electrical behavior of solids. However, we shall see in later chapters that the transport of charge through a metal or a semiconductor depends not only on the properties of the electron but also on the arrangement of atoms in the solid. In the first chapter we shall discuss some of the physical properties of semiconductors compared with other solids, the atomic arrangements of various materials, and some methods of growing semiconductor crystals. Topics such as crystal structure and crystal growth technology are often the subjects of books rather than introductory chapters; thus we shall consider only a few of the more important and fundamental ideas that form the basis for understanding electronic properties of semiconductors and device fabrication.

1.1 SEMICONDUCTOR MATERIALS

Semiconductors are a group of materials having electrical conductivities intermediate between metals and insulators. It is significant that the conductivity of these materials can be varied over orders of magnitude by changes in temperature, optical excitation, and impurity content. This variability of electrical properties makes the semiconductor materials natural choices for electronic device investigations.

Semiconductor materials are found in column IV and neighboring columns of the periodic table (Table 1-1). The column IV semiconductors, silicon and germanium, are called *elemental* semiconductors because they are composed of single species of atoms. In addition to the elemental materials, compounds of column III and column V atoms, as well as certain combinations from II and VI, and from IV, make up the *compound* semiconductors.

Petitioner Canadian Solar (USA) Inc., Ex. 1030, p. 1

As Table 1-1 indicates, there are numerous semiconductor materials. As we shall see, the wide variety of electronic and optical properties of these semiconductors provides the device engineer with great flexibility in the design of electronic and optoelectronic functions. The elemental semiconductor Ge was widely used in the early days of semiconductor development for transistors and diodes. Silicon is now used for the majority of rectifiers, transistors, and integrated circuits. However, the compounds are widely used in high-speed devices and devices requiring the emission or absorption of light. The two-element (*binary*) III-V compounds such as GaN, GaP, and GaAs are common in light-emitting diodes (LEDs). As discussed in Section 1.2.4, three-element (*ternary*) compounds such as GaAsP and four-element (*quaternary*) compounds such as InGaAsP can be grown to provide added flexibility in choosing materials properties.

Fluorescent materials such as those used in television screens usually are II-VI compound semiconductors such as ZnS. Light detectors are commonly made with InSb, CdSe, or other compounds such as PbTe and HgCdTe. Si and Ge are also widely used as infrared and nuclear radiation detectors. An important microwave device, the Gunn diode, is usually made of GaAs or InP. Semiconductor lasers are made using GaAs, AlGaAs, and other ternary and quaternary compounds.

One of the most important characteristics of a semiconductor, which distinguishes it from metals and insulators, is its *energy band gap*. This property, which we will discuss in detail in Chapter 3, determines among other things the wavelengths of light that can be absorbed or emitted by the semiconductor. For example, the band gap of GaAs is about 1.43 electron volts (eV), which corresponds to light wavelengths in the near infrared. In contrast,

Table 1-1. Common semiconductor materials: (a) the portion of the periodic table where semiconductors occur; (b) elemental and compound semiconductors.

(a)	II	III	IV	V	VI
		B	C	N	
		Al	Si	P	S
	Zn	Ga	Ge	As	Se
	Cd	In		Sb	Te

(b)	Elemental	IV compounds	Binary III–V compounds	Binary II–VI compounds
	Si	SiC	AlP	ZnS
	Ge	SiGe	AlAs	ZnSe
			AlSb	ZnTe
			GaN	CdS
			GaP	CdSe
			GaAs	CdTe
			GaSb	
			InP	
			InAs	
			InSb	

GaP has a band gap of about 2.3 eV, corresponding to wavelengths in the green portion of the spectrum.[1] The band gap E_g for various semiconductor materials is listed along with other properties in Appendix III. As a result of the wide variety of semiconductor band gaps, light-emitting diodes and lasers can be constructed with wavelengths over a broad range of the infrared and visible portions of the spectrum.

The electronic and optical properties of semiconductor materials are strongly affected by impurities, which may be added in precisely controlled amounts. Such impurities are used to vary the conductivities of semiconductors over wide ranges and even to alter the nature of the conduction processes from conduction by negative charge carriers to positive charge carriers. For example, an impurity concentration of one part per million can change a sample of Si from a poor conductor to a good conductor of electric current. This process of controlled addition of impurities, called *doping*, will be discussed in detail in subsequent chapters.

To investigate these useful properties of semiconductors, it is necessary to understand the atomic arrangements in the materials. Obviously, if slight alterations in purity of the original material can produce such dramatic changes in electrical properties, then the nature and specific arrangement of atoms in each semiconductor must be of critical importance. Therefore, we begin our study of semiconductors with a brief introduction to crystal structure.

1.2 CRYSTAL LATTICES

In this section we discuss the arrangements of atoms in various solids. We shall distinguish between single crystals and other forms of materials and then investigate the periodicity of crystal lattices. Certain important crystallographic terms will be defined and illustrated in reference to crystals having a basic cubic structure. These definitions will allow us to refer to certain planes and directions within a lattice. Finally, we shall investigate the diamond lattice; this structure, with some variations, is typical of most of the semiconductor materials used in electronic devices.

1.2.1 Periodic Structures

A crystalline solid is distinguished by the fact that the atoms making up the crystal are arranged in a periodic fashion. That is, there is some basic arrangement of atoms that is repeated throughout the entire solid. Thus the crystal appears exactly the same at one point as it does at a series of other equivalent points, once the basic periodicity is discovered. However, not all solids are crystals (Fig. 1-1); some have no periodic structure at all (*amorphous* solids), and others are composed of many small regions of single-crystal material (*polycrystalline* solids). The high-resolution micrograph shown in Fig. 6-33 illustrates the periodic array of atoms in the single-crystal silicon of a transistor channel compared with the amorphous SiO_2 (glass) of the oxide layer.

[1] The conversion between the energy E of a photon of light (eV) and its wavelength $\lambda(\mu m)$ is $\lambda = 1.24/E$. For GaAs, $\lambda = 1.24/1.43 = 0.87\ \mu m$.

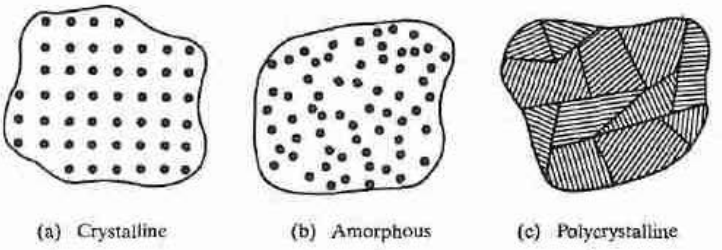

Figure 1–1
Three types of solids, classified according to atomic arrangement: (a) crystalline and (b) amorphous materials are illustrated by microscopic views of the atoms, whereas (c) polycrystalline structure is illustrated by a more macroscopic view of adjacent single-crystalline regions, such as (a).

The periodicity in a crystal is defined in terms of a symmetric array of points in space called the *lattice*. We can add atoms at each lattice point in an arrangement called a *basis*, which can be one atom or a group of atoms having the same spatial arrangement, to get a *crystal*. In every case, the lattice contains a volume or *cell* that represents the entire lattice and is regularly repeated throughout the crystal. As an example of such a lattice, Fig. 1–2 shows a two-dimensional arrangement of atoms called a rhombic lattice, with a *primitive* cell ODEF, which is the smallest such cell. Notice that we can define vectors **a** and **b** such that if the primitive cell is translated by integral multiples of these vectors, a new primitive cell identical to the original is found (e.g., O′D′E′F′). These vectors, **a** and **b** (and **c** if the lattice is three dimensional), are called the *primitive vectors* for the lattice. Points within the lattice are indistinguishable if the vector between the points is

$$\mathbf{r} = p\mathbf{a} + q\mathbf{b} + s\mathbf{c} \tag{1-1}$$

where p, q, and s are integers. A primitive cell has lattice points *only* at the corners of the cell. It is not unique, but the convention is to choose the smallest

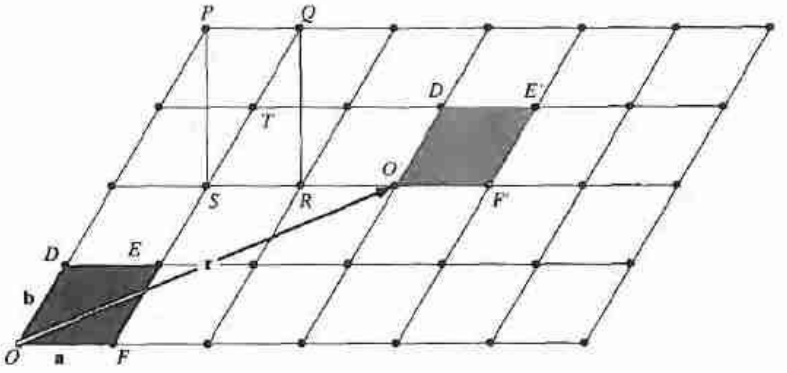

Figure 1–2
A two-dimensional lattice showing translation of a unit cell by $\mathbf{r} = 3\mathbf{a} + 2\mathbf{b}$.

primitive vectors. Note that, in a primitive cell, the lattice points at the corners are shared with adjacent cells; thus, the *effective* number of lattice points belonging to the primitive cell is always unity. Since there are many different ways of placing atoms in a volume, the distances and orientation between atoms can take many forms, but it is the *symmetry* that determines the lattice, not the magnitudes of the distances between the lattice points.

In many lattices, however, the primitive cell is not the most convenient to work with. For example, in Fig. 1-2, we see that the rhombic arrangement of the lattice points is such that it can also be considered to be rectangular (PQRS) with a lattice point in the center at T (a so-called *centered rectangular* lattice). [Note that this is not true of all rhombic lattices!] Clearly, it is simpler to deal with a rectangle rather than a rhombus. So, in this case we can choose to work with a larger rectangular *unit* cell, PQRS, rather than the smallest primitive cell, ODEF. A unit cell allows lattice points not only at the corners, but also at the face center (and body center in 3-D) if necessary. It is sometimes used instead of the primitive cell if it can represent the symmetry of the lattice better (in this example "centered rectangular" 2-D lattice). It replicates the lattice by integer translations of *basis* vectors.

The importance of the unit cell lies in the fact that we can analyze the crystal as a whole by investigating a representative volume. For example, from the unit cell we can find the distances between nearest atoms and next nearest atoms for calculation of the forces holding the lattice together; we can look at the fraction of the unit cell volume filled by atoms and relate the density of the solid to the atomic arrangement. But even more important for our interest in electronic devices, the properties of the periodic crystal lattice determine the allowed energies of electrons that participate in the conduction process. Thus the lattice determines not only the mechanical properties of the crystal but also its electrical properties.

1.2.2 Cubic Lattices

The simplest three-dimensional lattice is one in which the unit cell is a cubic volume, such as the three cells shown in Fig. 1-3. The *simple cubic* structure (abbreviated *sc*) has an atom located at each corner of the unit cell. The *body-centered cubic* (*bcc*) lattice has an additional atom at the center of the cube, and the *face-centered cubic* (*fcc*) unit cell has atoms at the eight corners and centered on the six faces. All three structures have different primitive cells, but the same cubic unit cell. We will generally work with unit cells.

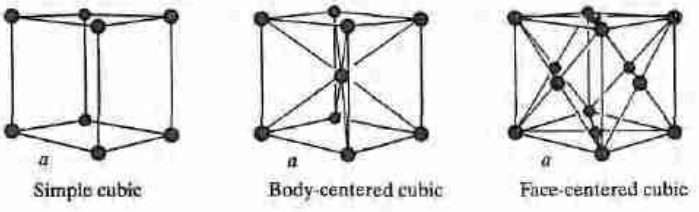

Figure 1-3
Unit cells for three types of cubic lattice structures.

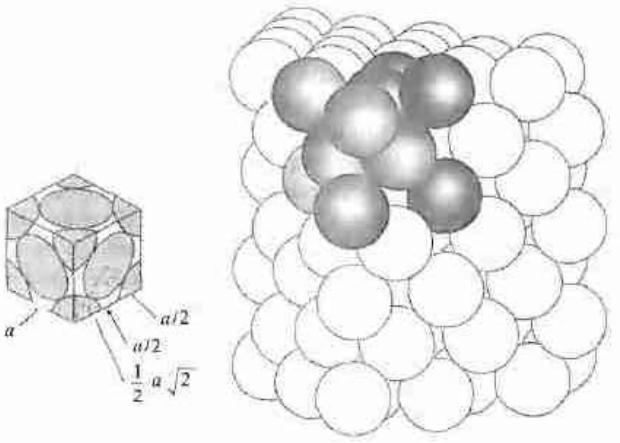

Figure 1–4 Packing of hard spheres in an fcc lattice.

As atoms are packed into the lattice in any of these arrangements, the distances between neighboring atoms will be determined by a balance between the forces that attract them together and other forces that hold them apart. We shall discuss the nature of these forces for particular solids in Section 3.1.1. For now, we can calculate the maximum fraction of the lattice volume that can be filled with atoms by approximating the atoms as hard spheres. For example, Fig. 1–4 illustrates the packing of spheres in a face-centered cubic cell of side a, such that the nearest neighbors touch. The dimension a for a cubic unit cell is called the *lattice constant*. For the fcc lattice the nearest neighbor distance is one-half the diagonal of a face, or $\frac{1}{2}(a\sqrt{2})$. Therefore, for the atom centered on the face to

EXAMPLE 1–1 For a bcc lattice of identical atoms with a lattice constant of 5 Å, calculate the maximum packing fraction and the radius of the atoms treated as hard spheres with the nearest neighbors touching.

SOLUTION Each corner atom in a cubic unit cell is shared with seven neighboring cells; thus, each unit cell contains one-eighth of a sphere at each of the eight corners for a total of one atom. The bcc cell contains one atom in the center of the cube. Thus, we have

$$\text{Nearest atoms are at a separation } \frac{1}{2} \times \sqrt{5^2 + 5^2 + 5^2} = 4.330 \text{ Å}$$

$$\text{Radius of each atom} = \frac{1}{2} \times 4.330 \text{ Å} = 2.165 \text{ Å}$$

$$\text{Volume of each atom} = \frac{4}{3}\pi(2.165)^3 = 42.5 \text{ Å}^3$$

$$\text{Number of atoms per cube} = 1 + 8 \times \frac{1}{8} = 2$$

$$\text{Packing fraction} = \frac{42.5 \times 2}{(5)^3} = 68\%$$

Therefore, if the atoms in a bcc lattice are packed as densely as possible, with no distance between the outer edges of nearest neighbors, 68% of the volume is filled. This is a relatively high percentage compared with some other lattice structures (Prob. 1.14).

just touch the atoms at each corner of the face, the radius of the sphere must be one-half the nearest neighbor distance, or $\frac{1}{4}(a\sqrt{2})$.

1.2.3 Planes and Directions

In discussing crystals it is very helpful to be able to refer to planes and directions within the lattice. The notation system generally adopted uses a set of three integers to describe the position of a plane or the direction of a vector within the lattice. We first set up an *xyz* coordinate system with the origin at any lattice point (it does not matter which one because they are all equivalent!), and the axes are lined up with the edges of the cubic unit cell. The three integers describing a particular plane are found in the following way:

1. Find the intercepts of the plane with the crystal axes and express these intercepts as integral multiples of the basis vectors (the plane can be moved in and out from the origin, retaining its orientation, until such an integral intercept is discovered on each axis).
2. Take the reciprocals of the three integers found in step 1 and reduce these to the smallest set of integers h, k, and l, which have the same relationship to each other as the three reciprocals.
3. Label the plane (hkl).

EXAMPLE 1-2

The plane illustrated in Fig. 1-5 has intercepts at **2a**, **4b**, and **1c** along the three crystal axes. Taking the reciprocals of these intercepts, we get $\frac{1}{2}$, $\frac{1}{4}$, and 1. These three fractions have the same relationship to each other as the integers 2, 1, and 4 (obtained by multiplying each fraction by 4). Thus the plane can be referred to as a (214) plane. The only exception is if the intercept is a fraction of the lattice constant a. In that case, we do not reduce it to the lowest set of integers. For example, in Fig. 1-3, planes parallel to the cube faces, but going through the body center atoms in the bcc lattice, would be (200) and not (100).

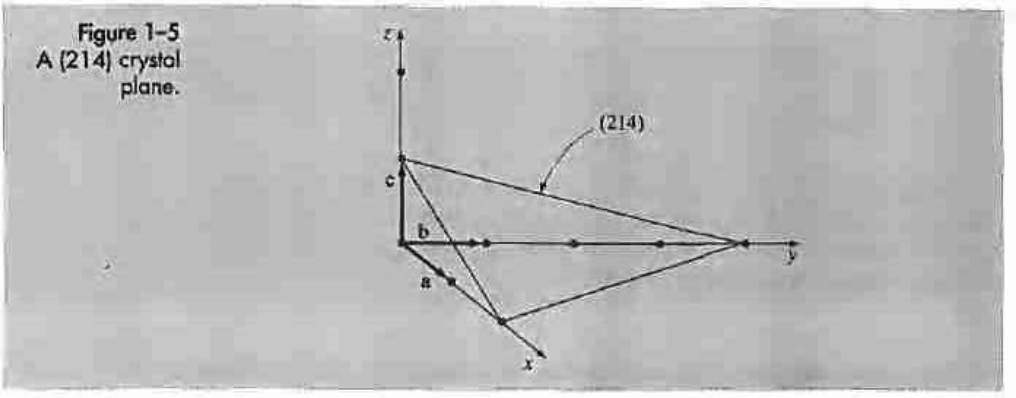

Figure 1-5 A (214) crystal plane.

The three integers h, k, and l are called the *Miller indices*; these three numbers define a set of parallel planes in the lattice. One advantage of taking the reciprocals of the intercepts is avoidance of infinities in the notation. One intercept is infinity for a plane parallel to an axis; however, the reciprocal of such an intercept is taken as zero. If a plane contains one of the axes, it is parallel to that axis and has a zero reciprocal intercept. If a plane passes through the origin, it can be translated to a parallel position for calculation of the Miller indices. If an intercept occurs on the negative branch of an axis, the minus sign is placed above the Miller index for convenience, such as $(h\bar{k}l)$.

From a crystallographic point of view, many planes in a lattice are equivalent; that is, a plane with given Miller indices can be shifted about in the lattice simply by choice of the position and orientation of the unit cell. The indices of such equivalent planes are enclosed in braces { } instead of parentheses. For example, in the cubic lattice of Fig. 1-6 all the cube faces are crystallographically equivalent in that the unit cell can be rotated in various directions and still appear the same. The six equivalent faces are collectively designated as {100}.

A direction in a lattice is expressed as a set of three integers with the same relationship as the components of a vector in that direction. The three vector components are expressed in multiples of the basis vectors, and the three integers are reduced to their smallest values while retaining the relationship among them. For example, the body diagonal in the cubic lattice (Fig. 1-7a) is composed of the components 1**a**, 1**b**, and 1**c**; therefore, this diagonal is the [111] direction. (Brackets are used for direction indices.) As in the case of planes, many directions in a lattice are equivalent, depending only on the arbitrary choice of orientation for the axes. Such equivalent direction indices are placed in angular brackets ⟨ ⟩. For example, the crystal axes in the cubic lattice [100], [010], and [001] are all equivalent and are called ⟨100⟩ directions (Fig. 1-7b).

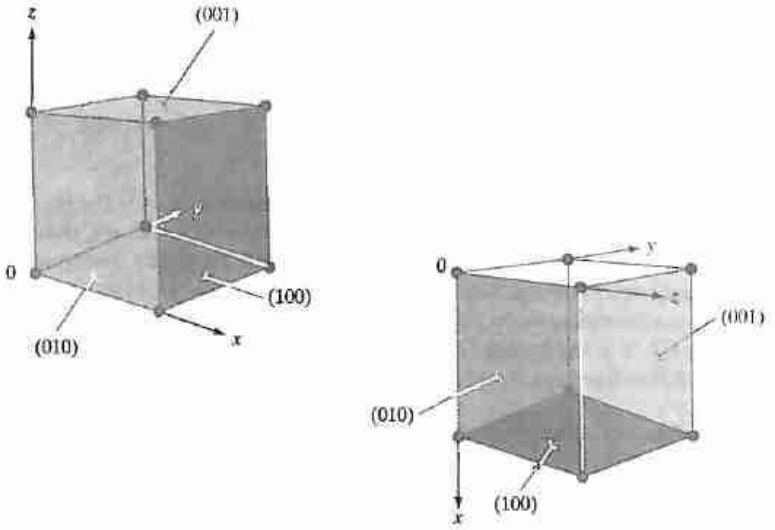

Figure 1–6 Equivalence of the cube faces ({100} planes) by rotation of the unit cell within the cubic lattice.

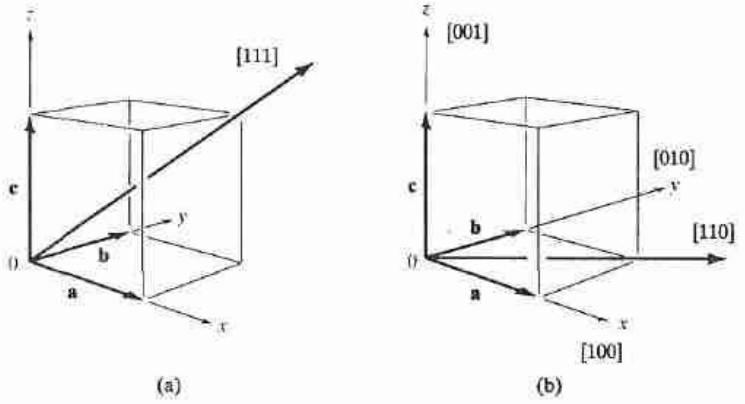

Figure 1–7 Crystal directions in the cubic lattice.

Two useful relationships in terms of Miller indices describe the distance between planes and angles between directions. The distance d between two adjacent planes labeled (hkl) is given in terms of the lattice constant, a, as

$$d = a/(h^2 + k^2 + l^2)^{1/2} \qquad (1\text{–}2a)$$

The angle θ between two different Miller index directions is given by

$$\cos\theta = h_1h_2 + k_1k_2 + l_1l_2/[(h_1^2 + k_1^2 + l_1^2)^{1/2}(h_2^2 + k_2^2 + l_2^2)^{1/2}] \qquad (1\text{–}2b)$$

Comparing Figs. 1-6 and 1-7, we notice that in cubic lattices a direction [*hkl*] is perpendicular to the plane (*hkl*). This is convenient in analyzing lattices with cubic unit cells, but it should be remembered that it is not necessarily true in noncubic systems.

1.2.4 The Diamond Lattice

The basic crystal structure for many important semiconductors is the fcc lattice with a basis of two atoms, giving rise to the *diamond* structure, characteristic of Si, Ge, and C in the diamond form. In many compound semiconductors, atoms are arranged in a basic diamond structure, but are different on alternating sites. This is called a *zinc blende* structure and is typical of the III–V compounds. One of the simplest ways of stating the construction of the diamond structure is the following:

> The diamond structure can be thought of as an fcc lattice with an extra atom placed at $\mathbf{a}/4 + \mathbf{b}/4 + \mathbf{c}/4$ from each of the fcc atoms.

Figure 1-8a illustrates the construction of a diamond lattice from an fcc unit cell. We notice that when the vectors are drawn with components one-fourth of the cube edge in each direction, only four additional points within the same unit cell are reached. Vectors drawn from any of the other fcc atoms simply determine corresponding points in adjacent unit cells. This method of constructing the diamond lattice implies that the original fcc has associated with it a second interpenetrating fcc displaced, by $\frac{1}{4}, \frac{1}{4}, \frac{1}{4}$. The two interpenetrating fcc *sublattices* can be visualized by looking down on the unit cell of Fig. 1-8a from the top (or along any ⟨100⟩ direction). In the top view of Fig. 1-8b, atoms belonging to the original fcc are represented by open circles, and the interpenetrating sublattice is shaded. If the atoms are all similar, we call this structure a diamond lattice; if the atoms differ on alternating

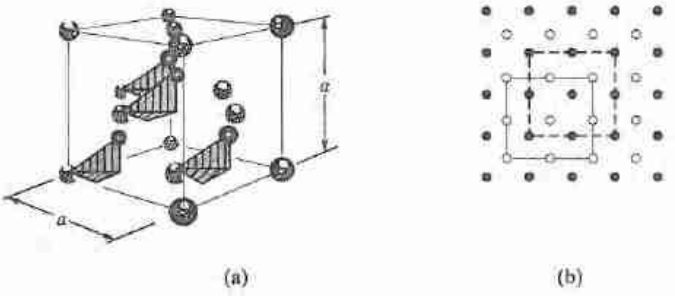

Figure 1-8
Diamond lattice structure: (a) a unit cell of the diamond lattice constructed by placing atoms $\frac{1}{4}, \frac{1}{4}, \frac{1}{4}$ from each atom in an fcc; (b) top view (along any ⟨100⟩ direction) of an extended diamond lattice. The colored circles indicate one fcc sublattice and the black circles indicate the interpenetrating fcc.

sites, it is a zinc blende structure. For example, if one fcc sublattice is composed of Ga atoms and the interpenetrating sublattice is As, the zinc blende structure of GaAs results. Most of the compound semiconductors have this type of lattice, although some of the II–VI compounds are arranged in a slightly different structure called the *wurtzite* lattice. We shall restrict our discussion here to the diamond and zinc blende structures, since they are typical of most of the commonly used semiconductors.

EXAMPLE 1–3

Calculate the volume density of Si atoms (number of atoms/cm^3), given that the lattice constant of Si is 5.43 Å. Calculate the areal density of atoms (number/cm^2) on the (100) plane.

SOLUTION

On the (100) plane, we have four atoms on corners and one on the face center.

$$\text{(100) plane: } \frac{4 \times \frac{1}{4} + 1}{(5.43 \times 10^{-8})(5.43 \times 10^{-8})} = 6.8 \times 10^{14}\ \text{cm}^{-2}$$

For Si, we have 8 corner lattice points, 6 face centered points, and 2 atoms

$$\text{Number of atoms per cube} = \left(8 \times \frac{1}{8} + \frac{1}{2} \times 6\right) \times 2 = 8$$

$$\text{Volume density} = \frac{8}{(5.43 \times 10^{-8})^3} = 5.00 \times 10^{22}\ \text{cm}^{-3}$$

A particularly interesting and useful feature of the III–V compounds is the ability to vary the mixture of elements on each of the two interpenetrating fcc sublattices of the zinc blende crystal. For example, in the ternary compound AlGaAs, it is possible to vary the composition of the ternary alloy by choosing the fraction of Al or Ga atoms on the column III sublattice. It is common to represent the composition by assigning subscripts to the various elements. For example, $Al_xGa_{1-x}As$ refers to a ternary alloy in which the column III sublattice in the zinc blende structure contains a fraction x of Al atoms and $1-x$ of Ga atoms. The composition $Al_{0.3}Ga_{0.7}As$ has 30 percent Al and 70 percent Ga on the column III sites, with the interpenetrating column V sublattice occupied entirely by As atoms. It is extremely useful to be able to grow ternary alloy crystals such as this with a given composition. For the $Al_xGa_{1-x}As$ example we can grow crystals over the entire composition range

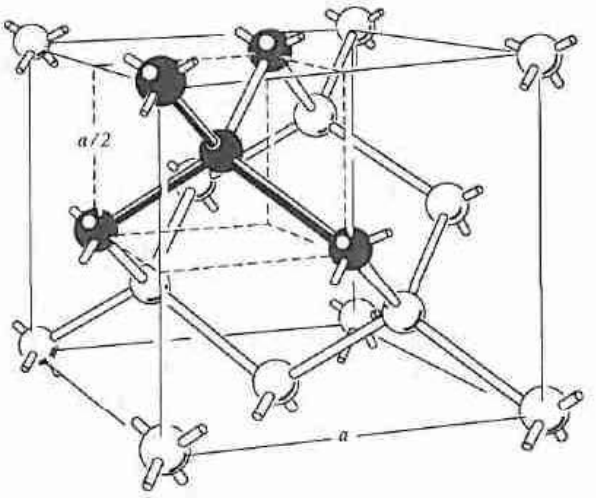

Figure 1–9 Diamond lattice unit cell, showing the four nearest neighbor structure. (From *Electrons and Holes in Semiconductors* by W. Shockley, © 1950 by Litton Educational Publishing Co., Inc.; by permission of Van Nostrand Reinhold Co., Inc.)

from $x = 0$ to $x = 1$, thus varying the electronic and optical properties of the material from that of GaAs ($x = 0$) to that of AlAs ($x = 1$). To vary the properties even further, it is possible to grow four-element (quaternary) compounds such as $In_xGa_{1-x}As_yP_{1-y}$ having a very wide range of properties.

It is important from an electronic point of view to notice that each atom in the diamond and zinc blende structures is surrounded by four nearest neighbors (Fig. 1-9). The importance of this relationship of each atom to its neighbors will become evident in Section 3.1.1 when we discuss the bonding forces which hold the lattice together.

The fact that atoms in a crystal are arranged in certain planes is important to many of the mechanical, metallurgical, and chemical properties of the material. For example, crystals often can be cleaved along certain atomic planes, resulting in exceptionally planar surfaces. This is a familiar result in cleaved diamonds for jewelry; the facets of a diamond reveal clearly the triangular, hexagonal, and rectangular symmetries of intersecting planes in various crystallographic directions. Semiconductors with diamond and zinc blende lattices have similar cleavage planes. Chemical reactions, such as etching of the crystal, often take place preferentially along certain directions. These properties serve as interesting illustrations of crystal symmetry, but in addition, each plays an important role in fabrication processes for many semiconductor devices.

1.3 BULK CRYSTAL GROWTH

The progress of solid state device technology since the invention of the transistor in 1948 has depended not only on the development of device concepts but also on the improvement of materials. For example, the fact that integrated circuits can be made today is the result of a considerable breakthrough

in the growth of pure, single-crystal Si in the early and mid-1950s. The requirements on the growing of device-grade semiconductor crystals are more stringent than those for any other materials. Not only must semiconductors be available in large single crystals, but also the purity must be controlled within extremely close limits. For example, Si crystals now being used in devices are grown with concentrations of most impurities of less than one part in ten billion. Such purities require careful handling and treatment of the material at each step of the manufacturing process.

1.3.1 Starting Materials

The raw feedstock for Si crystal is silicon dioxide (SiO_2). We react SiO_2 with C in the form of coke in an arc furnace at very high temperatures (~1800°C) to reduce SiO_2 according to the following reaction:

$$SiO_2 + 2C \rightarrow Si + 2CO \tag{1-3}$$

This forms metallurgical grade Si (MGS) which has impurities such as Fe, Al and heavy metals at levels of several hundred to several thousand parts per million (ppm). Refer back to Example 1-3 to see that 1 ppm of Si corresponds to an impurity level of $5 \times 10^{16}cm^{-3}$. While MGS is clean enough for metallurgical applications such as using Si to make stainless steel, it is not pure enough for electronic applications; it is also not single crystal.

The MGS is refined further to yield semiconductor-grade or electronic-grade Si (EGS), in which the levels of impurities are reduced to parts per billion or ppb (1 ppb$=5 \times 10^{13}cm^{-3}$). This involves reacting the MGS with dry HCl according to the following reaction to form trichlorosilane, $SiHCl_3$, which is a liquid with a boiling point of 32°C.

$$Si + 3HCl \rightarrow SiHCl_3 + H_2 \tag{1-4}$$

Along with $SiHCl_3$, chlorides of impurities such as $FeCl_3$ are formed which fortunately have boiling points that are different from that of $SiHCl_3$. This allows a technique called fractional distillation to be used, in which we heat up the mixture of $SiHCl_3$ and the impurity chlorides, and condense the vapors in different distillation towers held at appropriate temperatures. We can thereby separate pure $SiHCl_3$ from the impurities. $SiHCl_3$ is then converted to highly pure EGS by reaction with H_2,

$$2SiHCl_3 + 2H_2 \rightarrow 2Si + 6HCl \tag{1-5}$$

1.3.2 Growth of Single-Crystal Ingots

Next, we have to convert the high purity but still polycrystalline EGS to single-crystal Si ingots or boules. This is generally done today by a process commonly

called the *Czochralski* method. In order to grow single-crystal material, it is necessary to have a seed crystal which can provide a template for growth. We melt the EGS in a quartz-lined graphite crucible by resistively heating it to the melting point of Si (1412°C).

A seed crystal is lowered into the molten material and then is raised slowly, allowing the crystal to grow onto the seed (Fig. 1–10). Generally, the crystal is rotated slowly as it grows to provide a slight stirring of the melt and to average out any temperature variations that would cause inhomogeneous solidification. This technique is widely used in growing Si, Ge, and some of the compound semiconductors.

In pulling compounds such as GaAs from the melt, it is necessary to prevent volatile elements (e.g., As) from vaporizing. In one method a layer of B_2O_3, which is dense and viscous when molten, floats on the surface of the molten GaAs to prevent As evaporation. This growth method is called *liquid-encapsulated Czochralski* (*LEC*) growth.

In Czochralski crystal growth, the shape of the ingot is determined by a combination of the tendency of the cross section to assume a polygonal shape due to the crystal structure and the influence of surface tension, which encourages a circular cross section. The crystal facets are noticeable in the initial growth near the seed crystal in Fig. 1–10b. However, the cross section of the large ingot in Fig. 1–11 is almost circular.

In the fabrication of Si integrated circuits (Chapter 9) it is economical to use very large Si wafers, so that many IC chips can be made simultaneously. As a result, considerable research and development have gone into methods for growing very large Si crystals. For example, Fig. 1–11 illustrates a 12-inch-diameter Si ingot, 1.0 m long, weighing 140 kg.

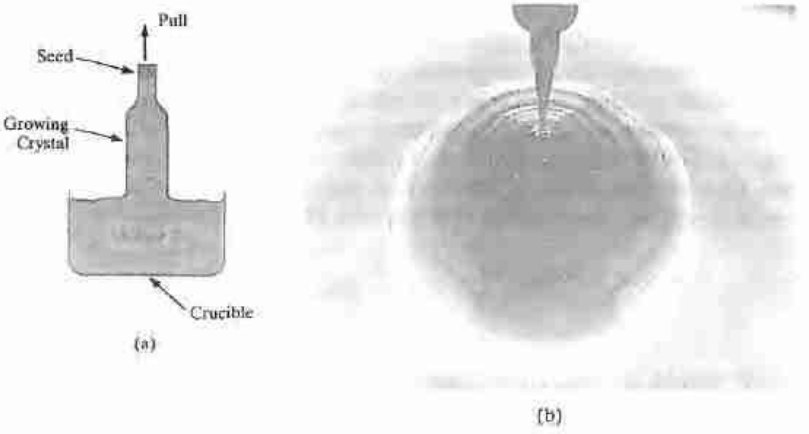

Figure 1–10 Pulling of a Si crystal from the melt (Czochralski method): (a) schematic diagram of the crystal growth process; (b) an 8-in. diameter, ⟨100⟩ oriented Si crystal being pulled from the melt. (Photograph courtesy of MEMC Electronics Intl.)

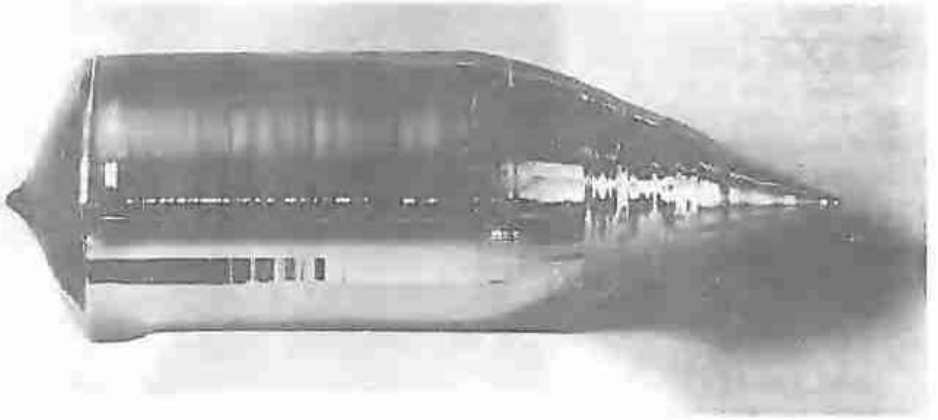

Figure 1–11
Silicon crystal grown by the Czochralski method. This large single-crystal ingot provides 300 mm (12-in.) diameter wafers when sliced using a saw. The ingot is about 1.0 m long (including the tapered regions), and weighs about 140 kg. (Photograph courtesy of MEMC Electronics Intl.)

1.3.3 Wafers

After the single-crystal ingot is grown, it is then mechanically processed to manufacture wafers. The first step involves mechanically grinding the more-or-less cylindrical ingot into a perfect cylinder with a precisely controlled diameter. This is important because in a modern integrated circuit fabrication facility many processing tools and wafer handling robots require tight tolerances on the size of the wafers. Using X-ray crystallography, crystal planes in the ingot are identified. For reasons discussed in Section 6.4.3, most Si ingots are grown along the ⟨100⟩ direction (Fig. 1–10). For such ingots, a small notch is ground on one side of the cylinder to delineate a {110} face of the crystal. This is useful because for ⟨100⟩ Si wafers, the {110} cleavage planes are orthogonal to each other. This notch then allows the individual integrated circuit chips to be made oriented along {110} planes so that when the chips are sawed apart, there is less chance of spurious cleavage of the crystal, which could cause good chips to be lost.

Next, the Si cylinder is sawed into individual wafers about 775 μm thick, by using a diamond-tipped inner-hole blade saw, or a wire saw (Fig. 1–12a). The resulting wafers are mechanically lapped and ground on both sides to achieve a flat surface, and to remove the mechanical damage due to sawing. Such damage would have a detrimental effect on devices. The flatness of the wafer is critical from the point of view of "depth of focus" or how sharp an image can be focussed on the wafer surface during photolithography, as discussed in Chapter 5. The Si wafers are then rounded or "chamfered" along the edges to minimize the likelihood of chipping the wafers during processing.

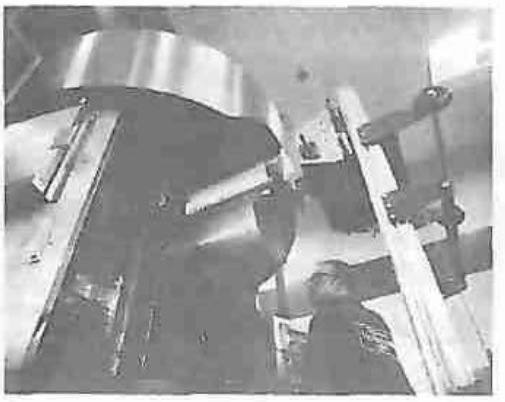

(a)

(b)

Figure 1–12 Steps involved in manufacturing Si wafers: (a) A 300 mm Si cylindrical ingot, with a notch on one side, being loaded into a wire saw to produce Si wafers; (b) a technician holding a cassette of 300 mm wafers. (Photographs courtesy of MEMC Electronics Intl.)

Finally, the wafers undergo chemical-mechanical polishing using a slurry of very fine SiO_2 particles in a basic NaOH solution to give the front surface of the wafer a mirror-like finish. The wafers are now ready for integrated circuit fabrication (Fig. 1-12b). The economic value added in this process is impressive. From sand (SiO_2) costing pennies, we can obtain Si wafers costing a few hundred dollars, on which we can make hundreds of microprocessors, for example, each costing several hundred dollars.

1.3.4 Doping

As previously mentioned, there are some impurities in the molten EGS. We may also add intentional impurities or dopants to the Si melt to change its electronic properties. At the solidifying interface between the melt and the

solid, there will be a certain distribution of impurities between the two phases. An important quantity that identifies this property is the *distribution coefficient* k_d, which is the ratio of the concentration of the impurity in the solid C_S to the concentration in the liquid C_L at equilibrium:

$$k_d = \frac{C_S}{C_L} \tag{1-6}$$

The distribution coefficient is a function of the material, the impurity, the temperature of the solid–liquid interface, and the growth rate. For an impurity with a distribution coefficient of one-half, the relative concentration of the impurity in the molten liquid to that in the refreezing solid is two to one. Thus the concentration of impurities in that portion of material that solidifies first is one-half the original concentration C_0. The distribution coefficient is thus important during growth from a melt. This can be illustrated by an example involving Czochralski growth:

EXAMPLE 1–4

A Si crystal is to be grown by the Czochralski method, and it is desired that the ingot contain 10^{16} phosphorus atoms/cm^3.

(a) What concentration of phosphorus atoms should the melt contain to give this impurity concentration in the crystal during the initial growth? For P in Si, $k_d = 0.35$.

(b) If the initial load of Si in the crucible is 5 kg, how many grams of phosphorus should be added? The atomic weight of phosphorus is 31.

SOLUTION

(a) Assume that $C_S = k_d C_L$ throughout the growth. Thus the initial concentration of P in the melt should be

$$\frac{10^{16}}{0.35} = 2.86 \times 10^{16}\ \text{cm}^{-3}$$

(b) The P concentration is so small that the volume of melt can be calculated from the weight of Si. From Appendix III the density of Si is 2.33 g/cm^3. In this example we will neglect the difference in density between solid and molten Si.

$$\frac{5000\ \text{g of Si}}{2.33\ \text{g/cm}^3} = 2146\ \text{cm}^3\ \text{of Si}$$

$$2.86 \times 10^{16}\ \text{cm}^{-3} \times 2146\ \text{cm}^3 = 6.14 \times 10^{19}\ \text{P atoms}$$

$$\frac{6.14 \times 10^{19}\ \text{atoms} \times 31\ \text{g/mole}}{6.02 \times 10^{23}\ \text{atoms/mole}} = 3.16 \times 10^{-3}\ \text{g of P}$$

Since the P concentration in the growing crystal is only about one-third of that in the melt, Si is used up more rapidly than P in the growth. Thus the melt becomes richer in P as the growth proceeds, and the crystal is doped more heavily in the latter stages of growth. This assumes that k_d is not varied; a more uniformly doped ingot can be grown by varying the pull rate (and therefore k_d) appropriately. Modern Czochralski growth systems use computer controls to vary the temperature, pull rate, and other parameters to achieve fairly uniformly doped ingots.

1.4 EPITAXIAL GROWTH

One of the most important and versatile methods of crystal growth for device applications is the growth of a thin crystal layer on a wafer of a compatible crystal. The substrate crystal may be a wafer of the same material as the grown layer or a different material with a similar lattice structure. In this process the substrate serves as the seed crystal onto which the new crystalline material grows. The growing crystal layer maintains the crystal structure and orientation of the substrate. The technique of growing an oriented single-crystal layer on a substrate wafer is called *epitaxial growth*, or *epitaxy*. As we shall see in this section, epitaxial growth can be performed at temperatures considerably below the melting point of the substrate crystal. A variety of methods are used to provide the appropriate atoms to the surface of the growing layer. These methods include *chemical vapor deposition* (*CVD*),[2] growth from a melt (*liquid-phase epitaxy, LPE*), and evaporation of the elements in a vacuum (*molecular beam epitaxy, MBE*). With this wide range of epitaxial growth techniques, it is possible to grow a variety of crystals for device applications, having properties specifically designed for the electronic or optoelectronic device being made.

1.4.1 Lattice-Matching in Epitaxial Growth

When Si epitaxial layers are grown on Si substrates, there is a natural matching of the crystal lattice, and high-quality single-crystal layers result. On the other hand, it is often desirable to obtain epitaxial layers that differ somewhat from the substrate, which is known as *heteroepitaxy*. This can be accomplished easily if the lattice structure and lattice constant a match for the two materials. For example, GaAs and AlAs both have the zinc blende structure, with a lattice constant of about 5.65 Å. As a result, epitaxial layers of the ternary alloy AlGaAs can be grown on GaAs substrates with little lattice mismatch. Similarly, GaAs can be grown on Ge substrates (see Appendix III).

[2]The generic term *chemical vapor deposition* includes the deposition of layers that may be polycrystalline or amorphous. When a CVD process results in a single-crystal epitaxial layer, a more specific term is *vapor-phase epitaxy* (*VPE*).

Since AlAs and GaAs have similar lattice constants, it is also true that the ternary alloy AlGaAs has essentially the same lattice constant over the entire range of compositions from AlAs to GaAs. As a result, one can choose the composition x of the ternary compound $Al_xGa_{1-x}As$ to fit the particular device requirement, and grow this composition on a GaAs wafer. The resulting epitaxial layer will be lattice-matched to the GaAs substrate.

Figure 1–13 illustrates the energy band gap E_g as a function of lattice constant a for several III–V ternary compounds as they are varied over their composition ranges. For example, as the ternary compound InGaAs is varied by choice of composition on the column III sublattice from InAs to GaAs, the band gap changes from 0.36 to 1.43 eV while the lattice constant of the crystal varies from 6.06 Å for InAs to 5.65 Å for GaAs. Clearly, we cannot grow this ternary compound over the entire composition range on a particular binary substrate, which has a fixed lattice constant. As Fig. 1–13 illustrates, however, it is possible to grow a specific composition of InGaAs on an InP substrate. The vertical (invariant lattice constant) line from InP to the InGaAs curve shows that a midrange ternary composition (actually, $In_{0.53}Ga_{0.47}As$) can be grown lattice-matched to an InP substrate. Similarly, a ternary InGaP alloy with about 50 percent Ga and 50 percent In on the column III sublattice can be grown lattice-matched to a GaAs substrate. To achieve a broader range of alloy compositions, grown lattice-matched on particular substrates, it is helpful to use quaternary alloys such as InGaAsP. The variation of compositions on both the column III and column V sublattices provides additional flexibility in choosing a particular band gap while providing lattice-matching to convenient binary substrates such as GaAs or InP.

In the case of GaAsP, the lattice constant is intermediate between that of GaAs and GaP, depending upon the composition. For example, GaAsP crystals used in red LEDs have 40 percent phosphorus and 60 percent arsenic on the column V sublattice. Since such a crystal cannot be grown directly on either a GaAs or a GaP substrate, it is necessary to gradually change the lattice constant as the crystal is grown. Using a GaAs or Ge wafer as a substrate, the growth is begun at a composition near GaAs. A region ~25 μm thick is grown while gradually introducing phosphorus until the desired As/P ratio is achieved. The desired epitaxial layer (e.g., 100 μm thick) is then grown on this graded layer. By this method epitaxial growth always occurs on a crystal of similar lattice constant. Although some crystal dislocations occur due to lattice strain in the graded region, such crystals are of high quality and can be used in LEDs.

In addition to the widespread use of lattice-matched epitaxial layers, the advanced epitaxial growth techniques described in the following sections allow the growth of very thin (~100 Å) layers of lattice-mismatched crystals. If the mismatch is only a few percent and the layer is thin, the epitaxial layer grows with a lattice constant in compliance with that of the seed crystal (Fig. 1–14). The resulting layer is in compression or tension along the surface plane as its lattice constant adapts to the seed crystal (Fig. 1–14). Such a layer is called

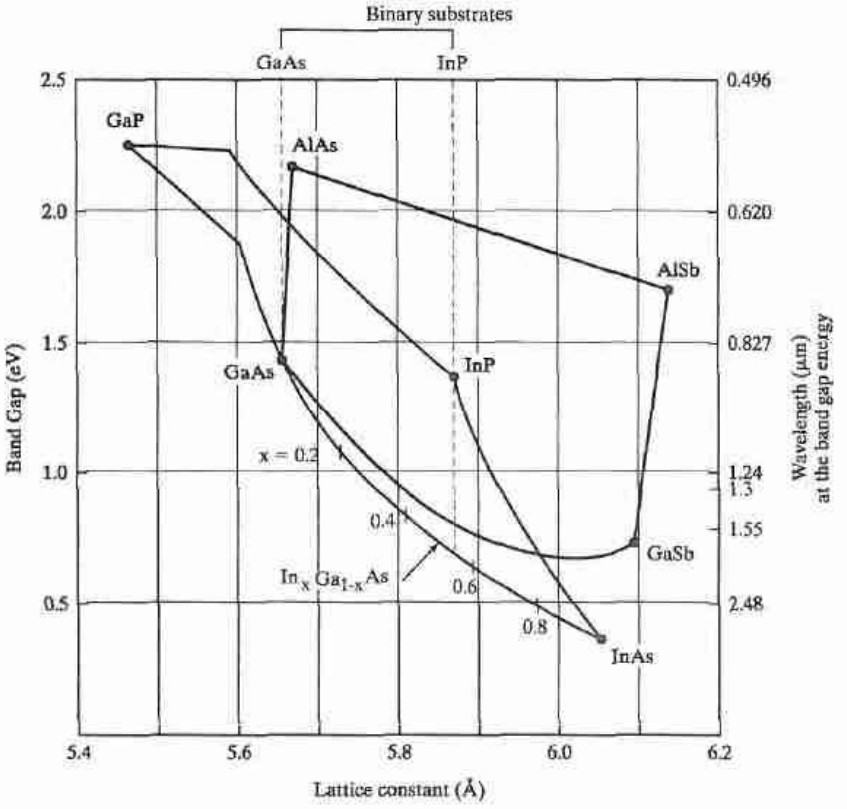

Figure 1–13
Relationship between band gap and lattice constant for alloys in the InGaAsP and AlGaAsSb systems. The dashed vertical lines show the lattice constants for the commercially available binary substrates GaAs and InP. For the marked example of $In_xGa_{1-x}As$, the ternary composition $x = 0.53$ can be grown lattice-matched on InP, since the lattice constants are the same. For quaternary alloys, the compositions on both the III and V sublattices can be varied to grow lattice-matched epitaxial layers along the dashed vertical lines between curves. For example, $In_xGa_{1-x}As_yP_{1-y}$ can be grown on InP substrates, with resulting band gaps ranging from 0.75 eV to 1.35 eV. In using this figure, assume the lattice constant a of a ternary alloy varies linearly with the composition x.

pseudomorphic because it is not lattice-matched to the substrate without strain. However, if the epitaxial layer exceeds a critical layer thickness, t_c, which depends on the lattice mismatch, the strain energy leads to formation of defects called *misfit dislocations*. Using thin alternating layers of slightly mismatched crystal layers, it is possible to grow a *strained-layer superlattice* (*SLS*) in which alternate layers are in tension and compression. The overall SLS lattice constant is an average of that of the two bulk materials.

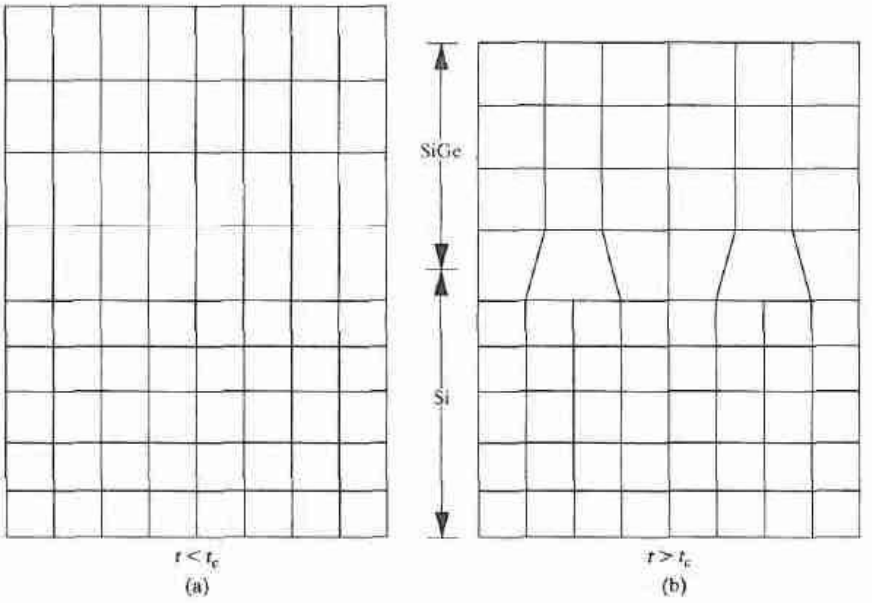

Figure 1–14
Heteroepitaxy and misfit dislocations. For example, in heteroepitaxy of a SiGe layer on Si, the lattice mismatch between SiGe and Si leads to compressive strain in the SiGe layer. The amount of strain depends on the mole fraction of Ge. (a) For layer thicknesses less than the critical layer thickness, t_c, pseudomorphic growth occurs. (b) However, above t_c, misfit dislocations form at the interface which may reduce the usefulness of the layers in device applications.

1.4.2 Vapor-Phase Epitaxy

The advantages of low temperature and high purity epitaxial growth can be achieved by crystallization from the vapor phase. Crystalline layers can be grown onto a seed or substrate from a chemical vapor of the semiconductor material or from mixtures of chemical vapors containing the semiconductor. *Vapor-phase epitaxy* (*VPE*) is a particularly important source of semiconductor material for use in devices. Some compounds such as GaAs can be grown with better purity and crystal perfection by vapor epitaxy than by other methods. Furthermore, these techniques offer great flexibility in the actual fabrication of devices. When an epitaxial layer is grown on a substrate, it is relatively simple to obtain a sharp demarcation between the type of impurity doping in the substrate and in the grown layer. The advantages of this freedom to vary the impurity will be discussed in subsequent chapters. We point out here, however, that Si integrated-circuit devices (Chapter 9) are usually built in layers grown by VPE on Si wafers.

Epitaxial layers are generally grown on Si substrates by the controlled deposition of Si atoms onto the surface from a chemical vapor containing Si. In one method, a gas of silicon tetrachloride reacts with hydrogen gas to give Si and anhydrous HCl:

$$SiCl_4 + 2H_2 \rightleftharpoons Si + 4HCl \qquad (1\text{-}7)$$

If this reaction occurs at the surface of a heated crystal, the Si atoms released in the reaction can be deposited as an epitaxial layer. The HCl remains gaseous at the reaction temperature and does not disturb the growing crystal. As indicated, this reaction is reversible. This is very important because it implies that by adjusting the process parameters, the reaction in Eq. (1-7) can be driven to the left (providing etching of the Si rather than deposition). This etching can be used for preparing an atomically clean surface on which epitaxy can occur.

This vapor epitaxy technique requires a chamber into which the gases can be introduced and a method for heating the Si wafers. Since the chemical reactions take place in this chamber, it is called a *reaction chamber* or, more simply, a *reactor*. Hydrogen gas is passed through a heated vessel in which $SiCl_4$ is evaporated; then the two gases are introduced into the reactor over the substrate crystal, along with other gases containing the desired doping impurities. The Si slice is placed on a graphite susceptor or some other material that can be heated to the reaction temperature with an rf heating coil or tungsten halogen lamps. This method can be adapted to grow epitaxial layers of closely controlled impurity concentration on many Si slices simultaneously (Fig. 1-15).

The reaction temperature for the hydrogen reduction of $SiCl_4$ is approximately 1150–1250°C. Other reactions may be employed at somewhat lower temperatures, including the use of dichlorosilane (SiH_2Cl_2) at 1000–1100°C, or

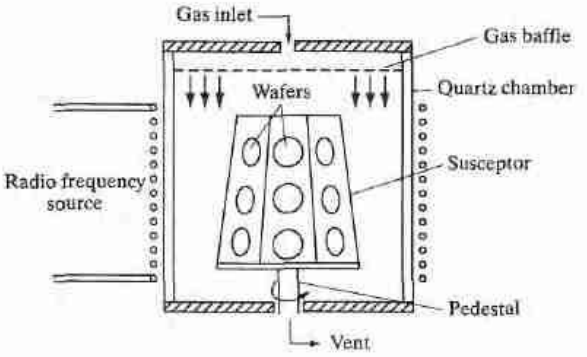

Figure 1-15 A barrel-type reactor for Si VPE. These are atmospheric pressure systems. The Si wafers are held in slots cut on the sides of a SiC-coated graphite susceptor that flares out near the base to promote gas flow patterns conducive to uniform epitaxy.

the pyrolysis of silane (SiH_4) at 500°C–1000°C. Pyrolysis involves the breaking up of the silane at the reaction temperature:

$$SiH_4 \rightarrow Si + 2H_2 \tag{1-8}$$

There are several advantages of the lower reaction temperature processes, including the fact that they reduce migration of impurities from the substrate to the growing epitaxial layer.

In some applications it is useful to grow thin Si layers on insulating substrates. For example, vapor-phase epitaxial techniques can be used to grow ~1μm Si films on sapphire and other insulators. This application of VPE is discussed in Section 9.3.2.

Vapor-phase epitaxial growth is also important in the III–V compounds, such as GaAs, GaP, and the ternary alloy GaAsP, which is widely used in the fabrication of LEDs. Substrates are held at about 800°C on a rotating wafer holder while phosphine, arsine, and gallium chloride gases are mixed and passed over the samples. The GaCl is obtained by reacting anhydrous HCl with molten Ga within the reactor. Variation of the crystal composition for GaAsP can be controlled by altering the mixture of arsine and phosphine gases.

Another useful method for epitaxial growth of compound semiconductors is called *metal-organic vapor-phase epitaxy* (*MOVPE*), or *organometallic vapor-phase epitaxy* (*OMVPE*). For example, the organometallic compound trimethylgallium can be reacted with arsine to form GaAs and methane:

$$(CH_3)_3Ga + AsH_3 \rightarrow GaAs + 3CH_4 \tag{1-9}$$

This reaction takes place at about 700°C, and epitaxial growth of high-quality GaAs layers can be obtained. Other compound semiconductors can also be grown by this method. For example, trimethylaluminum can be added to the gas mixture to grow AlGaAs. This growth method is widely used in the fabrication of a variety of devices, including solar cells and lasers. The convenient variability of the gas mixture allows the growth of multiple thin layers similar to those discussed below for molecular beam epitaxy.

1.4.3 Molecular Beam Epitaxy

One of the most versatile techniques for growing epitaxial layers is called *molecular beam epitaxy* (*MBE*). In this method the substrate is held in a high vacuum while molecular or atomic beams of the constituents impinge upon its surface (Fig. 1–16a). For example, in the growth of AlGaAs layers on GaAs substrates, the Al, Ga, and As components, along with dopants, are heated in separate cylindrical cells. Collimated beams of these constituents escape into the vacuum and are directed onto the surface of the substrate. The rates at which these atomic beams strike the surface can be closely controlled, and growth of very high quality crystals results. The sample is held at a relatively low temperature (about 600°C for GaAs) in this growth procedure. Abrupt

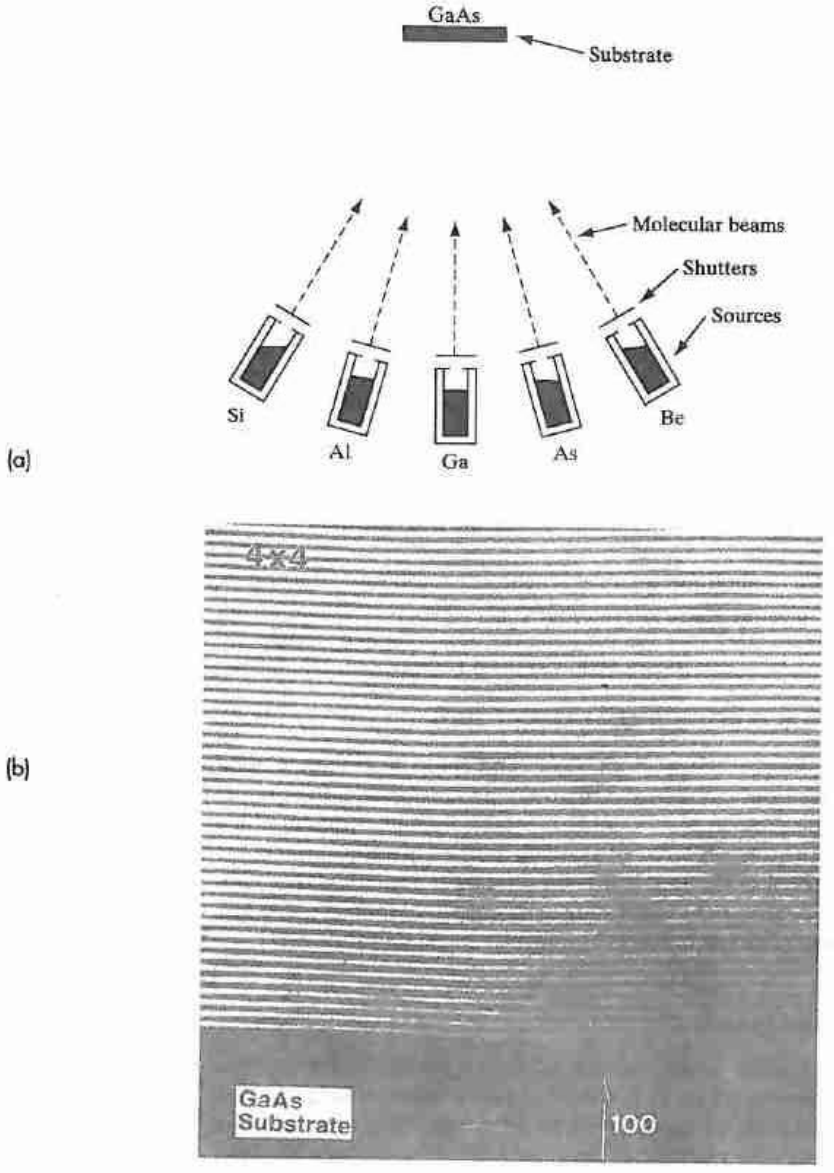

Figure 1–16
Crystal growth by molecular beam epitaxy (MBE): (a) evaporation cells inside a high-vacuum chamber directing beams of Al, Ga, As, and dopants onto a GaAs substrate; (b) scanning electron micrograph of the cross section of an MBE-grown crystal having alternating layers of GaAs (dark lines) and AlGaAs (light lines). Each layer is four monolayers ($4 \times a/2 = 11.3$ Å) thick. (Photograph courtesy of Bell Laboratories.)

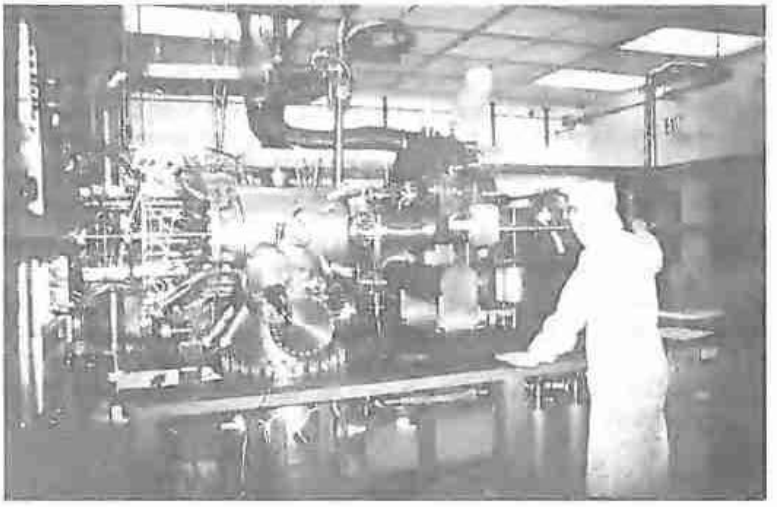

Figure 1–17 Molecular beam epitaxy facility in the Microelectronics Research Center at the University of Texas at Austin.

changes in doping or in crystal composition (e.g., changing from GaAs to AlGaAs) can be obtained by controlling shutters in front of the individual beams. Using slow growth rates (≤ 1 μm/h), it is possible to control the shutters to make composition changes on the scale of the lattice constant. For example, Fig. 1–16b illustrates a portion of a crystal grown with alternating layers of GaAs and AlGaAs only four monolayers thick. Because of the high vacuum and close controls involved, MBE requires a rather sophisticated setup (Fig. 1-17). However, the versatility of this growth method makes it very attractive for many applications.

As MBE has developed in recent years, it has become common to replace some of the solid sources shown in Fig. 1–16 with gaseous chemical sources. This approach, called *chemical beam epitaxy*, or *gas-source MBE*, combines many of the advantages of MBE and VPE.

SUMMARY

1.1 Semiconductor devices are at the heart of information technology. Elemental semiconductors such as Si appear in column IV of the periodic table, while compound semiconductors such as GaAs consist of elements symmetrically around column IV. More complicated alloy semiconductors are used to optimize optoelectronic properties.

1.2 These devices are generally made in single-crystal material for best performance. Single crystals have long-range order, while polycrystalline and amorphous materials have short-range and no order, respectively.

1.3 Lattices are determined by symmetry. In 3-D, these are called Bravais lattices. When we put a basis of atom(s) on the lattice sites, we get a crystal. Common

semiconductors have an fcc symmetry with a basis of two identical or different atoms, resulting in diamond or zinc blende crystals, respectively.

1.4 The fundamental building block of a lattice is a *primitive* cell with lattice points at its corners. Sometimes it is easier to describe the crystal in terms of a larger "unit" cell with lattice points not only at the corners, but also at body or face centers.

1.5 Translating unit cells by integer numbers of basis vectors can replicate the lattice. Planes and directions in a lattice can be defined in terms of Miller indices.

1.6 Real crystals can have defects in 0-, 1-, 2-, and 3-D, some of which are benign, but many of which are harmful for device operation.

1.7 Semiconductor bulk crystals are grown from a melt by the Czochralski method, starting from a seed. Single-crystal epitaxial layers can be grown on top of semiconductor wafers in various ways, such as vapor-phase epitaxy, MOCVD, or MBE. One can thereby optimize doping and band-structure properties for device fabrication.

PROBLEMS

1.1 Using Appendix III, which of the listed semiconductors in Table 1-1 has the largest band gap? The smallest? What are the corresponding wavelengths if light is emitted at the energy E_g? Is there a noticeable pattern in the band gap energy of III–V compounds related to the column III element?

1.2 Find the fraction of the fcc unit cell volume filled with hard spheres.

1.3 Label the planes illustrated in Fig. P1-3.

Figure P1-3

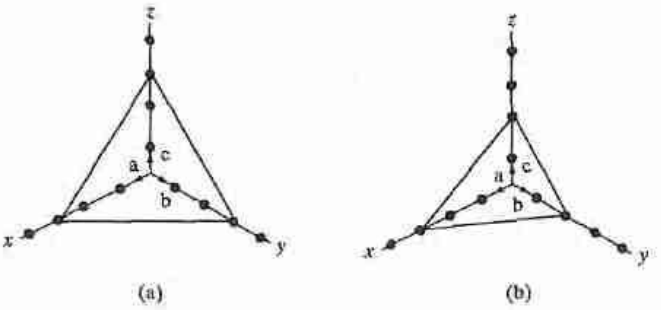

1.4 Calculate the densities of Si and GaAs from the lattice constants (Appendix III), atomic weights, and Avogadro's number. Compare the results with densities given in Appendix III. The atomic weights of Si, Ga, and As are 28.1, 69.7, and 74.9, respectively.

1.5 The atomic radii of In and Sb atoms are approximately 1.44 Å and 1.36 Å, respectively. Using the hard-sphere approximation, find the lattice constant of InSb (zinc blende structure), and the volume of the primitive cell. What is the atomic density on the (110) planes? (Hint: The volume of the primitive cell is one-fourth the fcc unit cell volume.)

1.6 A crystal with a simple cubic lattice and a monoatomic basis has an atomic radius of 2.5 Å and an atomic weight of 5.42. Calculate its density, assuming that the atoms touch each other.

1.7 Sketch a view down a ⟨110⟩ direction of a diamond lattice, using Fig. 1-9 as a guide. Include lines connecting nearest neighbors.

1.8 Show by a sketch that the bcc lattice can be represented by two interpenetrating sc lattices. To simplify the sketch, show a ⟨100⟩ view of the lattice.

1.9 (a) Find the number of atoms/cm^2 on the (100) surface of a Si wafer.

(b) What is the distance (in Å) between nearest In neighbors in InP?

1.10 The ionic radii of Na^+ (atomic weight 23) and Cl^- (atomic weight 35.5) are 1.0 and 1.8 Å, respectively. Treating the ions as hard spheres, calculate the density of NaCl. Compare this with the measured density of 2.17 g/cm^3.

1.11 Sketch an *sc* unit cell with lattice constant $\mathbf{a} = 4$ Å, whose diatomic basis of atom A is located at the lattice sites, and with atom B displaced by $(\mathbf{a}/2,0,0)$. Assume that both atoms have the same size and we have a close-packed structure (i.e., nearest neighbor atoms touch each other). Calculate

(i) the packing fraction (i.e., fraction of the total volume occupied by atoms),

(ii) the number of B atoms per unit *volume*,

(iii) the number of A atoms per unit *area* on (100) planes.

1.12 How many atoms are found inside a unit cell of an sc, a bcc, and an fcc crystal? How far apart in terms of lattice constant a are the nearest neighbor atoms in each case, measured from center to center?

1.13 Draw a cube such as Fig. 1-7, and show four {111} planes with different orientations. Repeat for {110} planes.

1.14 Find the maximum fractions of the unit cell volume that can be filled by hard spheres in the sc, fcc, and diamond lattices.

1.15 Calculate the densities of Ge and InP from the lattice constants (Appendix III), atomic weights, and Avogadro's number. Compare the results with the densities given in Appendix III.

1.16 Beginning with a sketch of an fcc lattice, add atoms at $(\frac{1}{4}, \frac{1}{4}, \frac{1}{4})$ from each fcc atom to obtain the diamond lattice. Show that only the four added atoms in Fig. 1-8a appear in the diamond unit cell.

1.17 Assuming that the lattice constant varies linearly with composition x for a ternary alloy (e.g., see the variation for InGaAs in Fig. 1-13), what composition of $AlSb_xAs_{1-x}$ is lattice-matched to InP? What composition of $In_xGa_{1-x}P$ is lattice-matched to GaAs? What is the band gap energy in each case?

(*Note*: Such linear variations of crystal properties (e.g., lattice constant and band gap) with mole fraction in alloys is known as *Vegard's law*. A second-order polynomial or quadratic fit to the data is called the *bowing* parameter.)

1.18 An Si crystal is to be pulled from the melt and doped with arsenic ($k_d = 0.3$). If the Si weighs 1 kg, how many grams of arsenic should be introduced to achieve 10^{15} cm^{-3} doping during the initial growth?

READING LIST

Ashcroft, N. W., and N. D. Mermin. *Solid State Physics.* Philadelphia: W.B. Saunders, 1976.

Denbaars, S. P. "Gallium–Nitride-Based Materials for Blue to Ultraviolet Optoelectronic Devices," *Proc. IEEE* 85(11) (November 1997): 1740–1749.

Kittel, C. *Introduction to Solid State Physics*, 7th ed. New York: Wiley, 1996.

Plummer, J. D., M. D. Deal, and P. B. Griffin, *Silicon VLSI Technology*. Upper Saddle River, NJ: Prentice Hall, 2000.

Stringfellow, G. B. *Organometallic Vapor-Phase Epitaxy.* New York: Academic Press, 1989.

Swaminathan, V., and A. T. Macrander. *Material Aspects of GaAs and InP Based Structures.* Englewood Cliffs, NJ: Prentice Hall, 1991.

SELF QUIZ

Question 1

(a) Label the following planes using the correct notation for a cubic lattice of unit cell edge length a (shown within the unit cell).

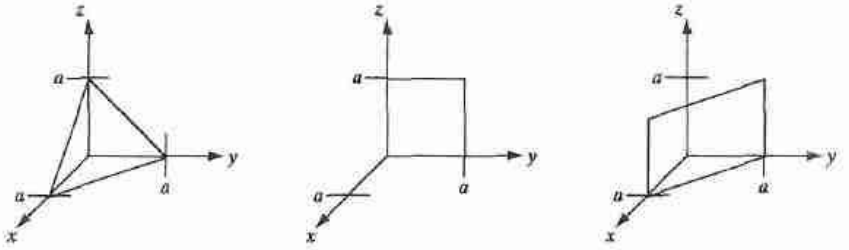

(b) Write out all of the equivalent ⟨100⟩ directions using the correct notation.

(c) On the two following sets of axes, (1) sketch the [011] direction and (2) a (111) plane (for a cubic system with primitive vectors $\boldsymbol{a}$, $\boldsymbol{b}$, and $\boldsymbol{c}$).

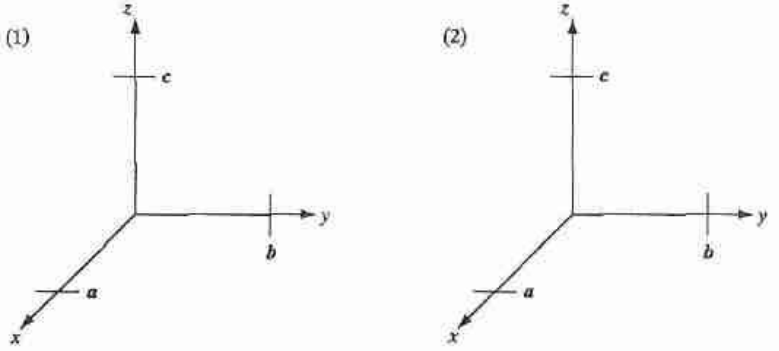

Question 2

(a) Which of the following three unit cells are *primitive cells* for the two-dimensional lattice? Circle the correct combination **in bold** below.

1 / 2 / 3 / 1 and 2 / 1 and 3 / 2 and 3 / 1, 2, and 3

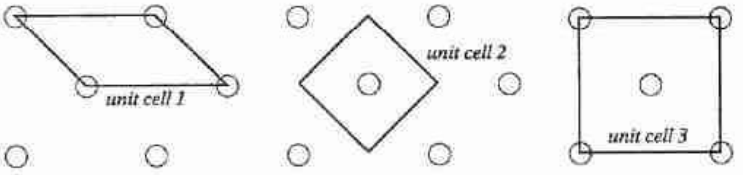

(b) The following planes (shown within the first quadrant for $0 < x,y,z < a$ only, with the dotted lines for reference only) are all from what one set of *equivalent* planes? Use correct notation:

answer:

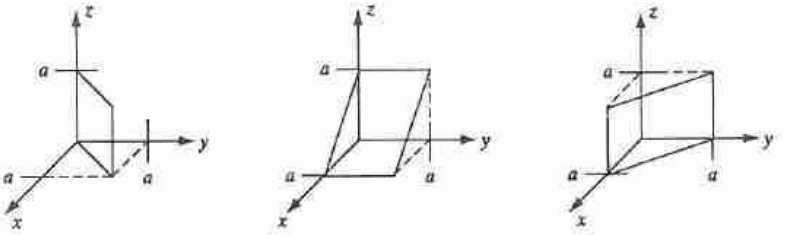

(c) Which of the following three planes (shown within the first quadrant only) is a (121) plane? Circle the correct diagram.

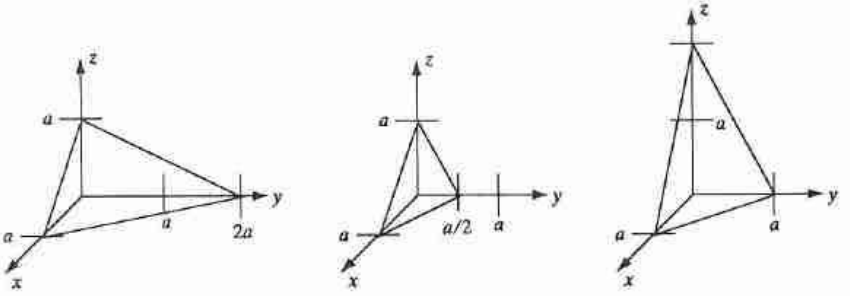

Question 3

(a) Diamond and zinc blende crystal structures are both composed of a Bravais lattice with a two-atom basis. Circle the correct unit cell for this Bravais lattice.

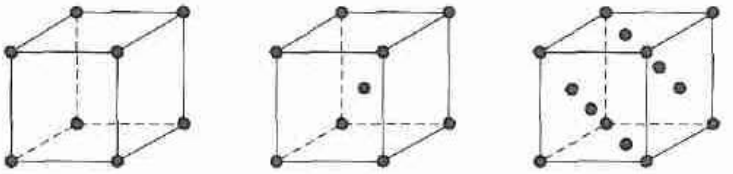

(b) Which statement below is true?

1. GaAs has a ***diamond / zinc blende*** crystal structure.
2. Si has a ***diamond / zinc blende*** crystal structure.

Question 4

Give some examples of zero-dimensional, one-dimensional, two-dimensional, and three-dimensional defects in a semiconductor.

Question 5

(a) What is the difference between a primitive cell and a unit cell? What is the utility of both concepts?

(b) What is the difference between a lattice and a crystal? How many different 1-D lattices can you have?

Question 6

Consider growing InAs on the following crystal substrates: InP, AlAs, GaAs, and GaP. For which case would the *critical thickness* of the InAs layer be greatest? You may use Fig. 1–13 from your text.

GaP / GaAs / AlAs / InP

Chapter 2

Atoms and Electrons

OBJECTIVES

1. Understand the wave-particle duality of nature in quantum mechanics
2. Study the Bohr model of atoms
3. Apply the Schrödinger equation to simple problems
4. Understand the electronic structure of atoms and the periodic table
5. Understand how semiconductor properties are determined

Since this book is primarily an introduction to solid state devices, it would be preferable not to delay this discussion with subjects such as atomic theory, quantum mechanics, and electron models. However, the behavior of solid state devices is directly related to these subjects. For example, it would be difficult to understand how an electron is transported through a semiconductor device without some knowledge of the electron and its interaction with the crystal lattice. Therefore, in this chapter we shall investigate some of the important properties of electrons, with special emphasis on two points: (1) the electronic structure of atoms, and (2) the interaction of atoms and electrons with excitation, such as the absorption and emission of light. By studying electron energies in an atom, we lay the foundation for understanding the influence of the lattice on electrons participating in current flow through a solid. Our discussions concerning the interaction of light with electrons form the basis for later descriptions of changes in the conductivity of a semiconductor with optical excitation, properties of light-sensitive devices, and lasers.

First, we shall investigate some of the experimental observations which led to the modern concept of the atom, and then we shall give a brief introduction to the theory of quantum mechanics. Several important concepts will emerge from this introduction: the electrons in atoms are restricted to certain energy levels by quantum rules; the electronic structure of atoms is determined from these quantum conditions; and this "quantization" defines certain allowable transitions involving absorption and emission of energy by the electrons.

Petitioner Canadian Solar (USA) Inc., Ex. 1030, p. 31

2.1 INTRODUCTION TO PHYSICAL MODELS

The main effort of science is to describe what happens in nature, in as complete and concise a form as possible. In physics this effort involves observing natural phenomena, relating these observations to previously established theory, and finally establishing a physical model for the observations. For example, we can explain the behavior of a spring-supported weight moving up and down periodically after an initial displacement, because the differential equations describing such a simple harmonic motion have been established by Newtonian classical mechanics.

When a new physical phenomenon is observed, it is necessary to find out how it fits into the established models and "laws" of physics. In the vast majority of cases this involves a direct extension of the mathematics of well-established models to the particular conditions of the new problem. In fact, it is not uncommon for a scientist or engineer to predict that a new phenomenon should occur before it is actually observed, simply by a careful study and extension of existing models and laws. The beauty of science is that natural phenomena are not isolated events but are related to other events by a few analytically describable laws. However, it does happen occasionally that a set of observations cannot be described in terms of existing theories. In such cases it is necessary to develop models which are based as far as possible on existing laws, but which contain new aspects arising from the new phenomena. Postulating new physical principles is a serious business, and it is done only when there is no possibility of explaining the observations with established theory. When new assumptions and models are made, their justification lies in the following question: "Does the model describe precisely the observations, and can reliable predictions be made based on the model?" The model is good or poor depending on the answer to this question.

In the 1920s it became necessary to develop a new theory to describe phenomena on the atomic scale. A long series of careful observations had been made that clearly indicated that many events involving electrons and atoms did not obey the classical laws of mechanics. It was necessary, therefore, to develop a new kind of mechanics to describe the behavior of particles on this small scale. This new approach, called *quantum mechanics*, describes atomic phenomena very well and also properly predicts the way in which electrons behave in solids—our primary interest here. Through the years, quantum mechanics has been so successful that now it stands beside the classical laws as a valid description of nature.

A special problem arises when students first encounter the theory of quantum mechanics. The problem is that quantum concepts are largely mathematical in nature and do not involve the "common sense" quality associated with classical mechanics. At first, many students find quantum concepts difficult, not so much because of the mathematics involved, but because they feel the concepts are somehow divorced from "reality." This is a reasonable reaction, since ideas which we consider to be real or intuitively satisfying are usually based on our own observation. Thus the classical laws of motion are easy to understand because we observe bodies in motion every day. On the

other hand, we observe the effects of atoms and electrons only indirectly, and naturally we have very little feeling for what is happening on the atomic scale. It is necessary, therefore, to depend on the facility of the theory to predict experimental results rather than to attempt to force classical analogs onto the nonclassical phenomena of atoms and electrons.

Our approach in this chapter will be to investigate the important experimental observations that led to the quantum theory, and then to indicate how the theory accounts for these observations. Discussions of quantum theory must necessarily be largely qualitative in such a brief presentation, and those topics that are most important to solid state theory will be emphasized here. Several good references for further individual study are given at the end of this chapter.

2.2 EXPERIMENTAL OBSERVATIONS

The experiments that led to the development of quantum theory were concerned with the interaction of light and matter. On the one hand, there were phenomena such as interference or diffraction which clearly indicated that light has a wave character as proposed by Huygens, in contrast to the particle or *corpuscular* view of light proposed by Newton. But on the other hand, many experiments at the turn of the 20th century clearly showed that a new theory of light was needed.

2.2.1 The Photoelectric Effect

An important observation by Planck indicated that radiation from a heated sample, known as blackbody radiation, is emitted in discrete units of energy called *quanta*; the energy units were described by $h\nu$, where ν is the frequency of the radiation, and h is a quantity now called Planck's constant ($h = 6.63 \times 10^{-34}$ J-s). Soon after Planck developed this hypothesis, Einstein interpreted an important experiment that clearly demonstrated the discrete nature (*quantization*) of light. This experiment involved absorption of optical energy by the electrons in a metal and the relationship between the amount of energy absorbed and the frequency of the light (Fig. 2-1). Let us suppose that monochromatic light is incident on the surface of a metal plate in a vacuum. The electrons in the metal absorb energy from the light, and some of the electrons receive enough energy to be ejected from the metal surface into the vacuum. This phenomenon is called the *photoelectric effect*. If the energy of the escaping electrons is measured, a plot can be made of the maximum energy as a function of the frequency ν of the incident light (Fig. 2-1b).

One simple way of finding the maximum energy of the ejected electrons is to place another plate above the one shown in Fig. 2-1a and then create an electric field between the two plates. The potential necessary to retard all electron flow between the plates gives the energy E_m. For a particular frequency of light incident on the sample, a maximum energy E_m is observed

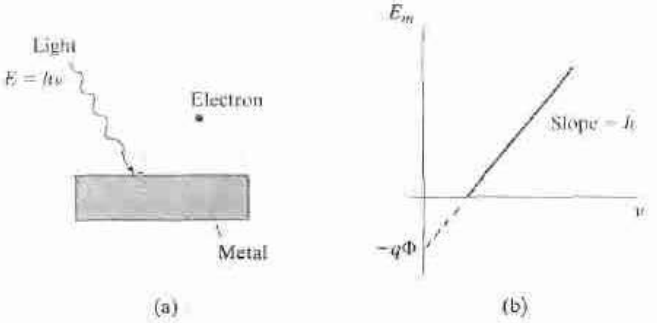

Figure 2–1 The photoelectric effect: (a) electrons are ejected from the surface of a metal when exposed to light of frequency ν in a vacuum; (b) plot of the maximum kinetic energy of ejected electrons vs. frequency of the incoming light.

for the emitted electrons. The resulting plot of E_m vs. ν is linear, with a slope equal to Planck's constant. The equation of the line shown in Fig. 2-1b is

$$E_m = h\nu - q\Phi \tag{2-1}$$

where q is the magnitude of the electronic charge. The quantity Φ (volts) is a characteristic of the particular metal used. When Φ is multiplied by the electronic charge, an energy (joules) is obtained which represents the minimum energy required for an electron to escape from the metal into a vacuum. The energy $q\Phi$ is called the *work function* of the metal. These results indicate that the electrons receive an energy $h\nu$ from the light and lose an amount of energy $q\Phi$ in escaping from the surface of the metal.

This experiment demonstrates clearly that Planck's hypothesis was correct—light energy is contained in discrete units rather than in a continuous distribution of energies. Other experiments also indicate that, in addition to the wave nature of light, the quantized units of light energy can be considered as localized packets of energy, called *photons*. (Interestingly, this is reminiscent of the Newtonian picture.) We get the Planck relationship

$$E = h\nu \tag{2-2a}$$

Some experiments emphasize the wave nature of light, while other experiments reveal the discrete nature of photons. This wave–particle duality is fundamental to quantum processes and does not imply an ambiguity in the theory. Based on the wave–particle duality of light, Louis de Broglie proposed that particles of matter (such as electrons) similarly could manifest a wave character in certain experiments. This observation was confirmed by the diffraction of electrons by the periodic array of atoms in a crystal observed by Davisson and Germer. De Broglie proposed that a particle of momentum $p = mv$ has a wavelength given by

$$\lambda = h/p = h/mv \tag{2-2b}$$

The Planck and de Broglie relationships are fundamental in quantum physics and are valid for *all* situations and objects, including photons and

electrons. They connect the wave description of phenomena (frequency and wavelength) to a particle description (energy and momentum).

The relation between frequency and wavelength, known as the *dispersion relationship*, however, is *not* the same for different objects. For example, for photons, the wavelength (λ) is related to frequency by $\lambda = c/\nu$, where c is the speed of light. For electrons, it is a different relationship, known as the band structure, as discussed in Chapter 3.

2.2.2 Atomic Spectra

One of the most valuable experiments of modern physics is the analysis of absorption and emission of light by atoms. For example, an electric discharge can be created in a gas, so that the atoms begin to emit light with wavelengths characteristic of the gas. We see this effect in a neon sign, which is typically a glass tube filled with neon or a gas mixture, with electrodes for creating a discharge. If the intensity of the emitted light is measured as a function of wavelength, one finds a series of sharp lines rather than a continuous distribution of wavelengths. By the early 1900s the characteristic spectra for several atoms were well known. A portion of the measured emission spectrum for hydrogen is shown in Fig. 2-2, in which the vertical lines represent the positions of observed emission peaks on the wavelength scale. Photon energy $h\nu$ is then related to wavelength by the dispersion relation $\lambda = c/\nu$.

The lines in Fig. 2-2 appear in several groups labeled the *Lyman*, *Balmer*, and *Paschen* series after their early investigators. Once the hydrogen spectrum was established, scientists noticed several interesting relationships among the lines. The various series in the spectrum were observed to follow certain empirical forms:

$$\text{Lyman:}\quad \nu = cR\left(\frac{1}{1^2} - \frac{1}{\mathbf{n}^2}\right),\quad \mathbf{n} = 2, 3, 4, \ldots \tag{2-3a}$$

$$\text{Balmer:}\quad \nu = cR\left(\frac{1}{2^2} - \frac{1}{\mathbf{n}^2}\right),\quad \mathbf{n} = 3, 4, 5, \ldots \tag{2-3b}$$

$$\text{Paschen:}\quad \nu = cR\left(\frac{1}{3^2} - \frac{1}{\mathbf{n}^2}\right),\quad \mathbf{n} = 4, 5, 6, \ldots \tag{2-3c}$$

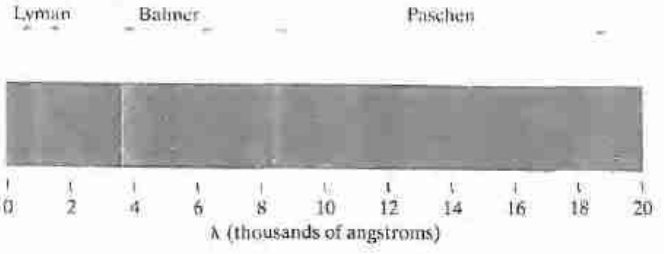

Figure 2-2 Some important lines in the emission spectrum of hydrogen.

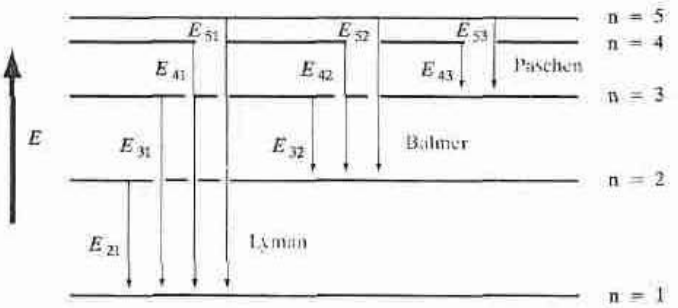

Figure 2–3 Relationships among photon energies in the hydrogen spectrum.

where R is a constant called the Rydberg constant ($R = 109{,}678\ \text{cm}^{-1}$). If the photon energies $h\nu$ are plotted for successive values of the integer **n**, we notice that each energy can be obtained by taking sums and differences of other photon energies in the spectrum (Fig. 2-3). For example, E_{42} in the Balmer series is the difference between E_{41} and E_{21} in the Lyman series. This relationship among the various series is called the *Ritz combination principle.* Naturally, these empirical observations stirred a great deal of interest in constructing a comprehensive theory for the origin of the photons given off by atoms.

2.3 THE BOHR MODEL

The results of emission spectra experiments led Niels Bohr to construct a model for the hydrogen atom, based on the mathematics of planetary systems. If the electron in the hydrogen atom has a series of planetary-type orbits available to it, it can be excited to an outer orbit and then can fall to any one of the inner orbits, giving off energy corresponding to one of the lines of Fig. 2-3. To develop the model, Bohr made several postulates:

1. Electrons exist in certain stable, circular orbits about the nucleus. This assumption implies that the orbiting electron does not give off radiation as classical electromagnetic theory would normally require of a charge experiencing angular acceleration; otherwise, the electron would not be stable in the orbit but would spiral into the nucleus as it lost energy by radiation.
2. The electron may shift to an orbit of higher or lower energy, thereby gaining or losing energy equal to the difference in the energy levels (by absorption or emission of a photon of energy $h\nu$).

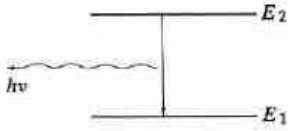

$$h\nu = E_2 - E_1 \qquad (2\text{-}4)$$

3. The angular momentum p_θ of the electron in an orbit is always an integral multiple of Planck's constant divided by 2π ($h/2\pi$ is often abbreviated $\hbar$ for convenience). This assumption,

$$p_\theta = \mathbf{n}\hbar, \quad \mathbf{n} = 1, 2, 3, 4, \ldots \qquad (2\text{-}5)$$

is necessary to obtain the observed results of Fig. 2-3. Although Bohr proposed this *ad hoc* relationship simply to explain the data, one can see that this is equivalent to having an integer number of de Broglie wavelengths fit within the circumference of the electron orbit (Prob. 2.2). These were called *pilot* waves, guiding the motion of the electrons around the nucleus. The de Broglie wave concept provided the inspiration for the Schrödinger wave equation in quantum mechanics discussed in Section 2.4.

If we visualize the electron in a stable orbit of radius r about the proton of the hydrogen atom, we can equate the electrostatic force between the charges to the centripetal force:

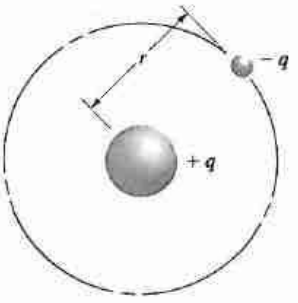

$$-\frac{q^2}{Kr^2} = -\frac{mv^2}{r} \qquad (2\text{-}6)$$

where $K = 4\pi\epsilon_0$ in MKS units, m is the mass of the electron, and v is its velocity. From assumption 3 we have

$$p_\theta = mvr = \mathbf{n}\hbar \qquad (2\text{-}7)$$

Since **n** takes on integral values, r should be denoted by r_n to indicate the **n**th orbit. Then Eq. (2-7) can be written

$$m^2v^2 = \frac{\mathbf{n}^2\hbar^2}{r_n^2} \tag{2-8}$$

Substituting Eq. (2-8) in Eq. (2-6) we find that

$$\frac{q^2}{Kr_n^2} = \frac{1}{mr_n} = \frac{\mathbf{n}^2\hbar^2}{r_n^2} \tag{2-9}$$

$$r_n = \frac{K\mathbf{n}^2\hbar^2}{mq^2} \tag{2-10}$$

for the radius of the **n**th orbit of the electron. Now we must find the expression for the total energy of the electron in this orbit, so that we can calculate the energies involved in transitions between orbits.

From Eqs. (2-7) and (2-10) we have

$$v = \frac{\mathbf{n}\hbar}{mr_n} \tag{2-11}$$

$$v = \frac{\mathbf{n}\hbar q^2}{K\mathbf{n}^2\hbar^2} = \frac{q^2}{K\mathbf{n}\hbar} \tag{2-12}$$

Therefore, the kinetic energy of the electron is

$$\text{K. E.} = \frac{1}{2}mv^2 = \frac{mq^4}{2K^2\mathbf{n}^2\hbar^2} \tag{2-13}$$

The potential energy is the product of the electrostatic force and the distance between the charges:

$$\text{P. E.} = -\frac{q^2}{Kr_n} = -\frac{mq^4}{K^2\mathbf{n}^2\hbar^2} \tag{2-14}$$

Thus the total energy of the electron in the **n**th orbit is

$$E_n = \text{K. E.} + \text{P. E.} = -\frac{mq^4}{2K^2\mathbf{n}^2\hbar^2} \tag{2-15}$$

The critical test of the model is whether energy differences between orbits correspond to the observed photon energies of the hydrogen spectrum. The transitions between orbits corresponding to the Lyman, Balmer, and Paschen series are illustrated in Fig. 2-4. The energy difference between orbits $\mathbf{n}_1$ and $\mathbf{n}_2$ is given by

$$E_{n2} - E_{n1} = \frac{mq^4}{2K^2\hbar^2}\left(\frac{1}{\mathbf{n}_1^2} - \frac{1}{\mathbf{n}_2^2}\right) \tag{2-16}$$

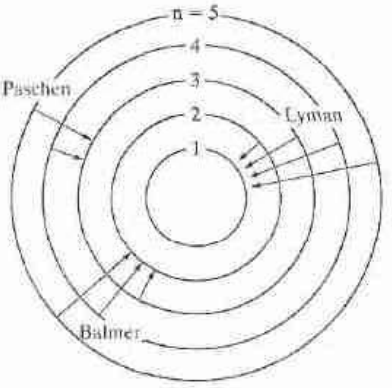

Figure 2–4
Electron orbits and transitions in the Bohr model of the hydrogen atom. Orbit spacing is not drawn to scale.

The frequency of light given off by a transition between these orbits is

$$\nu_{21} = \left[\frac{mq^4}{2K^2 - {}^2h}\right]\left(\frac{1}{\mathbf{n}_1^2} - \frac{1}{\mathbf{n}_2^2}\right) \tag{2–17}$$

The factor in brackets is essentially the Rydberg constant R times the speed of light c. A comparison of Eq. (2–17) with the experimental results summed up by Eq. (2–3) indicates that the Bohr theory provides a good model for electronic transitions within the hydrogen atom, as far as the early experimental evidence is concerned.

Whereas the Bohr model accurately describes the gross features of the hydrogen spectrum, it does not include many fine points. For example, experimental evidence indicates some splitting of levels in addition to the levels predicted by the theory. Also, difficulties arise in extending the model to atoms more complicated than hydrogen. Attempts were made to modify the Bohr model for more general cases, but it soon became obvious that a more comprehensive theory was needed. However, the partial success of the Bohr model was an important step toward the eventual development of the quantum theory. The concept that electrons are quantized in certain allowed energy levels, and the relationship of photon energy and transitions between levels, had been established firmly by the Bohr theory.

2.4 QUANTUM MECHANICS

The principles of quantum mechanics were developed from two different points of view at about the same time (the late 1920s). One approach, developed by Heisenberg, utilizes the mathematics of matrices and is called *matrix mechanics*. Independently, Schrödinger developed an approach utilizing a wave equation, now called *wave mechanics*. These two mathematical formulations appear to be quite different. However, closer examination

reveals that beyond the formalism, the basic principles of the two approaches are the same. It is possible to show, for example, that the results of matrix mechanics reduce to those of wave mechanics after mathematical manipulation. We shall concentrate here on the wave mechanics approach, since solutions to a few simple problems can be obtained with it, involving less mathematical discussion.

2.4.1 Probability and the Uncertainty Principle

It is impossible to describe with absolute precision events involving individual particles on the atomic scale. Instead, we must speak of the average values (*expectation values*) of position, momentum, and energy of a particle such as an electron. It is important to note, however, that the uncertainties revealed in quantum calculations are not based on some shortcoming of the theory. In fact, a major strength of the theory is that it describes the probabilistic nature of events involving atoms and electrons. The fact is that such quantities as the position and momentum of an electron *do not exist* apart from a particular uncertainty. The magnitude of this inherent uncertainty is described by the *Heisenberg uncertainty principle:*[1]

> In any measurement of the position and momentum of a particle, the uncertainties in the two measured quantities will be related by
>
> $$\boxed{(\Delta x)\,(\Delta p_x) \geq \hbar/2} \qquad (2\text{-}18)$$
>
> Similarly, the uncertainties in an energy measurement will be related to the uncertainty in the time at which the measurement was made by
>
> $$\boxed{(\Delta E)\,(\Delta t) \geq \hbar/2} \qquad (2\text{-}19)$$

These limitations indicate that simultaneous measurement of position and momentum or of energy and time are inherently inaccurate to some degree. Of course, Planck's constant h is a rather small number (6.63×10^{-34} J-s), and we are not concerned with this inaccuracy in the measurement of x and p_x for a truck, for example. On the other hand, measurements of the position of an electron and its speed are seriously limited by the uncertainty principle.

One implication of the uncertainty principle is that we cannot properly speak of *the* position of an electron, for example, but must look for the "probability" of finding an electron at a certain position. Thus one of the important results of quantum mechanics is that a *probability density function* can be

[1]This is often called the *principle of indeterminacy*.

obtained for a particle in a certain environment, and this function can be used to find the expectation value of important quantities such as position, momentum, and energy. We are familiar with the methods for calculating discrete (single-valued) probabilities from common experience. For example, it is clear that the probability of drawing a particular card out of a random deck is $^1/_{52}$, and the probability that a tossed coin will come up heads is $^1/_2$. The techniques for making predictions when the probability varies are less familiar, however. In such cases it is common to define a probability of finding a particle within a certain volume. Given a probability density function $P(x)$ for a one-dimensional problem, the probability of finding the particle in a range from x to $x + dx$ is $P(x)dx$. Since the particle will be *somewhere*, this definition implies that

$$\int_{-\infty}^{\infty} P(x)dx = 1 \tag{2-20}$$

if the function $P(x)$ is properly chosen. Equation (2-20) is implied by stating that the function $P(x)$ is *normalized* (i.e., the integral equals unity).

To find the average value of a function of x, we need only multiply the value of that function in each increment dx by the probability of finding the particle in that dx and sum over all x. Thus the average value of $f(x)$ is

$$\langle f(x)\rangle = \int_{-\infty}^{\infty} f(x)P(x)dx \tag{2-21a}$$

If the probability density function is not normalized, this equation should be written

$$\langle f(x)\rangle = \frac{\int_{-\infty}^{\infty} f(x)P(x)dx}{\int_{-\infty}^{\infty} P(x)dx} \tag{2-21b}$$

2.4.2 The Schrödinger Wave Equation

There are several ways to develop the wave equation by applying quantum concepts to various classical equations of mechanics. One of the simplest approaches is to consider a few basic postulates, develop the wave equation from them, and rely on the accuracy of the results to serve as a justification of the postulates. In more advanced texts these assumptions are dealt with in more convincing detail.

Basic Postulates

1. Each particle in a physical system is described by a wave function $\Psi(x, y, z, t)$. This function and its space derivative $(\partial\Psi/\partial x + \partial\Psi/\partial y + \partial\Psi/\partial z)$ are continuous, finite, and single valued.

2. In dealing with classical quantities such as energy E and momentum p, we must relate these quantities with abstract quantum mechanical operators defined in the following way:

Classical variable	Quantum operator
x	x
$f(x)$	$f(x)$
$\mathsf{p}(x)$	$\frac{\hbar}{j}\frac{\partial}{\partial x}$
E	$-\frac{\hbar}{j}\frac{\partial}{\partial t}$

and similarly for the other two directions.

3. The probability of finding a particle with wave function Ψ in the volume $dx\,dy\,dz$ is $\Psi^*\Psi\,dx\,dy\,dz$.[2] The product $\Psi^*\Psi$ is normalized according to Eq. (2-20) so that

$$\int_{-\infty}^{\infty} \Psi^*\Psi\,dx\,dy\,dz = 1$$

and the average value $\langle Q\rangle$ of any variable Q is calculated from the wave function by using the operator form Q_{op} defined in postulate 2:

$$\langle Q\rangle = \int_{-\infty}^{\infty} \Psi^* Q_{op}\,\Psi\,dx\,dy\,dz$$

Once we find the wave function Ψ for a particle, we can calculate its average position, energy, and momentum, within the limits of the uncertainty principle. Thus, a major part of the effort in quantum calculations involves solving for Ψ within the conditions imposed by a particular physical system. We notice from assumption 3 that the probability density function is $\Psi^*\Psi$, or $|\Psi|^2$.

The classical equation for the energy of a particle can be written:

$$\begin{array}{ccccc} \text{Kinetic energy} & + & \text{potential energy} & = & \text{total energy} \\ \frac{1}{2m}\mathsf{p}^2 & + & \mathsf{V} & = & E \end{array} \qquad (2\text{-}22)$$

[2] Ψ^* is the *complex conjugate* of Ψ, obtained by reversing the sign on each j. Thus, $[e^{jx}]^* = e^{-jx}$.

In quantum mechanics we use the operator form for these variables (postulate 2); the operators are allowed to operate on the wave function Ψ. For a one-dimensional problem Eq. (2-22) becomes[3]

$$-\frac{\hbar^2}{2m}\frac{\partial^2\Psi(x,t)}{\partial x^2} + V(x)\Psi(x,t) = -\frac{\hbar}{j}\frac{\partial\Psi(x,t)}{\partial t} \tag{2-23}$$

which is the Schrödinger wave equation. In three dimensions the equation is

$$\boxed{-\frac{\hbar^2}{2m}\nabla^2\Psi + V\Psi = -\frac{\hbar}{j}\frac{\partial\Psi}{\partial t}} \tag{2-24}$$

where $\nabla^2\Psi$ is

$$\frac{\partial^2\Psi}{\partial x^2} + \frac{\partial^2\Psi}{\partial y^2} + \frac{\partial^2\Psi}{\partial z^2}$$

The wave function Ψ in Eqs. (2-23) and (2-24) includes both space and time dependencies. It is common to calculate these dependencies separately and combine them later. Furthermore, many problems are time independent, and only the space variables are necessary. Thus we try to solve the wave equation by breaking it into two equations by the technique of separation of variables. Let $\Psi(x, t)$ be represented by the product $\psi(x)\phi(t)$. Using this product in Eq. (2-23) we obtain

$$-\frac{\hbar^2}{2m}\frac{\partial^2\psi(x)}{\partial x^2}\phi(t) + V(x)\psi(x)\phi(t) = -\frac{\hbar}{j}\psi(x)\frac{\partial\phi(t)}{\partial t} \tag{2-25}$$

Now the variables can be separated to obtain the time-dependent equation in one dimension,

$$\boxed{\frac{d\phi(t)}{dt} + \frac{jE}{\hbar}\phi(t) = 0} \tag{2-26}$$

and the time-independent equation,

$$\boxed{\frac{d^2\psi(x)}{dx^2} + \frac{2m}{\hbar^2}[E - V(x)]\psi(x) = 0} \tag{2-27}$$

We can show that the separation constant E corresponds to the energy of the particle when particular solutions are obtained, such that a wave function ψ_n (eigenfunction) corresponds to a particle energy E_n (eigenenergy).

These equations are the basis of wave mechanics. From them we can determine the wave functions for particles in various simple systems. For calculations involving electrons, the potential term $V(x)$ usually results from an electrostatic or magnetic field.

[3]The operational interpretation of $(\partial/\partial x)^2$ is the second-derivative form $\partial^2/\partial x^2$; the square of j is -1.

2.4.3 Potential Well Problem

It is quite difficult to find solutions to the Schrödinger equation for most realistic potential fields. One can solve the problem with some effort for the hydrogen atom, for example, but solutions for more complicated atoms are hard to obtain. There are several important problems, however, which illustrate the theory without complicated manipulation. The simplest problem is the potential energy well with infinite boundaries. Let us assume a particle is trapped in a potential well with $V(x)$ zero except at the boundaries $x = 0$ and L, where it is infinitely large (Fig. 2-5a):

$$\begin{aligned} V(x) &= 0, \quad 0 < x < L \\ V(x) &= \infty, \quad x = 0, L \end{aligned} \tag{2-28}$$

Inside the well we set $V(x) = 0$ in Eq. (2-27):

$$\frac{d^2\psi(x)}{dx^2} + \frac{2m}{\hbar^2} E\psi(x) = 0, \quad 0 < x < L \tag{2-29}$$

This is the wave equation for a free particle; it applies to the potential well problem in the region with no potential $V(x)$.

Possible solutions to Eq. (2-29) are $\sin kx$ and $\cos kx$, where k is $\sqrt{2mE}/\hbar$. In choosing a solution, however, we must examine the boundary conditions. The only allowable value of ψ at the walls is zero. Otherwise, there would be a nonzero $|\psi|^2$ outside the potential well, which is impossible because a particle cannot penetrate an infinite barrier. Therefore, we must choose only the sine solution and define k such that $\sin kx$ goes to zero at $x = L$:

$$\psi = A \sin kx, \quad k = \frac{\sqrt{2mE}}{\hbar} \tag{2-30}$$

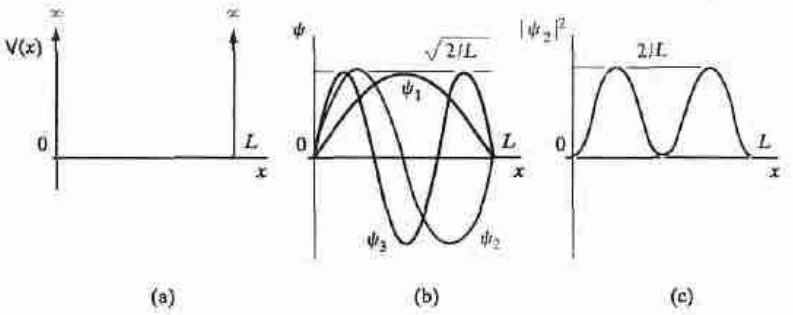

Figure 2-5 The problem of a particle in a potential well: (a) potential energy diagram; (b) wave functions in the first three quantum states; (c) probability density distribution for the second state.

The constant A is the amplitude of the wave function and will be evaluated from the normalization condition (postulate 3). If ψ is to be zero at $x = L$, then k must be some integral multiple of π/L:

$$\mathrm{k} = \frac{\mathbf{n}\pi}{L}, \quad \mathbf{n} = 1, 2, 3, \ldots \tag{2-31}$$

From Eqs. (2-30) and (2-31) we can solve for the total energy E_n for each value of the integer $\mathbf{n}$:

$$\frac{\sqrt{2mE_n}}{\hbar} = \frac{\mathbf{n}\pi}{L} \tag{2-32}$$

$$E_n = \frac{\mathbf{n}^2\pi^2\hbar^2}{2mL^2} \tag{2-33}$$

Thus for each allowable value of $\mathbf{n}$ the particle energy is described by Eq. (2-33). We notice that the *energy is quantized*. Only certain values of energy are allowed. The integer $\mathbf{n}$ is called a *quantum number*; the particular wave function ψ_n and corresponding energy state E_n describe the *quantum state* of the particle.

The quantized energy levels described by Eq. (2-33) appear in a variety of small-geometry structures encountered in semiconductor devices. We shall return to this potential well problem (often called the "particle in a box" problem) in later discussions.

The constant A is found from postulate 3:

$$\int_{-\infty}^{\infty} \psi^*\psi \, dx = \int_0^L A^2\left(\sin\frac{\mathbf{n}\pi}{L}x\right)^2 dx = A^2\frac{L}{2} \tag{2-34}$$

Setting Eq. (2-34) equal to unity we obtain

$$A = \sqrt{\frac{2}{L}}, \quad \psi_n = \sqrt{\frac{2}{L}}\sin\frac{\mathbf{n}\pi}{L}x \tag{2-35}$$

The first three wave functions ψ_1, ψ_2, ψ_3 are sketched in Fig. 2-5b. The probability density function $\psi^*\psi$, or $|\psi|^2$, is sketched for ψ_2 in Fig. 2-5c.

EXAMPLE 2-1

Given a plane wave $\psi = A\exp(jk_x x)$, what is the expectation value for p_x, the x-component of momentum?

SOLUTION

$$\langle p_x \rangle = \frac{\displaystyle\int_{-\infty}^{\infty} A^* e^{-jk_x x}\left(\frac{\hbar}{j}\frac{\partial}{\partial x}\right) A e^{jk_x x}\, dx}{\displaystyle\int_{-\infty}^{\infty} |A|^2 e^{-jk_x x} e^{jk_x x}\, dx} = (\hbar k_x) \text{ after normalization}$$

If we try to evaluate these integrals directly, we run into the problem that both numerator and denominator tend to infinity, because an *ideal* plane wave is strictly not a normalizable wave function. The trick to use is to choose the limits of integration from, say, $-L/2$ to $+L/2$ in a region of length L. The factor L cancels out in the numerator and denominator. *Then* we can consider L approaches infinity. For wave functions that are normalizable, such a mathematical "trick" does not have to be used.

2.4.4 Tunneling

The wave functions are relatively easy to obtain for the potential well with infinite walls, since the boundary conditions force ψ to zero at the walls. A slight modification of this problem illustrates a principle that is very important in some solid state devices—the quantum mechanical *tunneling* of an electron through a barrier of finite height and thickness. Let us consider the potential barrier of Fig. 2-6. If the barrier is not infinite, the boundary conditions do not force ψ to zero at the barrier. Instead, we must use the condition that ψ and its slope $d\psi/dx$ are continuous at each boundary of the barrier (postulate 1). Thus ψ must have a nonzero value within the barrier and also on the other side. Since ψ has a value to the right of the barrier, $\psi^*\psi$ exists there also, implying that there is some probability of finding the particle beyond the barrier. We notice that the particle does not go over the barrier; its total energy is assumed to be less than the barrier height V_0. The mechanism by which the particle "penetrates" the barrier is called tunneling. However, no classical analog, including classical descriptions of tunneling through barriers, in appropriate for this effect. Quantum mechanical

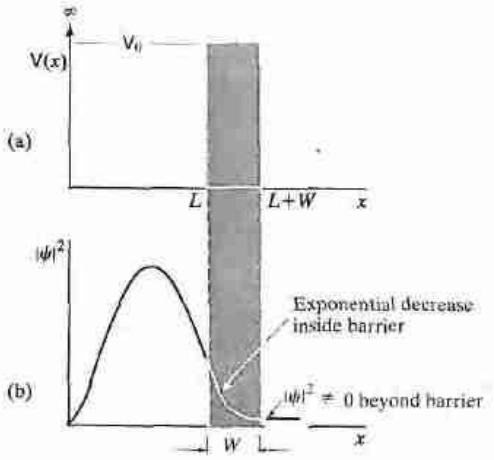

Figure 2-6 Quantum mechanical tunneling: (a) potential barrier of height V_0 and thickness W; (b) probability density for an electron with energy $E < V_0$, indicating a nonzero value of the wave function beyond the barrier.

tunneling is intimately bound to the uncertainty principle. If the barrier is sufficiently thin, we cannot say with certainty that the particle exists only on one side. However, the wave function amplitude for the particle is reduced by the barrier as Fig. 2-6 indicates, so that by making the thickness W greater, we can reduce ψ on the right-hand side to the point that negligible tunneling occurs. Tunneling is important only over very small dimensions, but it can be of great importance in the conduction of electrons in solids, as we shall see in Chapters 5, 6, and 10.

A novel electronic device called the resonant tunneling diode has been developed. This device operates by tunneling electrons through "particle in a potential well" energy levels of the type described in Section 2.4.3.

2.5 ATOMIC STRUCTURE AND THE PERIODIC TABLE

The Schrödinger equation describes accurately the interactions of particles with potential fields, such as electrons within atoms. Indeed, the modern understanding of atomic theory (the modern atomic *models*) comes from the wave equation and from Heisenberg's matrix mechanics. It should be pointed out, however, that the problem of solving the Schrödinger equation directly for complicated atoms is extremely difficult. In fact, only the hydrogen atom is generally solved directly; atoms of atomic number greater than one are usually handled by techniques involving approximations. Many atoms such as the alkali metals (Li, Na, etc.), which have a neutral core with a single electron in an outer orbit, can be treated by a rather simple extension of the hydrogen atom results. The hydrogen atom solution is also important in identifying the basic selection rules for describing allowed electron energy levels. These quantum mechanical results must coincide with the experimental spectra, and we expect the energy levels to include those predicted by the Bohr model. Without actually working through the mathematics for the hydrogen atom, in this section we shall investigate the energy level schemes dictated by the wave equation.

2.5.1 The Hydrogen Atom

Finding the wave functions for the hydrogen atom requires a solution of the Schrödinger equation in three dimensions for a coulombic potential field. Since the problem is spherically symmetric, the spherical coordinate system is used in the calculation (Fig. 2-7). The term $V(x, y, z)$ in Eq. (2-24) must be replaced by $V(r, \theta, \phi)$, representing the Coulomb potential which the electron experiences in the vicinity of the proton. The Coulomb potential varies only with r in spherical coordinates

$$V(r, \theta, \phi) = V(r) = -(4\pi\epsilon_0)^{-1}\frac{q^2}{r} \tag{2-36}$$

as in Eq. (2-14).

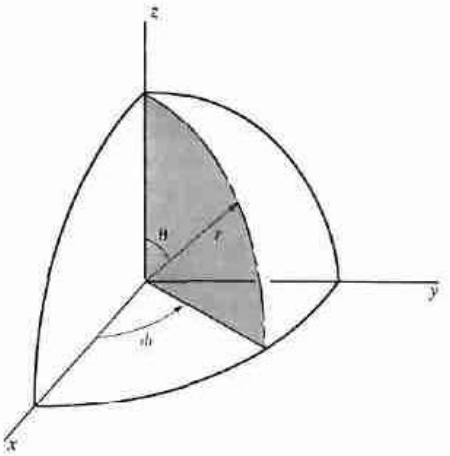

Figure 2–7 The spherical coordinate system.

When the separation of variables is made, the time-independent equation can be written as

$$\psi(r, \theta, \phi) = R(r)\Theta(\theta)\Phi(\phi) \tag{2-37}$$

Thus the wave functions are found in three parts. Separate solutions must be obtained for the r-dependent equation, the θ-dependent equation, and the ϕ-dependent equation. After these three equations are solved, the total wave function ψ is obtained from the product.

As in the simple potential well problem, each of the three hydrogen atom equations gives a solution which is quantized. Thus we would expect a quantum number to be associated with *each* of the three parts of the wave equation. As an illustration, the ϕ-dependent equation obtained after separation of variables is

$$\frac{d^2\Phi}{d\phi^2} + \mathbf{m}^2\Phi = 0 \tag{2-38}$$

where $\mathbf{m}$ is a quantum number. The solution to this equation is

$$\Phi_m(\phi) = Ae^{j\mathbf{m}\phi} \tag{2-39}$$

where A can be evaluated by the normalization condition, as before:

$$\int_0^{2\pi} \Phi_m^*(\phi)\Phi_m(\phi)d\phi = 1 \tag{2-40}$$

$$A^2\int_0^{2\pi} e^{-j\mathbf{m}\phi}e^{j\mathbf{m}\phi}\, d\phi = A^2\int_0^{2\pi} d\phi = 2\pi A^2 \tag{2-41}$$

Thus the value of A is

$$A = \frac{1}{\sqrt{2\pi}} \tag{2-42}$$

and the ϕ-dependent wave function is

$$\Phi_m(\phi) = \frac{1}{\sqrt{2\pi}} e^{jm\phi} \tag{2-43}$$

Since values of ϕ repeat every 2π radians, Φ should repeat also. This occurs if **m** is an integer, including negative integers and zero. Thus the wave functions for the ϕ-dependent equation are quantized with the following selection rule for the quantum numbers:

$$\mathbf{m} = \ldots, -3, -2, -1, 0, +1, +2, +3, \ldots \tag{2-44}$$

By similar treatments, the functions $R(r)$ and $\Theta(\theta)$ can be obtained, each being quantized by its own selection rule. For the r-dependent equation, the quantum number **n** can be any positive integer (not zero), and for the θ-dependent equation the quantum number $\boldsymbol{l}$ can be zero or a positive integer. However, there are interrelationships among the equations which restrict the various quantum numbers used with a single wave function ψ_{nlm}:

$$\psi_{nlm}(r, \theta, \phi) = R_n(r)\Theta_l(\theta)\Phi_m(\phi) \tag{2-45}$$

These restrictions are summarized as follows:

$$\mathbf{n} = 1, 2, 3, \ldots \tag{2-46a}$$

$$\boldsymbol{l} = 0, 1, 2, \ldots, (\mathbf{n} - 1) \tag{2-46b}$$

$$\mathbf{m} = -\boldsymbol{l}, \ldots, -2, -1, 0, +1, +2, \ldots, +\boldsymbol{l} \tag{2-46c}$$

In addition to the three quantum numbers arising from the three parts of the wave equation, there is an important quantization condition on the "spin" of the electron. Investigations of electron spin employ the theory of relativity as well as quantum mechanics; therefore, we shall simply state that the intrinsic angular momentum **s** of an electron with ψ_{nlm} specified is

$$\mathbf{s} = \pm \frac{\hbar}{2} \tag{2-47}$$

That is, in units of $\hbar$, the electron has a spin of $\frac{1}{2}$, and the angular momentum produced by this spin is positive or negative depending on whether the electron is "spin up" or "spin down." The important point for our discussion is that each allowed energy state of the electron in the hydrogen atom is uniquely described by four quantum numbers: **n**, $\boldsymbol{l}$, **m** and **s**.[4]

[4]In many texts, the numbers we have called **m** and **s** are referred to as $\mathbf{m}_l$ and $\mathbf{m}_s$, respectively.

Using these four quantum numbers, we can identify the various states which the electron can occupy in a hydrogen atom. The number **n**, called the *principal* quantum number, specifies the "orbit" of the electron in Bohr terminology. Of course, the concept of orbit is replaced by probability density functions in quantum mechanical calculations. It is common to refer to states with a given principal quantum number as belonging to a *shell* rather than an orbit.

There is considerable fine structure in the energy levels about the Bohr orbits, due to the dictates of the other three quantum conditions. For example, an electron with $\mathbf{n} = 1$ (the first Bohr orbit) can have only $\boldsymbol{l} = 0$ and $\mathbf{m} = 0$ according to Eq. (2-46), but there are two spin states allowed from Eq. (2-47). For $\mathbf{n} = 2$, $\boldsymbol{l}$ can be 0 or 1, and **m** can be -1, 0, or $+1$. The various allowed combinations of quantum numbers appear in the first four columns of Table 2-1. From these combinations it is apparent that the electron in a hydrogen atom can occupy any one of a large number of excited states in addition to the lowest (*ground*) state ψ_{100}. Energy differences between the various states properly account for the observed lines in the hydrogen spectrum.

2.5.2 The Periodic Table

The quantum numbers discussed in Section 2.5.1 arise from the solutions to the hydrogen atom problem. Thus the energies obtainable from the wave functions are unique to the hydrogen atom and cannot be extended to more complicated atoms without appropriate alterations. However, the quantum number selection rules are valid for more complicated structures, and we can use these rules to gain an understanding of the arrangement of atoms in the periodic table of chemical elements. Without these selection rules, it is difficult to understand why only two electrons fit into the first Bohr orbit of an atom, whereas eight electrons are allowed in the second orbit. After even the brief discussion of quantum numbers given above, we should be able to answer these questions with more insight.

Before discussing the periodic table, we must be aware of an important principle of quantum theory, the *Pauli exclusion principle*. This rule states that no two electrons in an interacting system[5] can have the same set of quantum numbers **n**, $\boldsymbol{l}$, **m**, **s**. In other words, only two electrons can have the same three quantum numbers **n**, $\boldsymbol{l}$, **m**, and those two must have opposite spin. The importance of this principle cannot be overemphasized; it is basic to the electronic structure of all atoms in the periodic table. One implication of this principle is that by listing the various combinations of quantum numbers, we can determine into which shell each electron of a complicated atom fits, and how many electrons are allowed per shell. The quantum states summarized in Table 2-1 can be

[5]An interacting system is a system in which electron wave functions overlap—in this case, an atom with two or more electrons.

Table 2–1 Quantum numbers to **n** = 3 and allowable states for the electron in a hydrogen atom: The first four columns show the various combinations of quantum numbers allowed by the selection rules of Eq (2–46); the last two columns indicate the number of allowed states (combinations of **n**, ***l***, **m**, and **s**) for each ***l*** (subshell) and **n** (shell, or Bohr orbit).

n	l	m	s/ħ	Allowable states in subshell	Allowable states in complete shell
1	0	0	$\pm\frac{1}{2}$	2	2
2	0	0	$\pm\frac{1}{2}$	2	8
	1	−1	$\pm\frac{1}{2}$	6	
		0	$\pm\frac{1}{2}$		
		1	$\pm\frac{1}{2}$		
3	0	0	$\pm\frac{1}{2}$	2	18
	1	−1	$\pm\frac{1}{2}$	6	
		0	$\pm\frac{1}{2}$		
		1	$\pm\frac{1}{2}$		
	2	−2	$\pm\frac{1}{2}$	10	
		−1	$\pm\frac{1}{2}$		
		0	$\pm\frac{1}{2}$		
		1	$\pm\frac{1}{2}$		
		2	$\pm\frac{1}{2}$		

used to indicate the electronic configurations for atoms in the lowest energy state.

In the first electronic shell (**n** = 1), ***l*** can be only zero since the maximum value of ***l*** is always **n** − 1. Similarly, **m** can be only zero since **m** runs from the negative value of ***l*** to the positive value of ***l***. Two electrons with opposite spin can fit in this ψ_{100} state; therefore, the first shell can have at most two electrons. For the helium atom (atomic number $Z = 2$) in the ground state, both electrons will be in the first Bohr orbit (**n** = 1), both will have ***l*** = 0 and **m** = 0, and they will have opposite spin. Of course, one or both of the He atom electrons can be excited to one of the higher energy states of Table 2-1 and subsequently relax to the ground state, giving off a photon characteristic of the He spectrum.

As Table 2-1 indicates, there can be two electrons in the ***l*** = 0 subshell, six electrons when ***l*** = 1, and ten electrons for ***l*** = 2. The electronic configurations of various atoms in the periodic table can be deduced from this list of allowed states. The ground state electron structures for a number of atoms are listed in Table 2-2. There is a simple shorthand notation for

Table 2–2 Electronic configurations for atoms in the ground state.

Atomic number (Z)	Element	n = 1, l = 0	2: 0	2: 1	3: 0	3: 1	3: 2	4: 0	4: 1	Shorthand notation
		1s	2s	2p	3s	3p	3d	4s	4p	
		Number of electrons								
1	H	1								$1s^1$
2	He	2								$1s^2$
3	Li		1							$1s^2\ 2s^1$
4	Be		2							$1s^2\ 2s^2$
5	B		2	1						$1s^2\ 2s^2\ 2p^1$
6	C	helium core,	2	2						$1s^2\ 2s^2\ 2p^2$
7	N	2 electrons	2	3						$1s^2\ 2s^2\ 2p^3$
8	O		2	4						$1s^2\ 2s^2\ 2p^4$
9	F		2	5						$1s^2\ 2s^2\ 2p^5$
10	Ne		2	6						$1s^2\ 2s^2\ 2p^6$
11	Na				1					[Ne] $3s^1$
12	Mg				2					$3s^2$
13	Al				2	1				$3s^2\ 3p^1$
14	Si	neon core,			2	2				$3s^2\ 3p^2$
15	P	10 electrons			2	3				$3s^2\ 3p^3$
16	S				2	4				$3s^2\ 3p^4$
17	Cl				2	5				$3s^2\ 3p^5$
18	Ar				2	6				$3s^2\ 3p^6$
19	K							1		[Ar] $4s^1$
20	Ca							2		$4s^2$
21	Sc						1	2		$3d^1\ 4s^2$
22	Ti						2	2		$3d^2\ 4s^2$
23	V						3	2		$3d^3\ 4s^2$
24	Cr						5	1		$3d^5\ 4s^1$
25	Mn						5	2		$3d^5\ 4s^2$
26	Fe						6	2		$3d^6\ 4s^2$
27	Co	argon core,					7	2		$3d^7\ 4s^2$
28	Ni	18 electrons					8	2		$3d^8\ 4s^2$
29	Cu						10	1		$3d^{10}\ 4s^1$
30	Zn						10	2		$3d^{10}\ 4s^2$
31	Ga						10	2	1	$3d^{10}\ 4s^2\ 4p^1$
32	Ge						10	2	2	$3d^{10}\ 4s^2\ 4p^2$
33	As						10	2	3	$3d^{10}\ 4s^2\ 4p^3$
34	Se						10	2	4	$3d^{10}\ 4s^2\ 4p^4$
35	Br						10	2	5	$3d^{10}\ 4s^2\ 4p^5$
36	Kr						10	2	6	$3d^{10}\ 4s^2\ 4p^6$

electronic structures which is commonly used instead of such a table. The only new convention to remember in this notation is the naming of the l values:

$$l = 0, 1, 2, 3, 4, \ldots$$
$$s, p, d, f, g, \ldots$$

This convention was created by early spectroscopists who referred to the first four spectral groups as *s*harp, *p*rincipal, *d*iffuse, and *f*undamental. Alphabetical order is used beyond *f*. With this convention for l, we can write an electron state as follows:

$$(\mathbf{n} = 3)\ 3p^6\ (l = 1)$$

6 electrons in the $3p$ subshell

For example, the total electronic configuration for Si ($Z = 14$) in the ground state is

$$1s^2 2s^2 2p^6 3s^2 3p^2$$

We notice that Si has a closed Ne configuration (see Table 2-2) plus four electrons in an outer $\mathbf{n} = 3$ orbit ($3s^2 3p^2$). These are the four valence electrons of Si; two valence electrons are in an s state and two are in a p state. The Si electronic configuration can be written [Ne] $3s^2 3p^2$ for convenience, since the Ne configuration $1s^2 2s^2 2p^6$ forms a closed shell (typical of the inert elements).

Figure 2-8a shows the orbital model of a Si atom, which has a nucleus consisting of 14 protons (with a charge of +14) and neutrons, 10 core electrons in shells $n = 1$ and 2, and 4 valence electrons in the $3s$ and $3p$ subshells. Figure 2-8b shows the energy levels of the various electrons in the coulombic potential well of the nucleus. Since unlike charges attract each other, there is an attractive potential between the negatively charged electrons and the positively charged nucleus. As indicated in Eq. (2-36), a Coulomb potential varies as $1/r$ as a function of distance from the charge, in this case the Si nucleus. The potential energy gradually goes to zero when we approach infinity. We end up getting "particle-in-a-box" states for these electrons in this potential well, as discussed in Section 2.4.3 and Eq. (2-33). Of course, in this case the shape of the potential well is not rectangular, as shown in Fig. 2-5a, but coulombic, as shown in Fig. 2-8b. Therefore, the energy levels have a form closer to those of the H atom as shown in Eq. (2-15), rather than in Eq. (2-33).

If we solve the Schrödinger equation for the Si atom as we did in Section 2.5.1 for the H atom, we can get the radial and angular dependence of the wavefunctions or "orbitals" of the electrons. Let us focus on the valence shell, $\mathbf{n} = 3$, where we have two $3s$ and two $3p$ electrons. It turns out that the $3s$ orbital is spherically symmetric with no angular dependence, and is positive everywhere. It can hold 2 electrons with opposite spin according to the Pauli

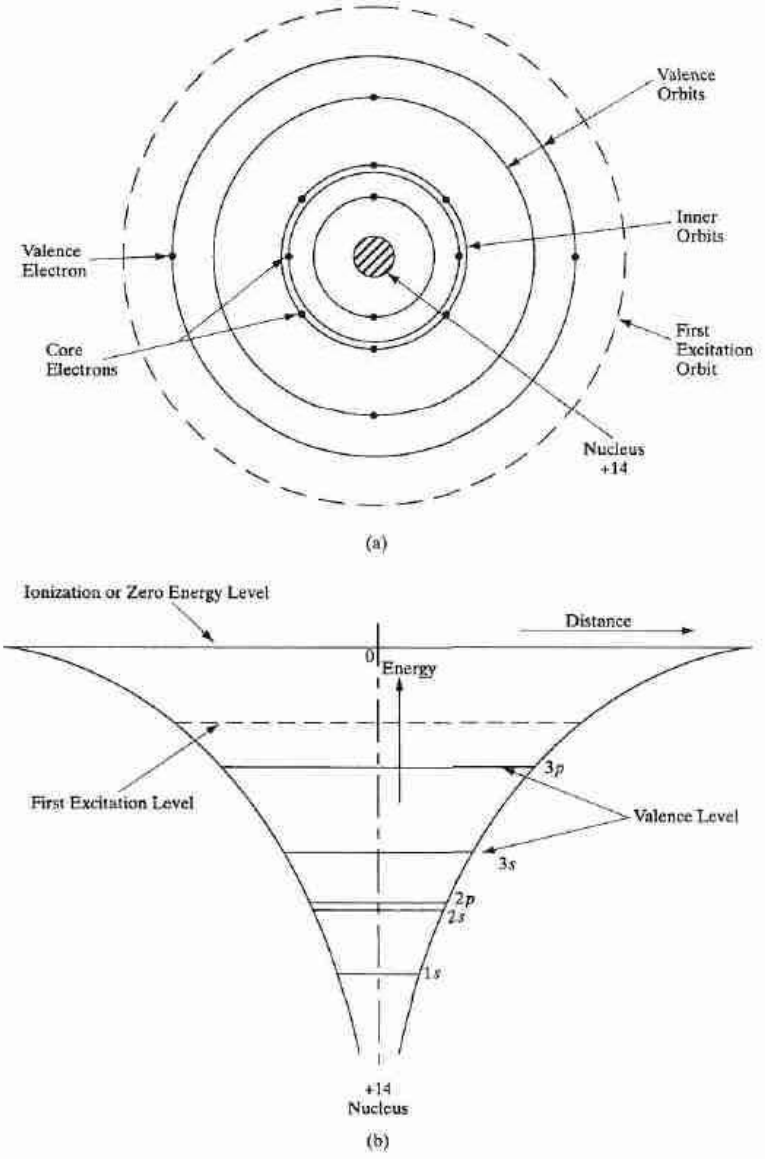

Figure 2–8
Electronic structure and energy levels in a Si atom: (a) The orbital model of a Si atom showing the 10 core electrons (n = 1 and 2), and the 4 valence electrons (n = 3); (b) energy levels in the coulombic potential of the nucleus are also shown schematically.

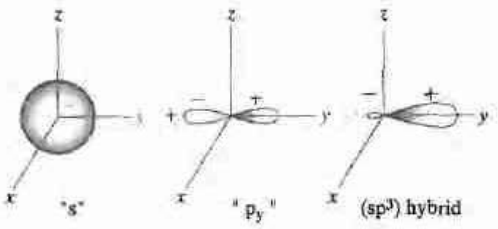

Figure 2–9 Orbitals in a Si atom: The spherically symmetric "*s*" type wave functions or orbitals are positive everywhere, while the three mutually perpendicular "p" type orbitals (p_x, p_y, p_z) are dumbbell shaped and have a positive lobe and a negative lobe. The four sp^3 "hybridized" orbitals, only one of which is shown here, point symmetrically in space and lead to the diamond lattice in Si.

principle. There are $3p$-orbitals which are mutually perpendicular. These are shaped like dumbbells with a positive lobe and a negative lobe (Fig. 2–9). The $3p$ subshell can hold up to 6 electrons, but in the case of Si has only 2. Interestingly, in a Si crystal when we bring individual atoms very close together, the s- and p-orbitals overlap so much that they lose their distinct character, and lead to four mixed sp^3 orbitals. The negative part of the p orbital cancels the s-type wavefunction, while the positive part enhances it, thereby leading to a "directed" bond in space. As shown in Fig. 2–9, these *linear combinations of atomic orbitals (LCAO)* or "hybridized" sp^3 orbitals point symmetrically in space along the 4 tetragonal directions (see Fig. 1–9). In Chapter 3 we shall see that these "directed" chemical bonds are responsible for the tetragonal diamond or zinc blende lattice structure in most semiconductors. They are also very important in the understanding of energy bands, and in the conduction of charges in these semiconductors.

The column IV semiconductor Ge ($Z = 32$) has an electronic structure similar to Si, except that the four valence electrons are outside a closed $\mathbf{n} = 3$ shell. Thus the Ge configuration is [Ar] $3d^{10}4s^24p^2$. There are several cases in Table 2–2 that do not follow the most straightforward choice of quantum numbers. For example, we notice that in K ($Z = 19$) and Ca ($Z = 20$) the $4s$ state is filled before the $3d$ state; in Cr ($Z = 24$) and Cu ($Z = 29$) there is a transfer of an electron back to the $3d$ state. These exceptions, required by minimum energy considerations, are discussed more fully in most atomic physics texts.

SUMMARY

2.1 In *classical* physics, *matter* (including electrons) was described as *particles* by Newtonian mechanics, while *light* was described as *waves*, consistent with phenomena such as interference and diffraction of light.

2.2 Phenomena such as blackbody radiation and the photoelectric effect forced Planck and Einstein to introduce a *particle* aspect to light (photons). Analysis of atomic spectra then led Bohr and de Broglie to analogously introduce a *wave aspect* to *subatomic particles* such as electrons. This led to a *wave-particle duality* and a *quantum mechanical* description of nature by Heisenberg and Schrödinger.

2.3 To understand how electrons move in semiconductor devices or interact w light, we need to determine a *complex wave function* of the electron. The wa function has to be mathematically well behaved, consistent with the interpre tation that the *wave function magnitude squared is the probability density* o finding the electron in space and time.

2.4 We get the wave function by solving Schrödinger's time-dependent partial differential equation. The application of *boundary conditions* (the potential energy profile) allows certain (proper) *eigenfunctions* as valid solutions, with corresponding *eigenenergies*, determined by *allowed quantum numbers*. Results of physical measurements are *no longer deterministic* (as in classical mechanics), but *probabilistic*, with an *expectation* value given by an average using the wave function of appropriate quantum mechanical *operators* corresponding to physical quantities.

2.5 Application of these principles to the simplest atom (H) introduces four quantum numbers—**n**, **l**, **m**, and **s**, which are subject to appropriate quantum mechanical rules. Extrapolating these ideas to more complicated atoms such as Si leads to the idea of electronic structure and the *periodic table*, if we apply the *Pauli exclusion principle* that one can have a maximum of one electron for one set of these quantum numbers.

PROBLEMS

2.1 (a) Sketch a simple vacuum tube device and the associated circuitry for measuring E_m in the photoelectric effect experiment. The electrodes can be placed in a sealed glass envelope.

(b) Sketch the photocurrent I vs. retarding voltage V that you would expect to measure for a given electrode material and configuration. Make the sketch for several intensities of light at a given wavelength.

(c) The work function of platinum is 4.09 eV. What retarding potential will be required to reduce the photocurrent to zero in a photoelectric experiment with Pt electrodes if the wavelength of incident light is 2440 Å? Remember that an energy of $q\Phi$ is lost by each electron in escaping the surface.

2.2 Show that the third Bohr postulate, Eq. (2–5), is equivalent to an integer number of de Broglie waves fitting within the circumference of a Bohr circular orbit.

2.3 (a) Show that the various lines in the hydrogen spectrum can be expressed in angstroms as

$$\lambda(\text{Å}) = \frac{911\mathbf{n}_1^2\mathbf{n}^2}{\mathbf{n}^2 - \mathbf{n}_1^2}$$

where $\mathbf{n}_1 = 1$ for the Lyman series, 2 for the Balmer series, and 3 for the Paschen series. The integer $\mathbf{n}$ is larger than $\mathbf{n}_1$.

(b) Calculate λ for the Lyman series to $\mathbf{n} = 5$, the Balmer series to $\mathbf{n} = 7$, and the Paschen series to $\mathbf{n} = 10$. Plot the results as in Fig. 2–2. What are the wavelength limits for each of the three series?

2.4 Show that the calculated Bohr expression for frequency of emitted light in the hydrogen spectrum, Eq. (2-17), corresponds to the experimental expressions, Eq. (2-3).

2.5 (a) The position of an electron is determined to within 1 Å. What is the minimum uncertainty in its momentum?

(b) An electron's energy is measured with an uncertainty of 1 eV. What is the minimum uncertainty in the time over which the measurement was made?

2.6 What is the de Broglie wavelength (in Å) of an electron at 100 eV? What is the wavelength for electrons at 12 keV, which is typical of electron microscopes? Comparing this to visible light, comment on the advantages of electron microscopes.

2.7 A sample of radioactive material undergoes decay such that the number of atoms $N(t)$ remaining in the unstable state at time t is related to the number N_0 at $t = 0$ by the relation $N(t) = N_0 \exp(-t/\tau)$. Show that τ is the average lifetime $\langle t \rangle$ of an atom in the unstable state before it spontaneously decays. Equation (2-21b) can be used with t substituted for x.

2.8 We define a potential well having energies V as a function of position x, as follows: $V = \infty$ for $x = -0.5$ nm to 0; $V = 0$ eV for $x = 0$ to 5 nm; $V = 10$ eV for $x = 5$ to 6 nm, and $V = 0$ for $x > 6$ nm and $x < -0.5$ nm. We put an electron with energy 7 eV in the region x, between 0 and 5 nm. What is the probability of finding the electron at $x < 0$ nm? Is the probability of finding the electron at $x > 6$ nm zero or nonzero? What is this probability for $x > 6$ nm if the electron was described by classical mechanics and not quantum mechanics?

2.9 An electron is described by a plane-wave wave function $\psi(x,t) = Ae^{i(10x+3y-4t)}$. Calculate the expectation value of a function defined as $[4p_x^2 + 2p_z^3 + 7E/m]$, where m is the mass of the electron, p_x and p_z are the x and z components of momentum, and E is energy. (Give values in terms of the Planck constant.)

2.10 A particle is trapped in the ground state (lowest energy level) of a potential well of width L. To understand how the particle is localized, a common measure is the standard deviation Δx defined by $\Delta x = \sqrt{\langle x^2 \rangle - \langle x \rangle^2}$, where $\langle x^2 \rangle$ and $\langle x \rangle$ are the expectation values of x^2 and x, respectively. Find the uncertainty Δx in the position of the particle in terms of length L and estimate the minimum uncertainty in the momentum of the particle, using the Heisenberg uncertainty principle in terms of L and the Planck's constant h. *Note*: $\frac{2}{L}\int_0^L x\left(\sin\frac{\pi x}{L}\right)^2 dx = 0.5L$ and $\frac{2}{L}\int_0^L x^2\left(\sin\frac{\pi x}{L}\right)^2 dx = 0.28L$.

2.11 Calculate the first three energy levels for an electron in a quantum well of width 10 Å with infinite walls.

2.12 Schematically show the number of electrons in the various subshells of an atom with the electronic shell structure $1s^2 2s^2 2p^4$ and an atomic weight of 21. Indicate how many protons and neutrons there are in the nucleus. Is this atom chemically reactive, and why?

READING LIST

Ashcroft, N. W., and N. D. Mermin. *Solid State Physics.* Philadelphia: W.B. Saunders, 1976.

Capasso, F., and S. Datta. "Quantum Electron Devices." *Physics Today* 43 (February 1990): 74–82.

Cassidy, D. C. "Heisenberg: Uncertainty and the Quantum Revolution." *Scientific American* 266 (May 1992): 106–12.

Chang, L. L., and L. Esaki. "Semiconductor Quantum Heterostructures." *Physics Today* 45 (October 1992): 36–43.

Cohen-Tannoudji, C., B. Diu, and F. Laloe. *Quantum Mechanics.* New York: Wiley, 1977.

Datta, S. *Modular Series on Solid State Devices: Vol. 8. Quantum Phenomena.* Reading, MA: Addison-Wesley, 1989.

Feynman, R. P. *The Feynman Lectures on Physics, Vol. 3. Quantum Mechanics.* Reading, MA: Addison-Wesley, 1965.

Kroemer, H. *Quantum Mechanics.* Englewood Cliffs, NJ: Prentice Hall, 1994.

Singh, J. *Semiconductor Devices.* New York: McGraw-Hill, 1994.

SELF QUIZ

Question 1

Decide whether *each* of the following one-dimensional functions defined between the limits x approaches negative infinity and x approaches positive infinity is an allowed quantum mechanical wave function (circle one answer in each case):

1. $\Psi(x) = C$ for $-|a| < x < |a|$; $\Psi(x) = 0$ otherwise — **allowed / not allowed**
2. $\Psi(x) = C(e^{x/a} + e^{-x/a})$ — **allowed / not allowed**
3. $\Psi(x) = C\exp(-x^2/|a|)$ — **allowed / not allowed**

where both C and a are nonzero and finite constants.

Question 2

Consider the finite potential well sketched below.

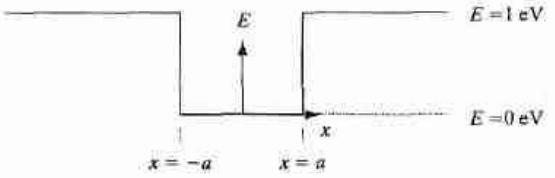

1. Can the measured value of a particle's energy in the well be 0 eV?
2. If the particle has an energy of $E < 1$ eV, can the measured value of the particle's position be $|x| > a$?

Question 3

(a) For a particle in the following potential well of minimum potential energy equal to 0 eV, could the ground state eigenenergy E_1 of the particle be equal to zero? Circle one choice below.

yes / no / not enough information provided

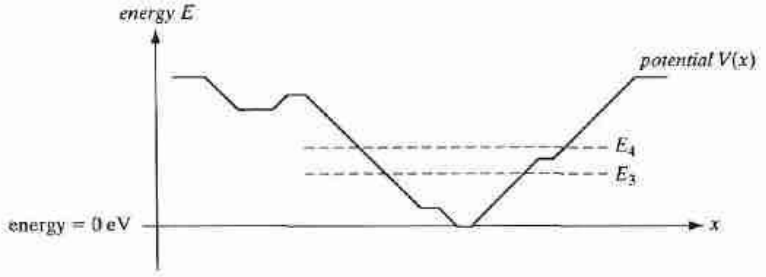

(b) Given the 3rd and 4th most energetic eigenstates of energies as shown above, is it possible under any circumstances that the expectation value of the particle's energy could be exactly $0.5(E_3 + E_4)$? (Do not assume the particle is in an energy eigenstate.) Circle one choice below.

yes / no / not enough information provided

(c) Consider the following *continuous*, *smooth*, and *normalizable* wavefunction $\Psi(x)$. Is this wave function an allowed quantum mechanical wave function for a particle (currently) above the potential $V(x)$ of part (a)? (Circle one.)

yes / no / can't tell

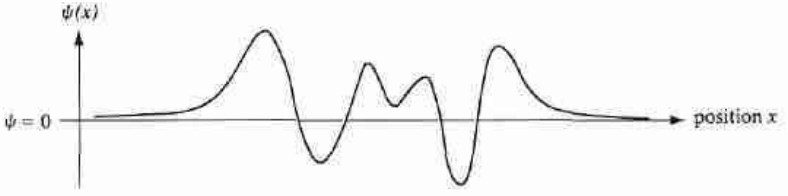

Question 4

Consider quantum mechanical particles incident from the left having well-defined energy as indicated by the vertical positions of the arrows, in the two systems shown below. Will the probability of being reflected be greater for the incident particle in System 1 than for the incident particle in System 2? Circle one choice below.

yes / no / not enough information provided

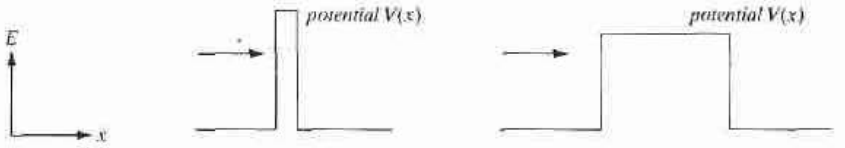

System 1
(narrow high potential barrier)

System 2
(wide low potential barrier)

Question 5

Suppose five precise measurements were made on a particle in rapid succession, such that the time evolution of the particle wave function *between* measurements could be neglected, in the following order: (1) position, (2) momentum, (3) momentum, (4) position, (5) momentum. If the results of the first two measurements were x_o and p_o, respectively, what would be the results of the next three measurements (circle one each)?

measurement (3): momentum	p_o **/ unknown**
measurement (4): position	x_o **/ unknown**
measurement (5): momentum	p_o **/ unknown**

Question 6

If the photoelectric effect were governed by classical physics rather than quantum mechanics, what would be result of the following experiments:

(a) By changing the intensity of the incident radiation, what would happen to the energy and number of ejected electrons?

(b) How about changing the frequency of the light?

Chapter 3

Energy Bands and Charge Carriers in Semiconductors

OBJECTIVES

1. Understand conduction and valence energy bands, and how bandgaps are formed
2. Appreciate the idea of doping in semiconductors
3. Use the density of states and Fermi Dirac statistics to calculate carrier concentrations
4. Calculate drift currents in an electric field in terms of carrier mobility, and how mobility is affected by scattering
5. Discuss the idea of "effective" masses

In this chapter we begin to discuss the specific mechanisms by which current flows in a solid. In examining these mechanisms we shall learn why some materials are good conductors of electric current, whereas others are poor conductors. We shall see how the conductivity of a semiconductor can be varied by changing the temperature or the number of impurities. These fundamental concepts of charge transport form the basis for later discussions of solid state device behavior.

3.1 BONDING FORCES AND ENERGY BANDS IN SOLIDS

In Chapter 2 we found that electrons are restricted to sets of discrete energy levels within atoms. Large gaps exist in the energy scale in which no energy states are available. In a similar fashion, electrons in solids are restricted to certain energies and are not allowed at other energies. The basic difference between the case of an electron in a solid and that of an electron in an isolated atom is that in the solid the electron has a *range*, or *band*, of available energies. The discrete energy levels of the isolated atom spread into bands of energies in the solid because in the solid the wave functions of electrons in neighboring atoms overlap, and an electron is not necessarily localized at a particular atom. Thus, for example, an electron in the outer orbit of one atom feels the influence of neighboring atoms, and its overall wave function is altered. Naturally, this influence affects the potential energy term and the boundary conditions in the Schrödinger equation, and we would

Petitioner Canadian Solar (USA) Inc., Ex. 1030, p. 61

expect to obtain different energies in the solution. Usually, the influence of neighboring atoms on the energy levels of a particular atom can be treated as a small perturbation, giving rise to shifting and splitting of energy states into energy bands.

3.1.1 Bonding Forces in Solids

The interaction of electrons in neighboring atoms of a solid serves the very important function of holding the crystal together. For example, alkali halides such as NaCl are typified by *ionic bonding*. In the NaCl lattice, each Na atom

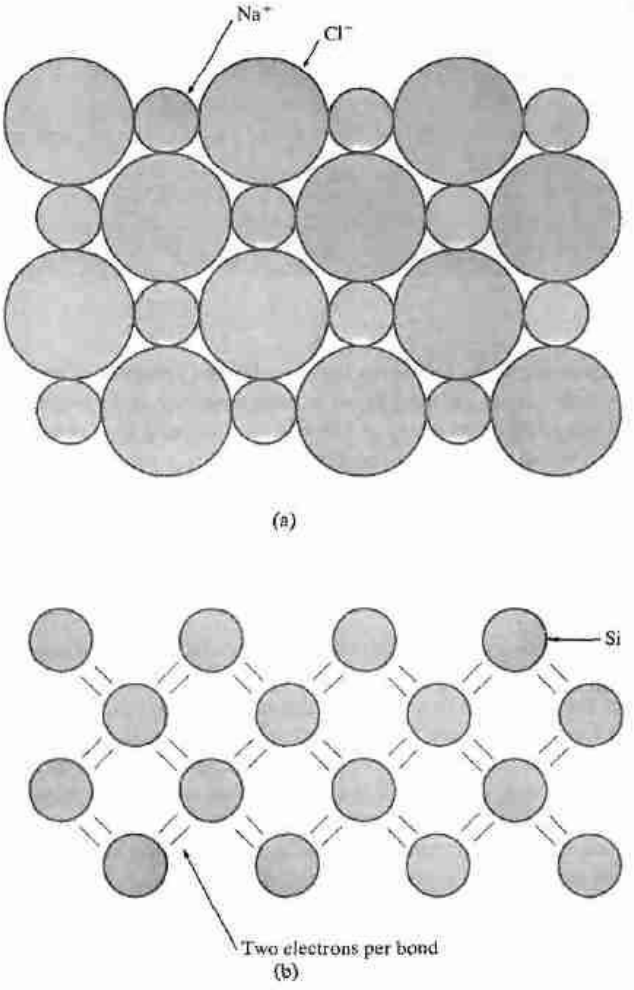

Figure 3–1 Different types of chemical bonding in solids: (a) an example of ionic bonding in NaCl; (b) covalent bonding in the Si crystal, viewed along a <100> direction (see also Figs. 1–8 and 1–9).

is surrounded by six nearest neighbor Cl atoms, and vice versa. Four of the nearest neighbors are evident in the two-dimensional representation shown in Fig. 3-1a. The electronic structure of Na ($Z = 11$) is [Ne] $3s^1$, and Cl ($Z = 17$) has the structure [Ne]$3s^2 3p^5$. In the lattice each Na atom gives up its outer $3s$ electron to a Cl atom, so that the crystal is made up of ions with the electronic structures of the inert atoms Ne and Ar (Ar has the electronic structure [Ne]$3s^2 3p^6$). However, the ions have net electric charges after the electron exchange. The Na^+ ion has a net positive charge, having lost an electron, and the Cl^- ion has a net negative charge, having gained an electron.

Each Na^+ ion exerts an electrostatic attractive force upon its six Cl^- neighbors, and vice versa. These coulombic forces pull the lattice together until a balance is reached with repulsive forces. A reasonably accurate calculation of the atomic spacing can be made by considering the ions as hard spheres being attracted together (Example 1-1).

An important observation in the NaCl structure is that all electrons are tightly bound to atoms. Once the electron exchanges have been made between the Na and Cl atoms to form the Na^+ and Cl^- ions, the outer orbits of all atoms are completely filled. Since the ions have the closed-shell configurations of the inert atoms Ne and Ar, there are no loosely bound electrons to participate in current flow; as a result, NaCl is a good insulator.

In a metal atom the outer electronic shell is only partially filled, usually by no more than three electrons. We have already noted that the alkali metals (e.g., Na) have only one electron in the outer orbit. This electron is loosely bound and is given up easily in ion formation. This accounts for the great chemical activity in the alkali metals, as well as for their high electrical conductivity. In the metal the outer electron of each alkali atom is contributed to the crystal as a whole, so that the solid is made up of ions with closed shells immersed in a sea of free electrons. The forces holding the lattice together arise from an interaction between the positive ion cores and the surrounding free electrons. This is one type of *metallic bonding*. Obviously, there are complicated differences in the bonding forces for various metals, as evidenced by the wide range of melting temperatures (234 K for Hg, 3643 K for W). However, the metals have the sea of electrons in common, and these electrons are free to move about the crystal under the influence of an electric field.

A third type of bonding is exhibited by the diamond lattice semiconductors. We recall that each atom in the Ge, Si, or C diamond lattice is surrounded by four nearest neighbors, each with four electrons in the outer orbit. In these crystals each atom shares its valence electrons with its four neighbors (Fig. 3-1b). Bonding between nearest neighbor atoms is illustrated in the diamond lattice diagram of Fig. 1-9. The bonding forces arise from a quantum mechanical interaction between the shared electrons. This is known as *covalent bonding;* each electron pair constitutes a covalent bond. In the sharing process it is no longer relevant to ask which electron belongs to a particular atom—both belong to the bond. The two electrons are indistinguishable, except that they must have opposite spin to satisfy the Pauli exclusion principle. Covalent bonding is also found in certain molecules, such as H_2.

As in the case of the ionic crystals, no free electrons are available to the lattice in the covalent diamond structure of Fig. 3-1b. By this reasoning Ge and Si should also be insulators. However, we have pictured an idealized lattice at 0 K in this figure. As we shall see in subsequent sections, an electron can be thermally or optically excited out of a covalent bond and thereby become free to participate in conduction. This is an important feature of semiconductors.

Compound semiconductors such as GaAs have mixed bonding, in which both ionic and covalent bonding forces participate. Some ionic bonding is to be expected in a crystal such as GaAs because of the difference in placement of the Ga and As atoms in the periodic table. The ionic character of the bonding becomes more important as the atoms of the compound become further separated in the periodic table, as in the II–VI compounds. Such electronic structure, and specifically the idea that the outermost valence shell is *complete* if it has a stable set of eight electrons (Ne, Ar, Kr), is the basis of most of chemistry and many of the semiconducting properties.

3.1.2 Energy Bands

As isolated atoms are brought together to form a solid, various interactions occur between neighboring atoms, including those described in the preceding section. The forces of attraction and repulsion between atoms will find a balance at the proper interatomic spacing for the crystal. In the process, important changes occur in the electron energy level configurations, and these changes result in the varied electrical properties of solids.

In Fig. 2-8, we showed the orbital model of a Si atom, along with the energy levels of the various electrons in the coulombic potential well of the nucleus. Let us focus on the outermost shell or valence shell, $\mathbf{n} = 3$, where two $3s$ and two $3p$ electrons interact to form the four "hybridized" sp^3 electrons when the atoms are brought close together. In Fig. 3-2, we schematically show the coulombic potential wells of two atoms close to each other, along with the wave functions of two electrons centered on the two nuclei. By solving the Schrödinger equation for such an interacting system, we find that the composite two-electron wave functions are *linear combinations* of the individual *atomic orbitals* (LCAO). The odd or antisymmetric combination is called the antibonding orbital, while the even or symmetric combination is the bonding orbital. It can be seen that the bonding orbital has a higher value of the wave function (and therefore the electron probability density) than the antibonding state in the region between the two nuclei. This corresponds to the covalent bond between the atoms.

To determine the energy levels of the bonding and the antibonding states, it is important to recognize that in the region between the two nuclei the coulombic potential energy $V(r)$ is lowered (solid line in Fig. 3-2) compared to isolated atoms (dashed lines). It is easy to see why the potential energy would be lowered in this region, because an electron here would be attracted by two nuclei, rather than just one. For the bonding state the electron

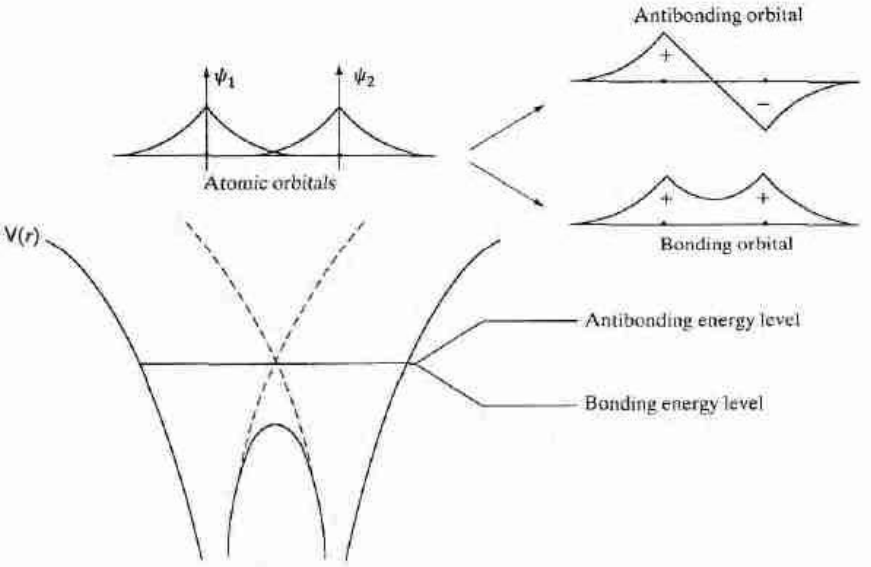

Figure 3–2
Linear combinations of atomic orbitals (LCAO): The LCAO when 2 atoms are brought together leads to 2 distinct "normal" modes—a higher energy antibonding orbital, and a lower energy bonding orbital. Note that the electron probability density is high in the region between the ion cores (covalent "bond"), leading to lowering of the bonding energy level and the cohesion of the crystal. If instead of 2 atoms, one brings together N atoms, there will be N distinct LCAO, and N closely spaced energy levels in a band.

probability density is higher in this region of lowered potential energy than for the antibonding state. As a result, the original isolated atomic energy level would be split into two, a lower bonding energy level and a higher antibonding level. It is the lowering of the energy of the bonding state that gives rise to cohesion of the crystal. For even smaller interatomic spacings, the energy of the crystal goes up because of repulsion between the nuclei, and other electronic interactions. Since the probability density is given by the square of the wave function, if the entire wave function is multiplied by -1, it does not lead to a different LCAO. The important point to note in this discussion is that the number of distinct LCAO, and the number of distinct energy levels, depends on the number of atoms that are brought together. The lowest energy level corresponds to the totally symmetric LCAO, the highest corresponds to the totally antisymmetric case, and the other combinations lead to energy levels in between.

Qualitatively, we can see that as atoms are brought together, the application of the Pauli exclusion principle becomes important. When two atoms are completely isolated from each other so that there is no interaction of electron wave functions between them, they can have identical electronic

structures. As the spacing between the two atoms becomes smaller, however, electron wave functions begin to overlap. The exclusion principle dictates that no two electrons in a given interacting system may have the same quantum state; thus there must be at most one electron per level after there is a splitting of the discrete energy levels of the isolated atoms into new levels belonging to the pair rather than to individual atoms.

In a solid, many atoms are brought together, so that the split energy levels form essentially continuous *bands* of energies. As an example, Fig. 3-3 illustrates the imaginary formation of a silicon crystal from isolated silicon atoms. Each isolated silicon atom has an electronic structure $1s^2 2s^2 2p^6 3s^2 3p^2$ in the ground state. Each atom has available two $1s$ states, two $2s$ states, six $2p$ states, two $3s$ states, six $3p$ states, and higher states (see Tables 2-1 and 2-2). If we consider N atoms, there will be $2N$, $2N$, $6N$, $2N$, and $6N$ states of type $1s$, $2s$, $2p$, $3s$, and $3p$, respectively. As the interatomic spacing decreases, these energy levels split into bands, beginning with the outer (**n** = 3) shell. As the "$3s$" and "$3p$" bands grow, they merge into a single band composed of a mixture of energy levels. This band of "$3s$-$3p$" levels contains $8N$ available states. As the

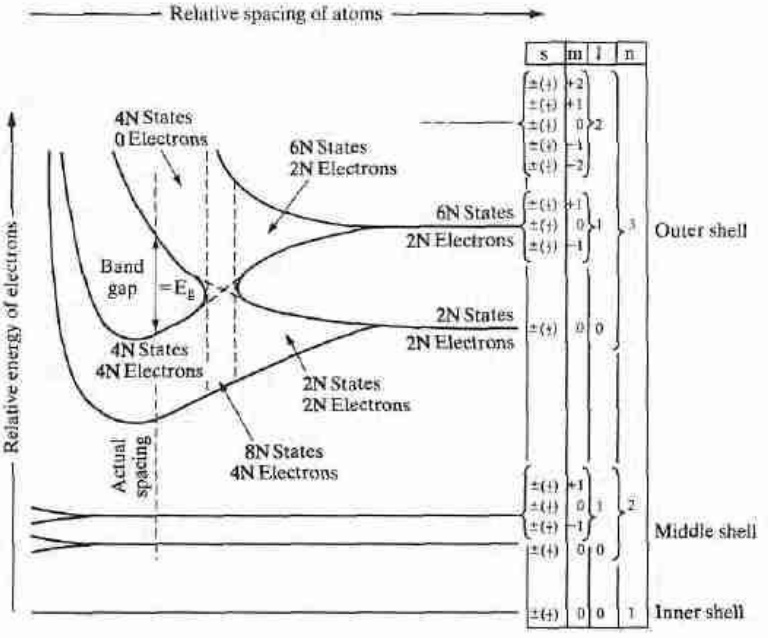

Figure 3-3
Energy levels in Si as a function of interatomic spacing. The core levels (**n** = 1,2) in Si are completely filled with electrons. At the actual atomic spacing of the crystal, the $2N$ electrons in the $3s$ subshell and the $2N$ electrons in the $3p$ subshell undergo sp^3 hybridization, and all end up in the lower $4N$ states (valence band), while the higher-lying $4N$ states (conduction band) are empty, separated by a band gap.

distance between atoms approaches the equilibrium interatomic spacing of silicon, this band splits into two bands separated by an *energy gap* E_g. The upper band (called the *conduction band*) contains $4N$ states, as does the lower (*valence*) band. Thus, apart from the low-lying and tightly bound "core" levels, the silicon crystal has two bands of available energy levels separated by an energy gap E_g wide, which contains no allowed energy levels for electrons to occupy. This gap is sometimes called a "forbidden band," since in a perfect crystal it contains no electron energy states.

We should pause at this point and count electrons. The lower "1*s*" band is filled with the $2N$ electrons which originally resided in the collective 1*s* states of the isolated atoms. Similarly, the 2*s* band and the 2*p* bands will have $2N$ and $6N$ electrons in them, respectively. However, there were $4N$ electrons in the original isolated $\mathbf{n} = 3$ shells ($2N$ in 3*s* states and $2N$ in 3*p* states). These $4N$ electrons must occupy states in the valence band or the conduction band in the crystal. At 0 K the electrons will occupy the lowest energy states available to them. In the case of the Si crystal, there are exactly $4N$ states in the valence band available to the $4N$ electrons. Thus at 0 K, *every* state in the valence band will be filled, while the conduction band will be completely empty of electrons. As we shall see, this arrangement of completely filled and empty energy bands has an important effect on the electrical conductivity of the solid.

3.1.3 Metals, Semiconductors, and Insulators

Every solid has its own characteristic energy band structure. This variation in band structure is responsible for the wide range of electrical characteristics observed in various materials. The silicon band structure of Fig. 3-3, for example, can give a good picture of why silicon in the diamond lattice is a good insulator. To reach such a conclusion, we must consider the properties of completely filled and completely empty energy bands in the current conduction process.

Before discussing the mechanisms of current flow in solids further, we can observe here that for electrons to experience acceleration in an applied electric field, they must be able to move into new energy states. This implies there must be empty states (allowed energy states which are not already occupied by electrons) available to the electrons. For example, if relatively few electrons reside in an otherwise empty band, ample unoccupied states are available into which the electrons can move. On the other hand, the silicon band structure is such that the valence band is completely filled with electrons at 0 K and the conduction band is empty. There can be no charge transport within the valence band, since no empty states are available into which electrons can move. There are no electrons in the conduction band, so no charge transport can take place there either. Thus silicon has a high resistivity typical of insulators.

Semiconductor materials at 0 K have basically the same structure as insulators—a filled valence band separated from an empty conduction band by a band gap containing no allowed energy states (Fig. 3-4). The difference lies in the size of the band gap E_g, which is much smaller in semiconductors

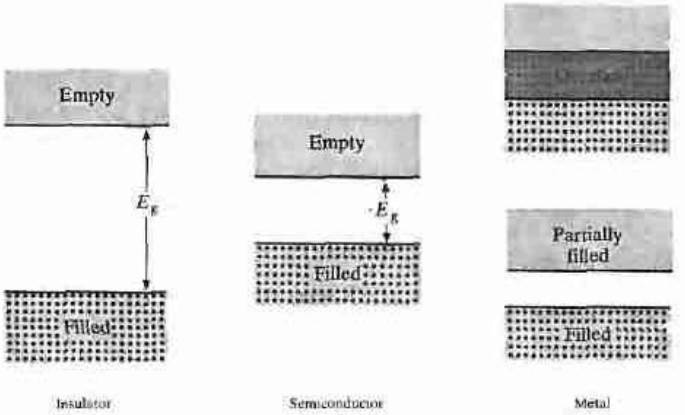

Figure 3–4 Typical band structures at 0 K.

than in insulators. For example, the semiconductor Si has a band gap of about 1.1 eV compared with 5 eV for diamond. The relatively small band gaps of semiconductors (Appendix III) allow for excitation of electrons from the lower (valence) band to the upper (conduction) band by reasonable amounts of thermal or optical energy. For example, at room temperature a semiconductor with a 1-eV band gap will have a significant number of electrons excited thermally across the energy gap into the conduction band, whereas an insulator with $E_g = 10$ eV will have a negligible number of such excitations. Thus an important difference between semiconductors and insulators is that the number of electrons available for conduction can be increased greatly in semiconductors by thermal or optical energy.

In metals the bands either overlap or are only partially filled. Thus electrons and empty energy states are intermixed within the bands so that electrons can move freely under the influence of an electric field. As expected from the metallic band structures of Fig. 3-4, metals have a high electrical conductivity.

3.1.4 Direct and Indirect Semiconductors

The "thought experiment" of Section 3.1.2, in which isolated atoms were brought together to form a solid, is useful in pointing out the existence of energy bands and some of their properties. Other techniques are generally used, however, when quantitative calculations are made of band structures. In a typical calculation, a single electron is assumed to travel through a perfectly periodic lattice. The wave function of the electron is assumed to be in the form of a plane wave[1] moving, for example, in the x- direction

[1]Discussions of plane waves are available in most sophomore physics texts or in introductory electromagnetics texts.

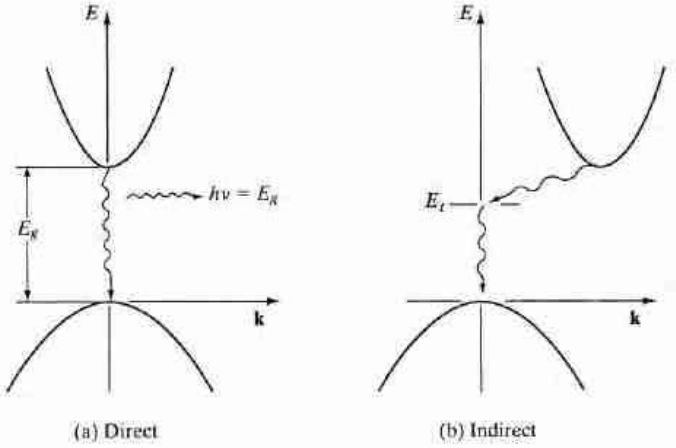

Figure 3–5 Direct and indirect electron transitions in semiconductors: (a) direct transition with accompanying photon emission; (b) indirect transition via a defect level.

with propagation constant **k**, also called a *wave vector*. The space-dependent wave function for the electron is

$$\psi_{\mathbf{k}}(x) = U(\mathbf{k}_x, x)e^{j\mathbf{k}_x x} \tag{3-1}$$

where the function $U(\mathbf{k}_x, x)$ modulates the wave function according to the periodicity of the lattice.

In such a calculation, allowed values of energy can be plotted vs. the propagation constant **k**. Since the periodicity of most lattices is different in various directions, the $(E, \mathbf{k})$ diagram must be plotted for the various crystal directions, and the full relationship between E and **k** is a complex surface which should be visualized in three dimensions.

The band structure of GaAs has a minimum in the conduction band and a maximum in the valence band for the same **k** value ($\mathbf{k} = 0$). On the other hand, Si has its valence band maximum at a different value of **k** than its conduction band minimum. Thus an electron making a smallest-energy transition from the conduction band to the valence band in GaAs can do so without a change in **k** value; on the other hand, a transition from the minimum point in the Si conduction band to the maximum point of the valence band requires some change in **k**. Thus there are two classes of semiconductor energy bands: *direct* and *indirect* (Fig. 3–5). We can show that an indirect transition, involving a change in **k**, requires a change of momentum for the electron.

EXAMPLE 3–1

Assuming that U is constant in Eq. (3–1) for an essentially free electron, show that the x-component of the electron momentum in the crystal is given by $\langle p_x \rangle = \hbar \mathbf{k}_x$.

SOLUTION From Eq. (3-1)

$$\psi_{\mathbf{k}}(x) = Ue^{j\mathbf{k}_x x}$$

Using Eq. (2-21b) and the momentum operator,

$$\langle \mathsf{p}_x \rangle = \frac{\displaystyle\int_{-\infty}^{\infty} U^2 e^{-j\mathbf{k}_x x} \frac{\hbar}{j} \frac{\partial}{\partial x} (e^{j\mathbf{k}_x x})\, dx}{\displaystyle\int_{-\infty}^{\infty} U^2\, dx}$$

$$= \frac{\hbar \mathbf{k}_x \displaystyle\int_{-\infty}^{\infty} U^2\, dx}{\displaystyle\int_{-\infty}^{\infty} U^2\, dx} = \hbar \mathbf{k}_x$$

With these limits of integration, both the numerator and denominator are infinite. For problems of this type, one integrates between the finite limits $-L/2$ and $+L/2$ and, in the final result, then assumes that L approaches infinity.

This result implies that $(E, \mathbf{k})$ diagrams such as shown in Fig. 3-5 can be considered plots of electron energy vs. momentum, with a scaling factor $\hbar$.

The direct and indirect semiconductors are identified in Appendix III In a direct semiconductor such as GaAs, an electron in the conduction band can fall to an empty state in the valence band, giving off the energy difference E_g as a photon of light. On the other hand, an electron in the conduction band minimum of an indirect semiconductor such as Si cannot fall directly to the valence band maximum but must undergo a momentum change as well as changing its energy. For example, it may go through some defect state (E_t) within the band gap. We shall discuss such defect states in Sections 4.2.1 and 4.3.2. In an indirect transition which involves a change in $\mathbf{k}$, part of the energy is generally given up as heat to the lattice rather than as an emitted photon. This difference between direct and indirect band structures is very important for deciding which semiconductors can be used in devices requiring light output. For example, semiconductor light emitters and lasers (Chapter 8) generally must be made of materials capable of direct band-to-band transitions or of indirect materials with vertical transitions between defect states.

Band diagrams such as those shown in Fig. 3-5 are cumbersome to draw in analyzing devices, and do not provide a view of the variation of electron energy with distance in the sample. Therefore, in most discussions we shall use simple band pictures such as those shown in Fig. 3-4, remembering that electron transitions across the band gap may be direct or indirect.

3.1.5 Variation of Energy Bands with Alloy Composition

As III–V ternary and quaternary alloys are varied over their composition ranges (see Sections 1.2.4 and 1.4.1), their band structures change. For example, Fig. 3–6 illustrates the band structure of GaAs and AlAs, and the way in which the bands change with composition x in the ternary compound $Al_xGa_{1-x}As$. The binary compound GaAs is a direct material, with a band gap of 1.43 eV at room temperature. For reference, we call the direct ($\mathbf{k} = 0$) conduction band minimum Γ. There are also two higher-lying indirect minima in the GaAs conduction band, but these are sufficiently far above Γ that few electrons reside there (we discuss an important exception in Chapter 10 in which high-field excitation of electrons into the indirect minima leads to the Gunn effect). We call the lowest-lying GaAs indirect minimum L and the other X. In AlAs the direct Γ minimum is much higher than the indirect X minimum, and this material is therefore indirect with a band gap of 2.16 eV at room temperature.

In the ternary alloy $Al_xGa_{1-x}As$ all of these conduction band minima move up relative to the valence band as the composition x varies from 0 (GaAs) to 1 (AlAs). However, the indirect minimum X moves up less than the others, and for compositions above about 38 percent Al this indirect minimum becomes the lowest-lying conduction band. Therefore, the ternary alloy AlGaAs is a direct semiconductor for Al compositions on the column III sublattice up to about 38 percent, and is an indirect semiconductor for higher Al mole fractions. The band gap energy E_g is shown in color on Fig. 3–6c.

The variation of energy bands for the ternary alloy $GaAs_{1-x}P_x$ is generally similar to that of AlGaAs shown in Fig. 3–6. GaAsP is a direct semiconductor from GaAs to about $GaAs_{.55}P_{.45}$ and is indirect from this composition to GaP (see Fig. 8–11). This material is often used in visible LEDs.

Since light emission is most efficient for direct materials, in which electrons can drop from the conduction band to the valence band without changing $\mathbf{k}$ (and therefore momentum), LEDs in GaAsP are generally made in material grown with a composition less than $x = 0.45$. For example, most red LEDs in this material are made at about $x = 0.4$, where the Γ minimum is still the lowest-lying conduction band edge, and where the photon resulting from a direct transition from this band to the valence band is in the red portion of the spectrum (about 1.9 eV). The use of impurities to enhance radiative recombination in indirect material will be discussed in Section 8.2.

3.2 CHARGE CARRIERS IN SEMICONDUCTORS

The mechanism of current conduction is relatively easy to visualize in the case of a metal; the metal atoms are imbedded in a "sea" of relatively free electrons, and these electrons can move as a group under the influence of an electric field. This free electron view is oversimplified, but many important conduction properties of metals can be derived from just such a model. However, we cannot account for all of the electrical properties of semiconductors

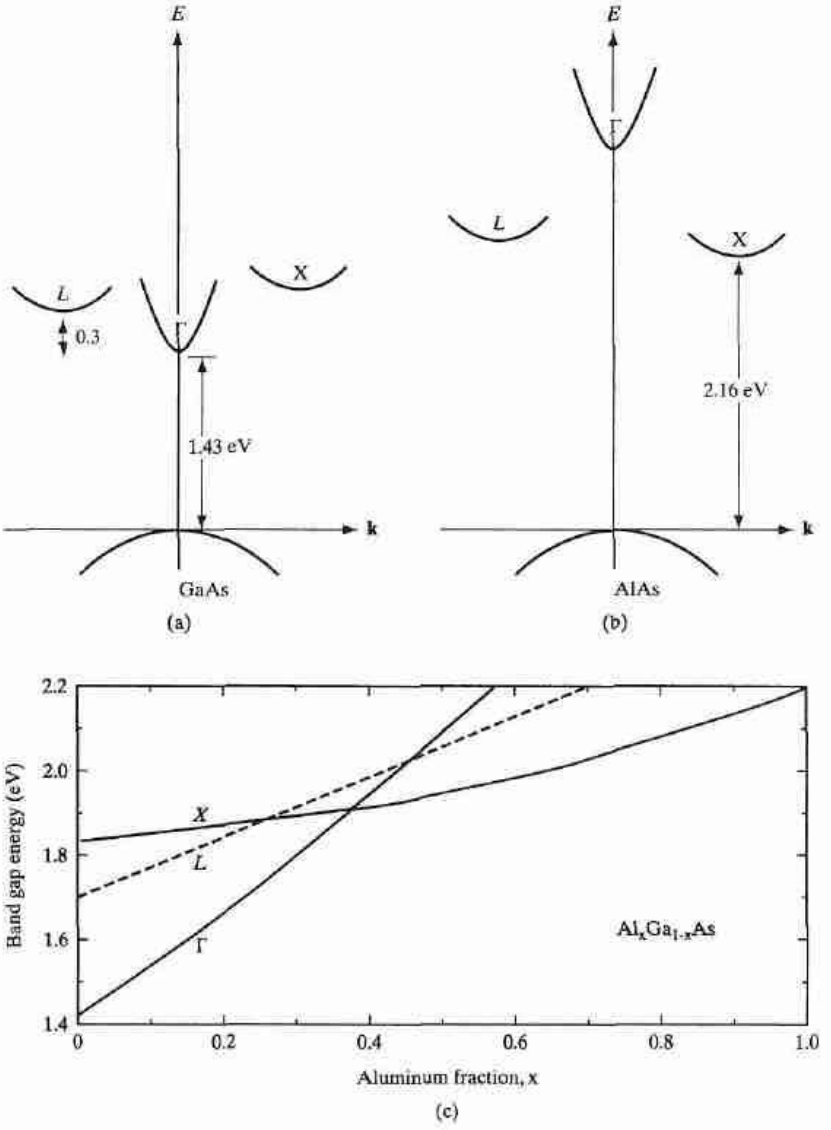

Figure 3–6
Variation of direct and indirect conduction bands in AlGaAs as a function of composition: (a) the (*E*,**k**) diagram for GaAs, showing three minima in the conduction band; (b) AlAs band diagram; (c) positions of the three conduction band minima in $Al_xGa_{1-x}As$ as *x* varies over the range of compositions from GaAs ($x = 0$) to AlAs ($x = 1$). The smallest band gap, E_g (shown in color), follows the direct Γ band to $x = 0.38$, and then follows the indirect X band.

in this way. Since the semiconductor has a filled valence band and an empty conduction band at 0 K, we must consider the increase in conduction band electrons by thermal excitations across the band gap as the temperature is raised. In addition, after electrons are excited to the conduction band, the empty states left in the valence band can contribute to the conduction process. The introduction of impurities has an important effect on the energy band structure and on the availability of charge carriers. Thus there is considerable flexibility in controlling the electrical properties of semiconductors.

3.2.1 Electrons and Holes

As the temperature of a semiconductor is raised from 0 K, some electrons in the valence band receive enough thermal energy to be excited across the band gap to the conduction band. The result is a material with some electrons in an otherwise empty conduction band and some unoccupied states in an otherwise filled valence band (Fig. 3-7).[2] For convenience, an empty state in the valence band is referred to as a *hole*. If the conduction band electron and the hole are created by the excitation of a valence band electron to the conduction band, they are called an *electron-hole pair* (abbreviated EHP).

After excitation to the conduction band, an electron is surrounded by a large number of unoccupied energy states. For example, the equilibrium number of electron-hole pairs in pure Si at room temperature is only about 10^{10} EHP/cm^3, compared to the Si atom density of 5×10^{22} atoms/cm^3. Thus the few electrons in the conduction band are free to move about via the many available empty states.

The corresponding problem of charge transport in the valence band is somewhat more complicated. However, it is possible to show that the effects of current in a valence band containing holes can be accounted for by simply keeping track of the holes themselves.

In a filled band, all available energy states are occupied. For every electron moving with a given velocity, there is an equal and opposite electron motion elsewhere in the band. If we apply an electric field, the net current is zero

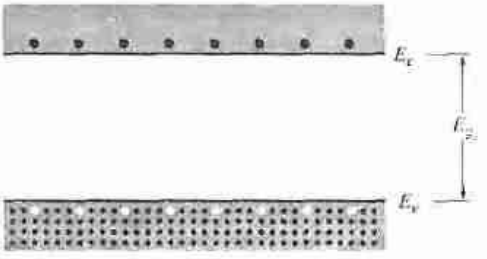

Figure 3-7 Electron-hole pairs in a semiconductor.

[2]In Fig. 3-7 and in subsequent discussions, we refer to the bottom of the conduction band as E_c and the top of the valence band as E_v.

because for every electron j moving with velocity $\mathbf{v}_j$ there is a corresponding electron j' with velocity $-\mathbf{v}_j$. Figure 3-8 illustrates this effect in terms of the electron energy vs. wave vector plot for the valence band. Since $\mathbf{k}$ is proportional to electron momentum, it is clear the two electrons have oppositely directed velocities. With N electrons/cm^3 in the band we express the current density using a sum over all of the electron velocities, and including the charge $-q$ on each electron. In a unit volume,

$$J = (-q)\sum_{i}^{N} \mathbf{v}_i = 0 \quad (\textit{filled band}) \tag{3-2a}$$

Now if we create a hole by removing the jth electron, the net current density in the valence band involves the sum over all velocities, minus the contribution of the electron we have removed:

$$J = (-q)\sum_{i}^{N} \mathbf{v}_i - (-q)\mathbf{v}_j \quad (j\text{th } \textit{electron missing}) \tag{3-2b}$$

But the first term is zero, from Eq. (3-2a). Thus the net current is $+q\mathbf{v}_j$. In other words, the current contribution of the hole is equivalent to that of a positively charged particle with velocity $\mathbf{v}_j$, that of the missing electron. Of course, the charge transport is actually due to the motion of the new uncompensated electron (j'). Its current contribution $(-q)\,(-\mathbf{v}_j)$ is equivalent to that of a positively charged particle with velocity $+\mathbf{v}_j$. For simplicity, it is customary to treat empty states in the valence band as charge carriers with positive charge and positive mass.

A simple analogy may help in understanding the behavior of holes. If we have two bottles, one completely filled with water and one completely empty, we can ask ourselves "Will there be any net transport of water when we tilt the bottles?" The answer is "no". In the case of the empty bottle, the answer is obvious. In the case of the completely full bottle also, there cannot be any net motion of water because there is no empty space for water to move into. Similarly, an empty conduction band completely devoid of electrons or a valence band completely full of electrons cannot give rise to a net motion of electrons, and thus to current conduction.

Next, we imagine transferring some water droplets from the full bottle into the empty bottle, leaving behind some air bubbles, and ask ourselves the same question. Now when we tilt the bottles there will be net transport of water: the water droplets will roll downhill in one bottle and the air bubbles will move uphill in the other. Similarly, a few electrons in an otherwise empty conduction band move opposite to an electric field, while holes in an otherwise filled valence band move in the direction of the field. The bubble analogy is imperfect, but it may provide a physical feel for why the charge and mass of a hole have opposite signs from those of an electron.

In all the following discussions we shall concentrate on the electrons in the conduction band and on the holes in the valence band. We can account for the current flow in a semiconductor by the motion of these two types of

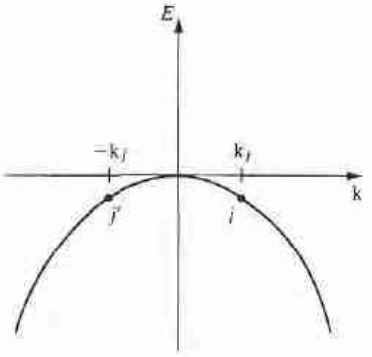

Figure 3–8
A valence band with all states filled, including states j and j', marked for discussion. The jth electron with wave vector k_j is matched by an electron at j' with the opposite wave vector $-k_j$. There is no net current in the band unless an electron is removed. For example, if the jth electron is removed, the motion of the electron at j' is no longer compensated.

charge carriers. We draw valence and conduction bands on an electron energy scale E, as in Fig. 3–8. However, we should remember that in the valence band, hole energy increases oppositely to electron energy, because the two carriers have opposite charge. Thus hole energy increases downward in Fig. 3–8 and holes, seeking the lowest energy state available, are generally found at the *top* of the valence band. In contrast, conduction band electrons are found at the bottom of the conduction band.

It would be instructive to compare the $(E, \mathbf{k})$ band diagrams with the "simplified" band diagrams that are used for routine device analysis (Fig. 3–9). As discussed in Examples 3–1 and 3–2, an $(E, \mathbf{k})$ diagram is a plot of the total electron energy (potential plus kinetic) as a function of the crystal-direction-dependent electron wave vector (which is proportional to the momentum and therefore the velocity) at some point in space. Hence, the bottom of the conduction band corresponds to zero electron velocity or kinetic energy, and simply gives us the potential energy at that point in space. For holes, the top of the valence band corresponds to zero kinetic energy. For simplified band diagrams, we plot the edges of the conduction and valence bands (i.e., the potential energy) as a function of position in the device. Energies higher in the band correspond to additional kinetic energy of the electron. Also, the fact that the band edge corresponds to the electron potential energy tells us that the variation of the band edge in space is related to the electric field at different points in the semiconductor. We will show this relationship explicitly in Section 4.4.2.

In Fig. 3–9, an electron at location A sees an electric field given by the slope of the band edge (potential energy), and gains kinetic energy (at the expense of potential energy) by moving to point B. Correspondingly, in the $(E, \mathbf{k})$ diagram, the electron starts at $k = 0$, but moves to a nonzero wave vector $\mathbf{k}_B$.

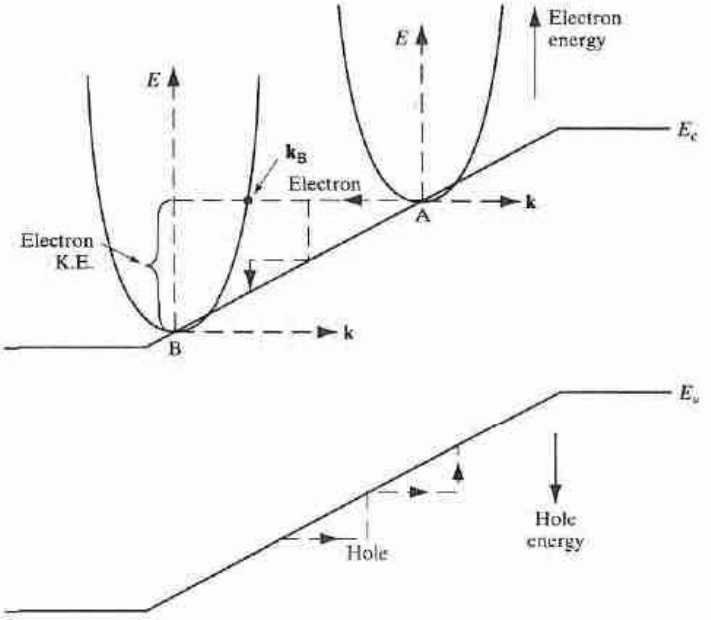

Figure 3–9 Superimposition of the (*E*,**k**) band structure on the *E*-versus-position simplified band diagram for a semiconductor in an electric field. Electron energies increase going up, while hole energies increase going down. Similarly, electron and hole wave vectors point in opposite directions and these charge carriers move opposite to each other, as shown.

The electron then loses kinetic energy to heat by scattering mechanisms (discussed in Section 3.4.3) and returns to the bottom of the band at B. The slopes of the (E, x) band edges at different points in space reflect the local electric fields at those points. In practice, the electron may lose its kinetic energy in stages by a series of scattering events, as shown by the colored dashed lines.

3.2.2 Effective Mass

The electrons in a crystal are not completely free, but instead interact with the periodic potential of the lattice. As a result, their "wave-particle" motion cannot be expected to be the same as for electrons in free space. Thus, in applying the usual equations of electrodynamics to charge carriers in a solid, we must use altered values of particle mass. In doing so, we account for most of the influences of the lattice, so that the electrons and holes can be treated as "almost free" carriers in most computations. The calculation of effective mass must take into account the shape of the energy bands in three-dimensional **k**-space, taking appropriate averages over the various energy bands.

EXAMPLE 3–2 Find the $(E, \mathbf{k})$ relationship for a free electron and relate it to the electron mass.

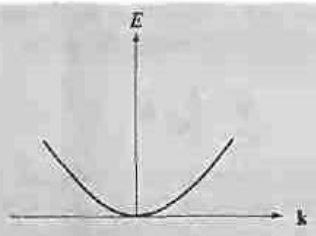

SOLUTION

From Example 3-1, the electron momentum is $\mathbf{p} = m\mathbf{v} = \hbar\mathbf{k}$. Then

$$E = \frac{1}{2}m\mathbf{v}^2 = \frac{1}{2}\frac{\mathbf{p}^2}{m} = \frac{\hbar^2}{2m}\mathbf{k}^2$$

Thus the electron energy is parabolic with wave vector $\mathbf{k}$. The electron mass is inversely related to the curvature (second derivative) of the (E, $\mathbf{k}$) relationship, since

$$\frac{d^2E}{d\mathbf{k}^2} = \frac{\hbar^2}{m}$$

Although electrons in solids are not free, most energy bands are close to parabolic at their minima (for conduction bands) or maxima (for valence bands). We can also approximate effective mass near those band extrema from the curvature of the band.

The effective mass of an electron in a band with a given (E, $\mathbf{k}$) relationship is found in Example 3-2 to be

$$m^* = \frac{\hbar^2}{d^2E/d\mathbf{k}^2} \tag{3-3}$$

Thus the curvature of the band determines the electron effective mass. For example, in Fig. 3-6a it is clear that the electron effective mass in GaAs is much smaller in the direct Γ conduction band (strong curvature) than in the L or X minima (weaker curvature, smaller value in the denominator of the m^* expression).

A particularly interesting feature of Figs. 3-5 and 3-6 is that the curvature of $d^2E/d\mathbf{k}^2$ is positive at the conduction band minima, but is negative at the valence band maxima. Thus, the electrons near the top of the valence band have *negative effective mass*, according to Eq. (3-3). Valence band electrons with negative charge and negative mass move in an electric field in the same direction as holes with positive charge and positive mass. As discussed in Section 3.2.1, we can fully account for charge transport in the valence band by considering hole motion.

For a band centered at $\mathbf{k} = 0$ (such as the Γ band in GaAs), the $(E, \mathbf{k})$ relationship near the minimum is usually parabolic:

$$E = \frac{\hbar^2}{2m^*}\mathbf{k}^2 + E_c \tag{3-4}$$

Comparing this relation to Eq. (3-3) indicates that the effective mass m^* is constant in a parabolic band. On the other hand, many conduction bands have complex $(E, \mathbf{k})$ relationships that depend on the direction of electron transport with respect to the principal crystal directions. In this case, the effective mass is a tensor quantity. However, we can use appropriate averages over such bands in most calculations.

Figure 3-10a shows the band structures for Si and GaAs viewed along two major directions. While the shape is parabolic near the band edges (as indicated in Figure 3-5 and Example 3-2), there are significant non-parabolicities at higher energies. The energies are plotted along the high symmetry [111] and [100] directions in the crystal. The $\mathbf{k} = 0$ point is denoted as Γ. When we go along

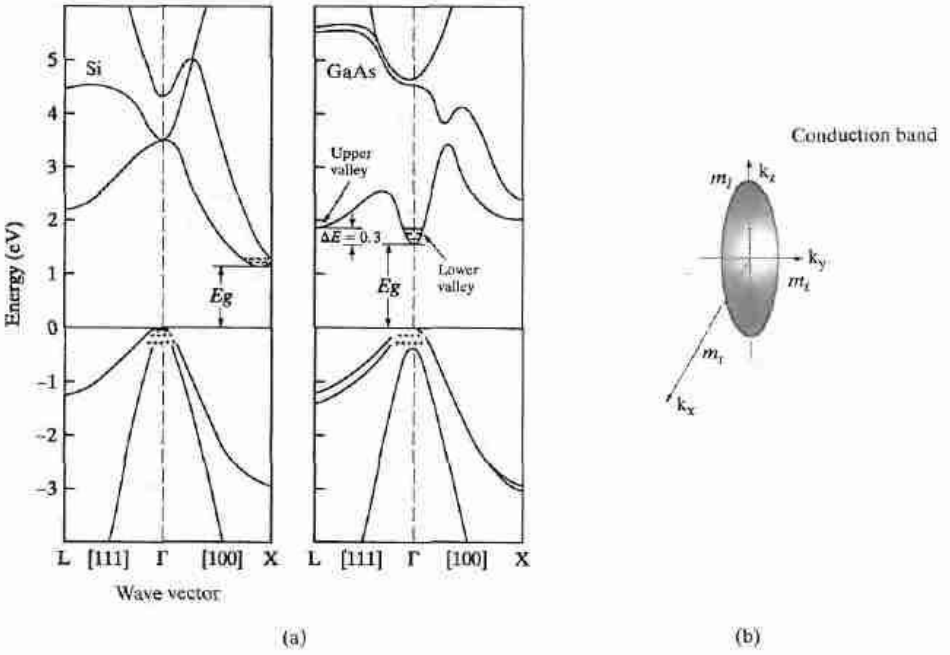

Figure 3-10
Realistic band structures in semiconductors: (a) Conduction and valence bands in Si and GaAs along [111] and [100]; (b) ellipsoidal constant energy surface for Si, near the 6 conduction band minima along the X directions. (From Chelikowsky and Cohen, Phys. Rev. B14, 556, 1976).

the [100] direction, we reach a valley near X, while we reach the L valley along the [111] direction. (Since the energies are plotted along different directions, the curves do not look symmetric.) The valence band maximum in most semiconductors is at the Γ point. It has three branches: the *heavy hole* band with the smallest curvature, a *light hole band* with a larger curvature, and a *split-off band* at a different energy. We notice that for GaAs the conduction band minimum and the valence band maximum are both at $\mathbf{k} = 0$; therefore it is direct band gap. Silicon, on the other hand, has 6 equivalent conduction minima at X along the 6 equivalent ⟨100⟩ directions; therefore, it is indirect.

Figure 3-10b shows the constant energy surface for electrons in one of the six conduction bands for Si. The way to relate these surfaces to the band structures shown in Fig. 3-10a is to consider a certain value of energy, and determine all the **k** vectors in 3 dimensions for which we get this energy. We find that for Si we have 6 cigar-shaped ellipsoidal equi-energy surfaces near the conduction band minima along the six equivalent X-directions, with a longitudinal effective mass, m_l, along the major axis, and two transverse effective masses, m_t, along the minor axes. For GaAs, the conduction band is more or less spherical for low energies. On the other hand, we have warped spherical surfaces in the valence band. The importance of these surfaces will be clear in Sections 3.3.2 and 3.4.1 when we consider different types of effective masses in semiconductors.

In any calculation involving the mass of the charge carriers, we must use effective mass values for the particular material involved. In all subsequent discussions, the electron effective mass is denoted by m_n^* and the hole effective mass by m_p^*. The n subscript indicates the electron as a negative charge carrier, and the p subscript indicates the hole as a positive charge carrier.

There is nothing mysterious about the concept of an "effective" mass, m_n^*, and about the fact that it is different in different semiconductors. Indeed, the "true" mass of an electron, m, is the same in Si, Ge, or GaAs—it is the same as for a free electron in vacuum. To understand why the effective mass is different from the true mass, consider Newton's second law, which states that the time rate of change of momentum is the force.

$$dp/dt = d(m\mathrm{v})/dt = \text{Force} \tag{3-5a}$$

An electron in a crystal experiences a total force $\mathrm{F}_{\mathrm{int}} + \mathrm{F}_{\mathrm{ext}}$, where $\mathrm{F}_{\mathrm{int}}$ is the collection of internal periodic crystal forces, and $\mathrm{F}_{\mathrm{ext}}$ is the externally applied force. It is inefficient to solve this complicated problem involving the periodic crystal potential (which is obviously different in different semiconductors) every time we try to solve a semiconductor device problem. It is better to solve the complicated problem of carrier motion in the periodic crystal potential just once, and encapsulate that information in what is called the bandstructure, $(E, \mathbf{k})$, whose curvature gives us the effective mass, m_n^*. The electron then responds to external forces with this new m_n^*. Newton's law is then written as:

$$d(m_n^*\mathrm{v})/dt = \mathrm{F}_{\mathrm{ext}} \tag{3-5b}$$

This is clearly an enormous simplification compared to the more detailed problem. Obviously, the periodic crystal forces depend on the details of a specific semiconductor; therefore, the effective mass is different in different materials.

Once we determine the band curvature effective mass components from the orientation-dependent $(E, \mathbf{k})$, we have to combine them appropriately for different types of calculations. We shall see in Section 3.3.2 that when we are interested in determining the numbers of carriers in the bands, we have to use a "density-of-states" effective mass by taking the geometric mean of the band curvature effective masses, and the number of equivalent band extrema. On the other hand we will find in Section 3.4.1 that in problems involving the motion of carriers, one must take the harmonic mean of the band curvature effective masses to get the "conductivity" effective mass.

3.2.3 Intrinsic Material

A perfect semiconductor crystal with no impurities or lattice defects is called an *intrinsic* semiconductor. In such material there are no charge carriers at 0 K, since the valence band is filled with electrons and the conduction band is empty. At higher temperatures electron-hole pairs are generated as valence band electrons are excited thermally across the band gap to the conduction band. These EHPs are the only charge carriers in intrinsic material.

The generation of EHPs can be visualized in a qualitative way by considering the breaking of covalent bonds in the crystal lattice (Fig. 3-11). If one of the Si valence electrons is broken away from its position in the bonding structure such that it becomes free to move about in the lattice, a conduction electron is created and a broken bond (hole) is left behind. The energy required to break the bond is the band gap energy E_g. This model helps in visualizing the physical mechanism of EHP creation, but the energy band model is more productive for purposes of quantitative calculation. One important difficulty in the "broken bond" model is that the free electron and the hole seem deceptively localized in the lattice. Actually, the positions of the free electron and the hole are spread out over several lattice spacings and should be considered quantum mechanically by probability distributions (see Section 2.4).

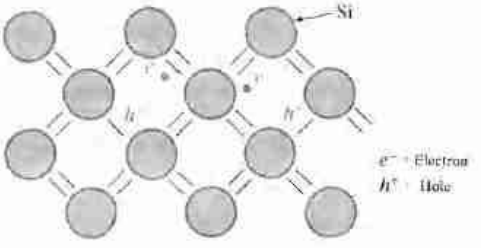

Figure 3–11 Electron–hole pairs in the covalent bonding model of the Si crystal.

Since the electrons and holes are created in pairs, the conduction band electron concentration n (electrons per cm^3) is equal to the concentration of holes in the valence band p (holes per cm^3). Each of these intrinsic carrier concentrations is commonly referred to as n_i. Thus *for intrinsic material*

$$n = p = n_i \tag{3-6}$$

At a given temperature there is a certain concentration of electron-hole pairs n_i. Obviously, if a steady state carrier concentration is maintained, there must be *recombination* of EHPs at the same rate at which they are generated. Recombination occurs when an electron in the conduction band makes a transition (direct or indirect) to an empty state (hole) in the valence band, thus annihilating the pair. If we denote the generation rate of EHPs as g_i (EHP/cm^3-s) and the recombination rate as r_i, equilibrium requires that

$$r_i = g_i \tag{3-7a}$$

Each of these rates is temperature dependent. For example, $g_i(T)$ increases when the temperature is raised, and a new carrier concentration n_i is established such that the higher recombination rate $r_i(T)$ just balances generation. At any temperature, we can predict that the rate of recombination of electrons and holes r_i is proportional to the equilibrium concentration of electrons n_0 and the concentration of holes p_0:

$$r_i = \alpha_r n_0 p_0 = \alpha_r n_i^2 = g_i \tag{3-7b}$$

The factor α_r is a constant of proportionality which depends on the particular mechanism by which recombination takes place. We shall discuss the calculation of n_i as a function of temperature in Section 3.3.3; recombination processes will be discussed in Chapter 4.

3.2.4 Extrinsic Material

In addition to the intrinsic carriers generated thermally, it is possible to create carriers in semiconductors by purposely introducing impurities into the crystal. This process, called *doping*, is the most common technique for varying the conductivity of semiconductors. By doping, a crystal can be altered so that it has a predominance of either electrons or holes. Thus there are two types of doped semiconductors, n-type (mostly electrons) and p-type (mostly holes). When a crystal is doped such that the equilibrium carrier concentrations n_0 and p_0 are different from the intrinsic carrier concentration n_i, the material is said to be *extrinsic*.

When impurities or lattice defects are introduced into an otherwise perfect crystal, additional levels are created in the energy band structure, usually within the band gap. For example, an impurity from column V of the periodic table (P, As, and Sb) introduces an energy level very near the conduction band in Ge or Si. This level is filled with electrons at 0 K, and very little thermal energy is required to excite these electrons to the conduction band (Fig. 3-12a). Thus at about 50–100 K virtually all of the electrons in the

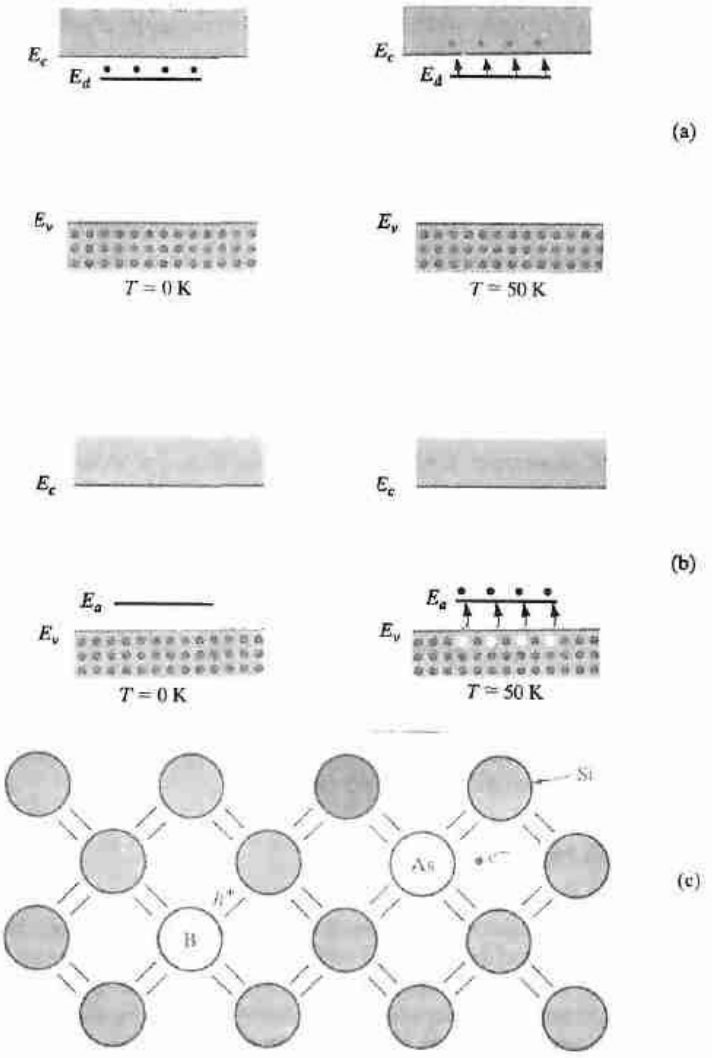

Figure 3–12 Energy band model and chemical bond model of dopants in semiconductors: (a) donation of electrons from donor level to conduction band; (b) acceptance of valence band electrons by an acceptor level, and the resulting creation of holes; (c) donor and acceptor atoms in the covalent bonding model of a Si crystal.

impurity level are "donated" to the conduction band. Such an impurity level is called a *donor* level, and the column V impurities in Ge or Si are called donor impurities. From Fig. 3–12a we note that the material doped with donor impurities can have a considerable concentration of electrons in the conduction band, even when the temperature is too low for the intrinsic EHP concentration to be appreciable. Thus semiconductors doped with a significant number of donor atoms will have $n_0 \gg (n_i, p_0)$ at room temperature. This is n-type material.

Atoms from column III (B, Al, Ga, and In) introduce impurity levels in Ge or Si near the valence band. These levels are empty of electrons at 0 K (Fig. 3-12b). At low temperatures, enough thermal energy is available to excite electrons from the valence band into the impurity level, leaving behind holes in the valence band. Since this type of impurity level "accepts" electrons from the valence band, it is called an *acceptor* level, and the column III impurities are acceptor impurities in Ge and Si. As Fig. 3-12b indicates, doping with acceptor impurities can create a semiconductor with a hole concentration p_0 much greater than the conduction band electron concentration n_0 (this type is p-type material).

In the covalent bonding model, donor and acceptor atoms can be visualized as shown in Fig. 3-12c. An As atom (column V) in the Si lattice has the four necessary valence electrons to complete the covalent bonds with the neighboring Si atoms, plus one extra electron. This fifth electron does not fit into the bonding structure of the lattice and is therefore loosely bound to the As atom. A small amount of thermal energy enables this extra electron to overcome its coulombic binding to the impurity atom and be donated to the lattice as a whole. Thus it is free to participate in current conduction. This process is a qualitative model of the excitation of electrons out of a donor level and into the conduction band (Fig. 3-12a). Similarly, the column III impurity B has only three valence electrons to contribute to the covalent bonding (Fig. 3-12c), thereby leaving one bond incomplete. With a small amount of thermal energy, this incomplete bond can be transferred to other atoms as the bonding electrons exchange positions. Again, the idea of an electron "hopping" from an adjacent bond into the incomplete bond at the B site provides some physical insight into the behavior of an acceptor, but the model of Fig. 3-12b is preferable for most discussions.

We can calculate rather simply the approximate energy required to excite the fifth electron of a donor atom into the conduction band (the donor *binding energy*). Let us assume for rough calculations that the As atom of Fig. 3-12c has its four covalent bonding electrons rather tightly bound and the fifth "extra" electron loosely bound to the atom. We can approximate this situation by using the Bohr model results, considering the loosely bound electron as ranging about the tightly bound "core" electrons in a hydrogen-like orbit. From Eq. (2-15) the magnitude of the ground-state energy ($\mathbf{n} = 1$) of such an electron is

$$E = \frac{mq^4}{2K^2\hbar^2} \tag{3-8}$$

The value of K must be modified from the free-space value $4\pi\epsilon_0$ used in the hydrogen atom problem to

$$K = 4\pi\epsilon_0\,\epsilon_r \tag{3-9}$$

where ϵ_r is the relative dielectric constant of the semiconductor material. In addition, we must use the conductivity effective mass m_n^* typical of the semiconductor, discussed in more detail in Section 3.4.1.

EXAMPLE 3–3 It was mentioned in Section 3.2 that the covalent bonding model gives a false impression of the localization of carriers. As an illustration, calculate the radius of the electron orbit around the donor in Fig. 3–12c, assuming a ground state hydrogen-like orbit in Si. Compare with the Si lattice constant. Use $m_n^* = 0.26m_0$ for Si.

SOLUTION From Eq. (2–10) with $n = 1$ and using $\epsilon_r = 11.8$ for Si,

$$r = \frac{4\pi\,\epsilon_r\epsilon_0\hbar^2}{m_n^* q^2} = \frac{11.8(8.85 \times 10^{-12})(6.63 \times 10^{-34})^2}{\pi(0.26)(9.11 \times 10^{-31})(1.6 \times 10^{-19})^2}$$

$$r = 2.41 \times 10^{-9} m = 24.1\ \text{Å}.$$

Note that this is more than four lattice spacings $a = 5.43$ Å.

Generally, the column V donor levels lie approximately 0.01 eV below the conduction band in Ge, and the column III acceptor levels lie about 0.01 eV above the valence band. In Si the usual donor and acceptor levels lie about 0.03–0.06 eV from a band edge.

In III–V compounds, column VI impurities occupying column V sites serve as donors. For example, S, Se, and Te are donors in GaAs, since they substitute for As and provide an extra electron compared with the As atom. Similarly, impurities from column II (Be, Zn, Cd) substitute for column III atoms to form acceptors in the III–V compounds. A more ambiguous case arises when a III–V material is doped with Si or Ge, from column IV. These impurities are called *amphoteric*, meaning that Si or Ge can serve as donors or acceptors depending on whether they reside on the column III or column V sublattice of the crystal. In GaAs it is common for Si impurities to occupy Ga sites. Since the Si has an extra electron compared with the Ga it replaces, it serves as a donor. However, an excess of As vacancies arising during growth or processing of the GaAs can cause Si impurities to occupy As sites, where they serve as acceptors.

The importance of doping will become obvious when we discuss electronic devices made from junctions between p-type and n-type semiconductor material. The extent to which doping controls the electronic properties of semiconductors can be illustrated here by considering changes in the sample resistance which occur with doping. In Si, for example, the intrinsic carrier concentration n_i is about 10^{10} cm^{-3} at room temperature. If we dope Si with 10^{15} As atoms/cm^3, the conduction electron concentration changes by five orders of magnitude. The resistivity of Si changes from about 2×10^5 Ω-cm to 5 Ω-cm with this doping.

When a semiconductor is doped n-type or p-type, one type of carrier dominates. In the example given above, the conduction band electrons outnumber the holes in the valence band by many orders of magnitude. We refer

to the small number of holes in n-type material as *minority carriers* and the relatively large number of conduction band electrons as *majority carriers*. Similarly, electrons are the minority carriers in p-type material, and holes are the majority carriers.

3.2.5 Electrons and Holes in Quantum Wells

We have discussed single-valued (*discrete*) energy levels in the band gap arising from doping, and a *continuum* of allowed states in the valence and conduction bands. A third possibility is the formation of discrete levels for electrons and holes as a result of quantum-mechanical confinement.

One of the most useful applications of MBE or OMVPE growth of multi-layer compound semiconductors, as described in Section 1.4, is the fact that a continuous single crystal can be grown in which adjacent layers have different band gaps. For example, Fig. 3-13 shows the spatial variation in conduction and valence bands for a multilayer structure in which a very thin layer of GaAs is sandwiched between two layers of AlGaAs, which has a wider band gap that the GaAs. We will discuss the details of such *heterojunctions* (junctions between dissimilar materials) in Section 5.8. It is interesting to point out here, however, that a consequence of confining electrons and holes in a very thin layer is that these particles behave according to the *particle in a potential well* problem, with quantum states calculated in Section 2.4.3. Therefore,

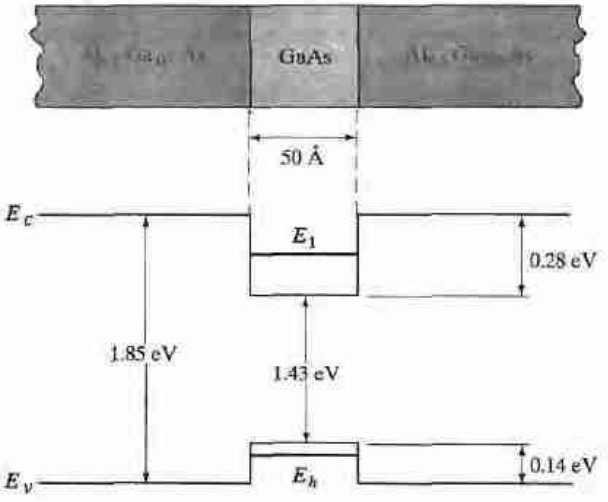

Figure 3-13
Energy band discontinuities for a thin layer of GaAs sandwiched between layers of wider band gap AlGaAs. In this case, the GaAs region is so thin that quantum states are formed in the valence and conduction bands. Electrons in the GaAs conduction band reside on "particle in a potential well" states such as E_1 shown here, rather than in the usual conduction band states. Holes in the quantum well occupy similar discrete states, such as E_h.

instead of having the continuum of states normally available in the conduction band, the conduction band electrons in the narrow-gap material are confined to discrete quantum states as described by Eq. (2-33), modified for effective mass and finite barrier height. Similarly, the states in the valence band available for holes are restricted to discrete levels in the quantum well. This is one of the clearest demonstrations of the quantum mechanical results discussed in Chapter 2. From a practical device point of view, the formation of discrete quantum states in the GaAs layer of Fig. 3-13 changes the energy at which photons can be emitted. An electron on one of the discrete conduction band states (E_1 in Fig. 3-13) can make a transition to an empty discrete valence band state in the GaAs quantum well (such as E_h), giving off a photon of energy $E_g + E_1 + E_h$, greater than the GaAs band gap. Semiconductor lasers have been made in which such a quantum well is used to raise the energy of the transition from the infrared, typical of GaAs, to the red portion of the spectrum. We will see other examples of quantum wells in semiconductor devices in later chapters.

3.3 CARRIER CONCENTRATIONS

In calculating semiconductor electrical properties and analyzing device behavior, it is often necessary to know the number of charge carriers per cm^3 in the material. The majority carrier concentration is usually obvious in heavily doped material, since one majority carrier is obtained for each impurity atom (for the standard doping impurities). The concentration of minority carriers is not obvious, however, nor is the temperature dependence of the carrier concentrations.

To obtain equations for the carrier concentrations we must investigate the distribution of carriers over the available energy states. This type of distribution is not difficult to calculate, but the derivation requires some background in statistical methods. Since we are primarily concerned here with the application of these results to semiconductor materials and devices, we shall accept the distribution function as given.

3.3.1 The Fermi Level

Electrons in solids obey *Fermi–Dirac* statistics.[3] In the development of this type of statistics, one must consider the indistinguishability of the electrons,

[3]Examples of other types of statistics are *Maxwell–Boltzmann* for classical particles (e.g., gas) and *Bose–Einstein* for photons. For two discrete energy levels, E_2 and E_1 (with $E_2 > E_1$), classical gas atoms follow a Boltzmann distribution; the number n_2 of atoms in state E_2 is related to the number n_1 in E_1 at thermal equilibrium by

$$\frac{n_2}{n_1} = \frac{N_2 e^{-E_2/kT}}{N_1 e^{-E_1/kT}} = \frac{N_2}{N_1} e^{-(E_2 - E_1)/kT}$$

assuming the two levels have N_2 and N_1 number of states, respectively. The exponential term $\exp[-\Delta E/kT]$ is commonly called the *Boltzmann factor*. It appears also in the denominator of the Fermi–Dirac distribution function. We shall return to the Boltzmann distribution in Chapter 8 in discussions of the properties of lasers.

their wave nature, and the Pauli exclusion principle. The rather simple result of these statistical arguments is that the distribution of electrons over a range of allowed energy levels at thermal equilibrium is

$$\boxed{f(E) = \frac{1}{1 + e^{(E-E_F)/kT}}} \tag{3-10}$$

where k is Boltzmann's constant ($k = 8.62 \times 10^{-5}$ eV/K $= 1.38 \times 10^{-23}$ J/K). The function $f(E)$, the *Fermi–Dirac distribution function*, gives the probability that an available energy state at E will be occupied by an electron at absolute temperature T. The quantity E_F is called the *Fermi level*, and it represents an important quantity in the analysis of semiconductor behavior. We notice that, for an energy E equal to the Fermi level energy E_F, the occupation probability is

$$f(E_F) = [1 + e^{(E_F - E_F)/kT}]^{-1} = \frac{1}{1+1} = \frac{1}{2} \tag{3-11}$$

Thus an energy state at the Fermi level has a probability of $^1/_2$ of being occupied by an electron.

A closer examination of $f(E)$ indicates that at 0 K the distribution takes the simple rectangular form shown in Fig. 3-14. With $T = 0$ in the denominator of the exponent, $f(E)$ is $1/(1 + 0) = 1$ when the exponent is negative ($E < E_F$), and is $1/(1 + \infty) = 0$ when the exponent is positive ($E > E_F$). This rectangular distribution implies that at 0 K every available energy state up to E_F is filled with electrons, and all states above E_F are empty.

At temperatures higher than 0 K, some probability exists for states above the Fermi level to be filled. For example, at $T = T_1$ in Fig. 3-14 there is some probability $f(E)$ that states above E_F are filled, and there is a corresponding probability $[1 - f(E)]$ that states below E_F are empty. The Fermi function is symmetrical about E_F for all temperatures; that is, the probability $f(E_F + \Delta E)$ that a state ΔE above E_F is filled is the same as the probability $[1 - f(E_F - \Delta E)]$ that a state ΔE below E_F is empty. The symmetry of the

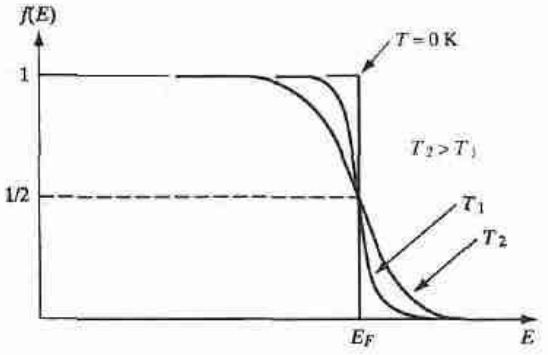

Figure 3–14
The Fermi–Dirac distribution function.

distribution of empty and filled states about E_F makes the Fermi level a natural reference point in calculations of electron and hole concentrations in semiconductors.

In applying the Fermi–Dirac distribution to semiconductors, we must recall that $f(E)$ is the probability of occupancy of an *available* state at E. Thus if there is no available state at E (e.g., in the band gap of a semiconductor), there is no possibility of finding an electron there. We can best visualize the relation between $f(E)$ and the band structure by turning the $f(E)$ vs. E diagram on its side so that the E scale corresponds to the energies of the band diagram (Fig. 3-15). For intrinsic material we know that the concentration of holes in the valence band is equal to the concentration of electrons in the conduction band. Therefore, the Fermi level E_F must lie at the middle of the band gap in intrinsic material.[4] Since $f(E)$ is symmetrical about E_F, the electron probability "tail" of $f(E)$ extending into the conduction band of Fig. 3-15a is symmetrical with the hole probability tail $[1 - f(E)]$ in the valence band. The distribution function has values within the band gap between

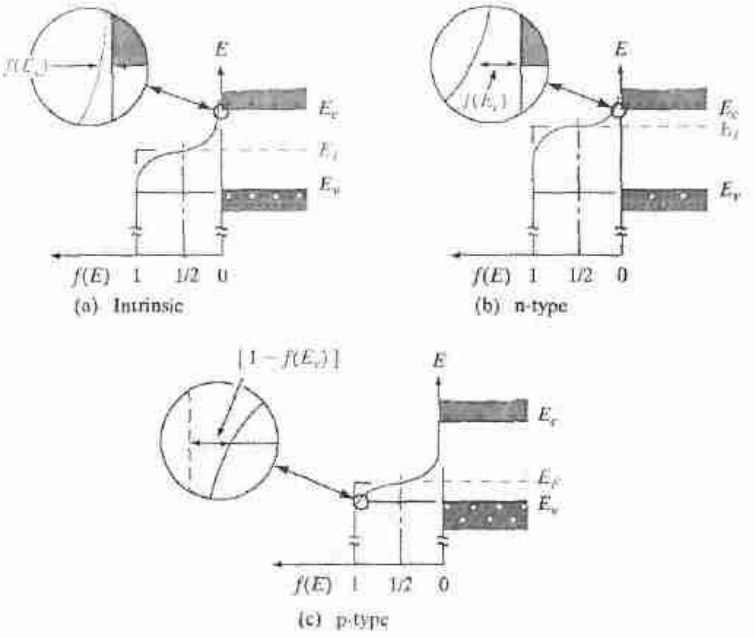

Figure 3-15 The Fermi distribution function applied to semiconductors: (a) intrinsic material; (b) n-type material; (c) p-type material.

[4]Actually the intrinsic E_F is displaced slightly from the middle of the gap, since the densities of available states in the valence and conduction bands are not equal (Section 3.3.2).

E_v and E_c, but there are no energy states available, and no electron occupancy results from $f(E)$ in this range.

The tails in $f(E)$ are exaggerated in Fig. 3-15 for illustrative purposes. Actually, the probability values at E_v and E_c are quite small for intrinsic material at reasonable temperatures. For example, in Si at 300 K, $n_i = p_i = 10^{10}$ cm^{-3}, whereas the densities of available states at E_v and E_c are on the order of 10^{19} cm^{-3}. Thus the probability of occupancy $f(E)$ for an individual state in the conduction band and the hole probability $[1 - f(E)]$ for a state in the valence band are quite small. Because of the relatively large density of states in each band, small changes in $f(E)$ can result in significant changes in carrier concentration.

In n-type material there is a high concentration of electrons in the conduction band compared with the hole concentration in the valence band (recall Fig. 3-12a). Thus in n-type material the distribution function $f(E)$ must lie above its intrinsic position on the energy scale (Fig. 3-15b). Since $f(E)$ retains its shape for a particular temperature, the larger concentration of electrons at E_c in n-type material implies a correspondingly smaller hole concentration at E_v. We notice that the value of $f(E)$ for each energy level in the conduction band (and therefore the total electron concentration n_0) increases as E_F moves closer to E_c. Thus the energy difference $(E_c - E_F)$ gives a measure of n; we shall express this relation mathematically in the following section.

For p-type material the Fermi level lies near the valence band (Fig. 3-15c) such that the $[1 - f(E)]$ tail below E_v is larger than the $f(E)$ tail above E_c. The value of $(E_F - E_v)$ indicates how strongly p-type the material is.

It is usually inconvenient to draw $f(E)$ vs. E on every energy band diagram to indicate the electron and hole distributions. Therefore, it is common practice merely to indicate the position of E_F in band diagrams. This is sufficient information, since for a particular temperature the position of E_F implies the distributions in Fig. 3-15.

3.3.2 Electron and Hole Concentrations at Equilibrium

The Fermi distribution function can be used to calculate the concentrations of electrons and holes in a semiconductor, if the densities of available states in the valence and conduction bands are known. For example, the concentration of electrons in the conduction band is

$$n_0 = \int_{E_c}^{\infty} f(E)N(E)dE \tag{3-12}$$

where $N(E)dE$ is the density of states (cm^{-3}) in the energy range dE. The subscript 0 used with the electron and hole concentration symbols (n_0, p_0) indicates equilibrium conditions. The number of electrons per unit volume in the energy range dE is the product of the density of states and the probability of occupancy $f(E)$. Thus the total electron concentration is the integral

over the entire conduction band, as in Eq. (3–12).[5] The function $N(E)$ can be calculated by using quantum mechanics and the Pauli exclusion principle (Appendix IV).

It is shown in Appendix IV that $N(E)$ is proportional to $E^{1/2}$, so the density of states in the conduction band increases with electron energy. On the other hand, the Fermi function becomes extremely small for large energies. The result is that the product $f(E)N(E)$ decreases rapidly above E_c, and very few electrons occupy energy states far above the conduction band edge. Similarly, the probability of finding an empty state (hole) in the valence band $[1 - f(E)]$ decreases rapidly below E_v, and most holes occupy states near the top of the valence band. This effect is demonstrated in Fig. 3–16, which shows the density of available states, the Fermi function, and the resulting number of electrons and holes occupying available energy states in the conduction and valence bands at thermal equilibrium (i.e., with no excitations except thermal energy). For holes, increasing energy points down in Fig. 3–16, since the E scale refers to electron energy.

The result of the integration of Eq. (3–12) is the same as that obtained if we represent all of the distributed electron states in the conduction band by an *effective density of states* N_c located at the conduction band edge E_c. Therefore, the conduction band electron concentration is simply the effective density of states at E_c times the probability of occupancy at E_c.[6]

$$n_0 = N_c f(E_c) \tag{3-13}$$

In this expression we assume the Fermi level E_F lies at least several kT below the conduction band. Then the exponential term is large compared with unity, and the Fermi function $f(E_c)$ can be simplified as

$$f(E_c) = \frac{1}{1 + e^{(E_c - E_F)/kT}} \simeq e^{-(E_c - E_F)/kT} \tag{3-14}$$

Since kT at room temperature is only 0.026 eV, this is generally a good approximation. For this condition the concentration of electrons in the conduction band is

$$\boxed{n_0 = N_c e^{-(E_c - E_F)/kT}} \tag{3-15}$$

The effective density of states N_c is shown in Appendix IV to be

$$N_c = 2\left(\frac{2\pi m_n^* kT}{h^2}\right)^{3/2} \tag{3-16a}$$

[5]The upper limit is actually improper in Eq. (3–12), since the conduction band does not extend to infinite energy. This is unimportant in the calculation of n_0, however, since $f(E)$ becomes negligibly small for large values of E. Most electrons occupy states near the bottom of the conduction band at equilibrium.

[6]The simple expression for n_0 obtained in Eq. (3–13) is the direct result of integrating Eq. (3–12), as in Appendix IV. Equations (3–15) and (3–19) properly include the effects of the conduction and valence bands through the density-of-states terms.

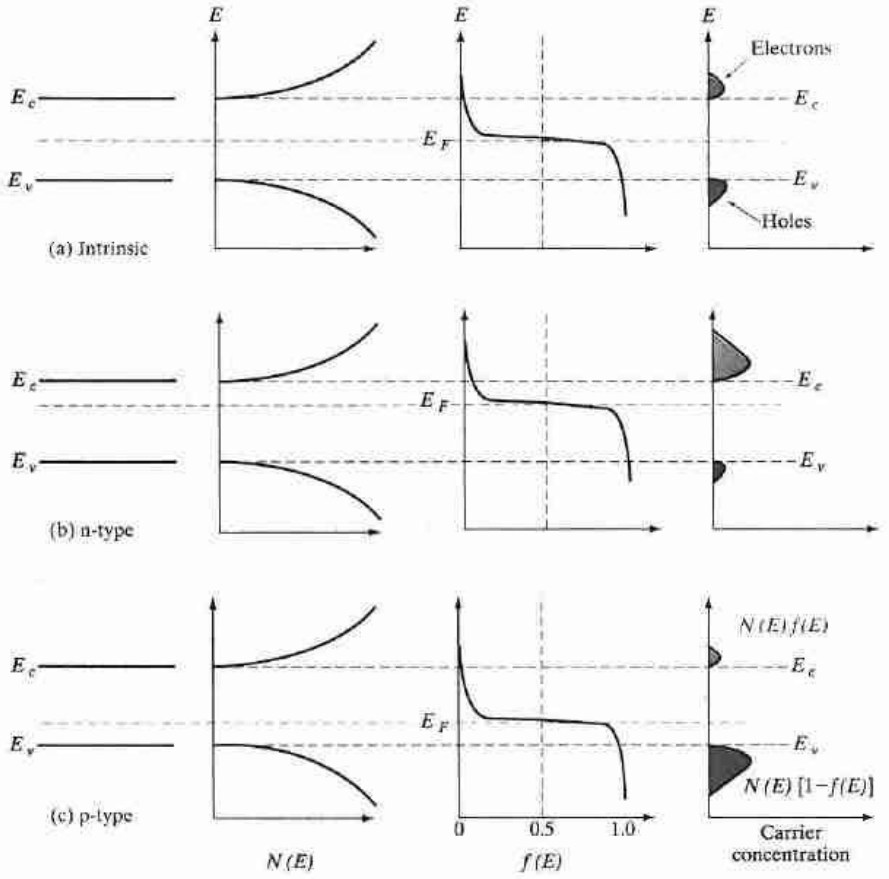

Figure 3–16
Schematic band diagram, density of states, Fermi–Dirac distribution, and the carrier concentrations for (a) intrinsic, (b) n-type, and (c) p-type semiconductors at thermal equilibrium.

Since the quantities in Eq. (3–16a) are known, values of N_c can be tabulated as a function of temperature. As Eq. (3–15) indicates, the electron concentration increases as E_F moves closer to the conduction band. This is the result we would predict from Fig. 3–15b.

In Eq. (3–16a), m_n^* is the density-of-states effective mass for electrons. To illustrate how it is obtained from the band curvature effective masses mentioned in Section 3.2.2, let us consider the 6 equivalent conduction

band minima along the X-directions for Si. Looking at the cigar-shaped equi-energy surfaces in Fig. 3-10b, we find that we have more than one band curvature to deal with in calculating effective masses. There is a longitudinal effective mass m_l along the major axis of the ellipsoid, and the transverse effective mass m_t along the two minor axes. Since we have $(m_n^*)^{3/2}$ appearing in the density-of-states expression Eq. (3-16a), by using dimensional equivalence and adding contributions from all 6 valleys, we get

$$(m_n^*)^{3/2} = 6(m_l m_t^2)^{1/2} \tag{3-16b}$$

It can be seen that this is the geometric mean of the effective masses.

EXAMPLE 3-4 Calculate the density-of-states effective mass of electrons in Si.

SOLUTION For Si, $m_l = 0.98\ m_0$; $m_t = 0.19\ m_0$ from Appendix III.
There are six equivalent X valleys in the conduction band.

$$m_n^* = 6^{2/3}[0.98(0.19)^2]^{1/3}\, m_0 = 1.1\ m_0$$

Note: For GaAs, the conduction band equi-energy surfaces are spherical. So there is only one band curvature effective mass, and it is equal to the density-of-states effective mass ($= 0.067\ m_0$).

By similar arguments, the concentration of holes in the valence band is

$$p_0 = N_v[1 - f(E_v)] \tag{3-17}$$

where N_v is the effective density of states in the valence band. The probability of finding an empty state at E_v is

$$1 - f(E_v) = 1 - \frac{1}{1 + e^{(E_v - E_F)/kT}} \simeq e^{-(E_F - E_v)/kT} \tag{3-18}$$

for E_F larger than E_v by several kT. From these equations, the concentration of holes in the valence band is

$$\boxed{p_0 = N_v e^{-(E_F - E_v)/kT}} \tag{3-19}$$

The effective density of states in the valence band reduced to the band edge is

$$N_v = 2\left(\frac{2\pi m_p^* kT}{h^2}\right)^{3/2} \tag{3-20}$$

As expected from Fig. 3-15c, Eq. (3-19) predicts that the hole concentration increases as E_F moves closer to the valence band.

The electron and hole concentrations predicted by Eqs. (3-15) and (3-19) are valid whether the material is intrinsic or doped, provided thermal equilibrium is maintained. Thus *for intrinsic material, E_F lies at some intrinsic level E_i* near the middle of the band gap (Fig. 3-15a), and the intrinsic electron and hole concentrations are

$$n_i = N_c e^{-(E_c - E_i)/kT}, \quad p_i = N_v e^{-(E_i - E_v)/kT} \tag{3-21}$$

The product of n_0 and p_0 at equilibrium is a constant for a particular material and temperature, even if the doping is varied:

$$n_0 p_0 = (N_c e^{-(E_c - E_F)/kT})(N_v e^{-(E_F - E_v)/kT}) = N_c N_v e^{-(E_c - E_v)/kT} \tag{3-22a}$$
$$= N_c N_v e^{-E_g/kT}$$
$$n_i p_i = (N_c e^{-(E_c - E_i)/kT})(N_v e^{-(E_i - E_v)/kT}) = N_c N_v e^{-E_g/kT} \tag{3-22b}$$

The intrinsic electron and hole concentrations are equal (since the carriers are created in pairs), $n_i = p_i$; thus the intrinsic concentration is

$$n_i = \sqrt{N_c N_v}\, e^{-E_g/2kT} \tag{3-23}$$

The constant product of electron and hole concentrations in Eq. (3-22) can be written conveniently as

$$\boxed{n_0 p_0 = n_i^2} \tag{3-24}$$

This is an important relation, and we shall use it extensively in later calculations. The intrinsic concentration for Si at room temperature is approximately $\overline{n}_i = 1.5 \times 10^{10}\ cm^{-3}$.

Comparing Eqs. (3-21) and (3-23), we note that the intrinsic level E_i is the middle of the band gap ($E_c - E_i = E_g/2$), if the effective densities of states N_c and N_v are equal. There is usually some difference in effective mass for electrons and holes, however, and N_c and N_v are slightly different as Eqs. (3-16) and (3-20) indicate. The intrinsic level E_i is displaced from the middle of the band gap, more for GaAs than for Ge or Si.

Another convenient way of writing Eqs. (3-15) and (3-19) is

$$\boxed{n_0 = n_i e^{(E_F - E_i)/kT}} \tag{3-25a}$$
$$\boxed{p_0 = n_i e^{(E_i - E_F)/kT}} \tag{3-25b}$$

obtained by the application of Eq. (3-21). This form of the equations indicates directly that the electron concentrations is n_i when E_F is at the intrinsic level E_i, and that n_0 increases exponentially as the Fermi level moves away from E_i toward the conduction band. Similarly, the hole concentration p_0 varies from n_i to larger values as E_F moves from E_i toward the valence band. Since these equations reveal the qualitative features of carrier concentration so directly, they are particularly convenient to remember.

EXAMPLE 3–5 A Si sample is doped with 10^{17} As atoms/cm^3. What is the equilibrium hole concentration p_0 at 300 K? Where is E_F relative to E_i?

SOLUTION Since $N_d \gg n_i$, we can approximate $n_0 = N_d$ and

$$p_0 = \frac{n_i^2}{n_0} = \frac{2.25 \times 10^{20}}{10^{17}} = 2.25 \times 10^3 \text{ cm}^{-3}$$

From Eq. (3-25a), we have

$$E_F - E_i = kT \ln \frac{n_0}{n_i} = 0.0259 \ln \frac{10^{17}}{1.5 \times 10^{10}} = 0.407 \text{ eV}$$

The resulting band diagram is:

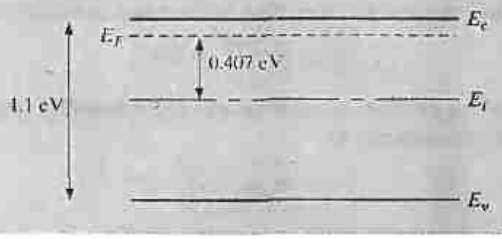

3.3.3 Temperature Dependence of Carrier Concentrations

The variation of carrier concentration with temperature is indicated by Eq. (3-25). Initially, the variation of n_0 and p_0 with T seems relatively straightforward in these relations. The problem is complicated, however, by the fact that n_i has a strong temperature dependence [Eq. (3-23)] and that E_F can also vary with temperature. Let us begin by examining the intrinsic carrier concentration. By combining Eqs. (3-23), (3-16a), and (3-20) we obtain

$$n_i(T) = 2\left(\frac{2\pi kT}{h^2}\right)^{3/2} (m_n^* m_p^*)^{3/4} e^{-E_g/2kT} \tag{3-26}$$

The exponential temperature dependence dominates $n_i(T)$, and a plot of ln n_i vs. $10^3/T$ appears linear (Fig. 3-17).[7] In this figure we neglect variations due to the $T^{3/2}$ dependence of the density-of-states function and the fact

[7]When plotting quantities such as carrier concentration, which involve a Boltzmann factor, it is common to use an inverse temperature scale. This allows terms which are exponential in $1/T$ to appear linear in the semi-logarithmic plot. When reading such graphs, remember that temperature increases from right to left.

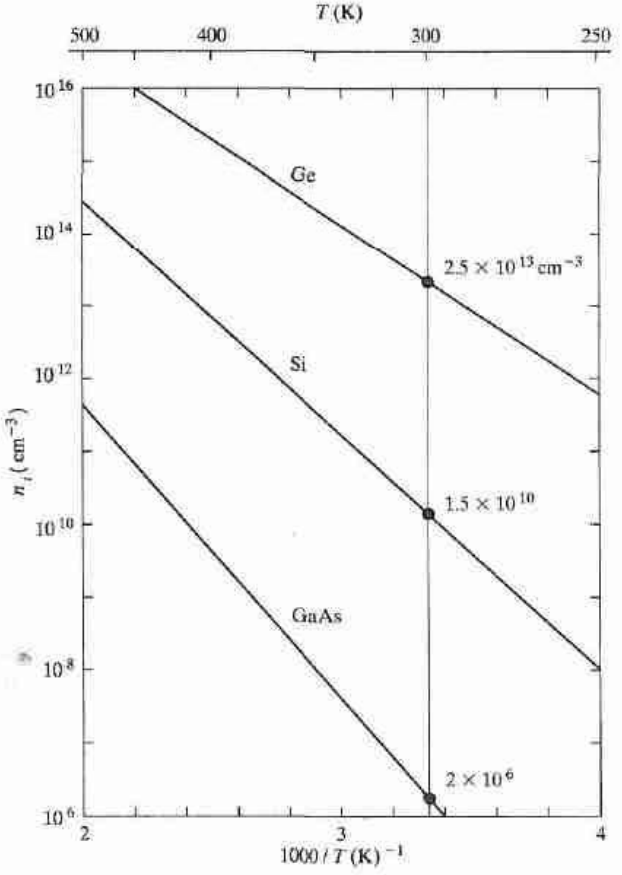

Figure 3–17 Intrinsic carrier concentration for Ge, Si, and GaAs as a function of inverse temperature. The room temperature values are marked for reference.

that E_g varies somewhat with temperature.[8] The value of n_i at any temperature is a definite number for a given semiconductor, and is known for most materials. Thus we can take n_i as given in calculating n_0 or p_0 from Eq. (3-25).[9]

With n_i and T given, the unknowns in Eq. (3-25) are the carrier concentrations and the Fermi level position relative to E_i. One of these two

[8]For Si the band gap E_g varies from about 1.11 eV at 300 K to about 1.16 eV at 0 K.

[9]Care must be taken to use consistent units in these calculations. For example, if an energy such as E_g is expressed in electron volts (eV), it should be multiplied by q (1.6×10^{-19} C) to convert to joules if k is in J/K; alternatively, E_g can be kept in eV and the value of k in eV/K can be used. At 300 K we can use $kT = 0.0259$ eV and E_g in eV.

quantities must be given if the other is to be found. If the carrier concentration is held at a certain value, as in heavily doped extrinsic material, E_F can be obtained from Eq. (3-25). The temperature dependence of electron concentration in a doped semiconductor can be visualized as shown in Fig. 3-18. In this example, Si is doped n-type with a donor concentration N_d of 10^{15} cm^{-3}. At very low temperatures (large $1/T$), negligible intrinsic EHPs exist, and the donor electrons are bound to the donor atoms. As the temperature is raised, these electrons are donated to the conduction band, and at about 100 K ($1000/T = 10$) all the donor atoms are ionized. This temperature range is called the *ionization* region. Once the donors are ionized, the conduction band electron concentration is $n_0 \simeq N_d = 10^{15}$ cm^{-3}, since one electron is obtained for each donor atom. When every available extrinsic electron has been transferred to the conduction band, n_0 is virtually constant with temperature until the concentration of intrinsic carriers n_i becomes comparable to the extrinsic concentration N_d. Finally, at higher temperatures n_i is much greater than N_d, and the intrinsic carriers dominate. In most devices it is desirable to control the carrier concentration by doping rather than by thermal EHP generation. Thus one usually dopes the material such that the extrinsic range extends beyond the highest temperature at which the device is to be used.

3.3.4 Compensation and Space Charge Neutrality

When the concept of doping was introduced, we assumed the material contained either N_d donors or N_a acceptors, so that the extrinsic majority carrier concentrations were $n_0 \simeq N_d$ or $p_0 \simeq N_a$, respectively, for the n-type or

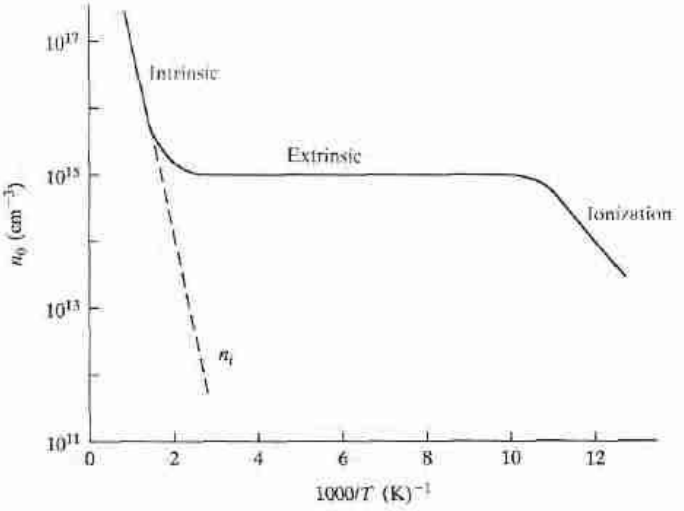

Figure 3-18 Carrier concentration vs. inverse temperature for Si doped with 10^{15} donors/cm^3.

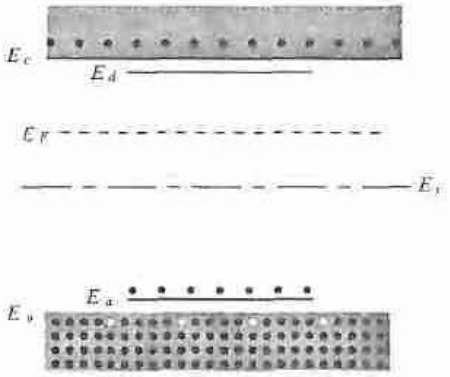

Figure 3–19 Compensation in an n-type semiconductor ($N_d > N_a$).

p-type material. It often happens, however, that a semiconductor contains both donors and acceptors. For example, Fig. 3–19 illustrates a semiconductor for which both donors and acceptors are present, but $N_d > N_a$. The predominance of donors makes the material n-type, and the Fermi level is therefore in the upper part of the band gap. Since E_F is well above the acceptor level E_a, this level is essentially filled with electrons. However, with E_F above E_i, we cannot expect a hole concentration in the valence band commensurate with the acceptor concentration. In fact, the filling of the E_a states occurs at the expense of the donated conduction band electrons. The mechanism can be visualized as follows: Assume an acceptor state is filled with a valence band electron as described in Fig. 3–12b, with a hole resulting in the valence band. This hole is then filled by recombination with one of the conduction band electrons. Extending this logic to all the acceptor atoms, we expect the resultant concentration of electrons in the conduction band to be $N_d - N_a$ instead of the total N_d. This process is called *compensation*. By this process it is possible to begin with an n-type semiconductor and add acceptors until $N_a = N_d$ and no donated electrons remain in the conduction band. In such compensated material, $n_0 = n_i = p_0$ and intrinsic conduction is obtained. With further acceptor doping the semiconductor becomes p-type with a hole concentration of essentially $N_a - N_d$.

The exact relationship among the electron, hole, donor, and acceptor concentrations can be obtained by considering the requirements for *space charge neutrality*. If the material is to remain electrostatically neutral, the sum of the positive charges (holes and ionized donor atoms) must balance the sum of the negative charges (electrons and ionized acceptor atoms):

$$p_0 + N_d^+ = n_0 + N_a^- \tag{3-27}$$

Thus in Fig. 3–19 the net electron concentration in the conduction band is

$$n_0 = p_0 + (N_d^+ - N_a^-) \tag{3-28}$$

If the material is doped n-type ($n_0 \gg p_0$) and all the impurities are ionized, we can approximate Eq. (3-28) by $n_0 \simeq N_d - N_a$.

Since the intrinsic semiconductor itself is electrostatically neutral and the doping atoms we add are also neutral, the requirement of Eq. (3-27) must be maintained at equilibrium. The electron and hole concentrations and the Fermi level adjust such that Eqs. (3-27) and (3-25) are satisfied.

3.4 DRIFT OF CARRIERS IN ELECTRIC AND MAGNETIC FIELDS

Knowledge of carrier concentrations in a solid is necessary for calculating current flow in the presence of electric or magnetic fields. In addition to the values of n and p, we must be able to take into account the collisions of the charge carriers with the lattice and with the impurities. These processes will affect the ease with which electrons and holes can flow through the crystal, that is, their *mobility* within the solid. As should be expected, these collision and scattering processes depend on temperature, which affects the thermal motion of the lattice atoms and the velocity of the carriers.

3.4.1 Conductivity and Mobility

The charge carriers in a solid are in constant motion, even at thermal equilibrium. At room temperature, for example, the thermal motion of an individual electron may be visualized as random scattering from lattice vibrations, impurities, other electrons, and defects (Fig. 3-20a). Since the scattering is random, there is no net motion of the group of n electrons/cm^3 over any period of time. This is not true of an individual electron, of course. The probability of

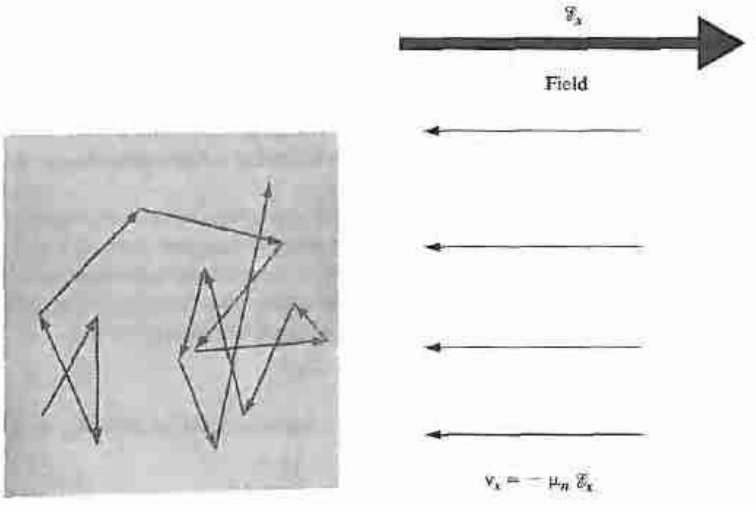

Figure 3-20 (a) Random thermal motion of an electron in a solid; (b) well-directed drift velocity with an applied electric field.

the electron in Fig. 3-20a returning to its starting point after some time t is negligibly small. However, if a large number of electrons is considered (e.g., 10^{16} cm^{-3} in an n-type semiconductor), there will be no preferred direction of motion for the group of electrons and no net current flow.

If an electric field $\mathscr{E}_x$ is applied in the x-direction, each electron experiences a net force $-q\mathscr{E}_x$ from the field. This force may be insufficient to alter appreciably the random path of an individual electron; the effect when averaged over all the electrons, however, is a net motion of the group in the $-x$-direction (Fig. 3-20b). If p_x is the x-component of the total momentum of the group, the force of the field on the n electrons/cm^3 is

$$-nq\mathscr{E}_x = \left.\frac{d\mathsf{p}_x}{dt}\right|_{\text{field}} \tag{3-29}$$

Initially, Eq. (3-29) seems to indicate a continuous acceleration of the electrons in the $-x$-direction. This is not the case, however, because the net acceleration of Eq. (3-29) is just balanced in steady state by the decelerations of the collision processes. Thus while the steady field $\mathscr{E}_x$ does produce a net momentum p_{-x}, the net rate of change of momentum when collisions are included must be zero in the case of steady state current flow.

To find the total rate of momentum change from collisions, we must investigate the collision probabilities more closely. If the collisions are truly random, there will be a constant probability of collision at any time for each electron. Let us consider a group of N_0 electrons at time $t = 0$ and define $N(t)$ as the number of electrons that *have not* undergone a collision by time t. The rate of decrease in $N(t)$ at any time t is proportional to the number left unscattered at t,

$$-\frac{dN(t)}{dt} = \frac{1}{\bar{t}}N(t) \tag{3-30}$$

where $\bar{t}^{\,-1}$ is a constant of proportionality.

The solution to Eq. (3-30) is an exponential function

$$N(t) = N_0 e^{-t/\bar{t}} \tag{3-31}$$

and $\bar{t}$ represents the mean time between scattering events,[10] called the *mean free time*. The probability that any electron has a collision in the time interval dt is $dt/\bar{t}$. Thus the differential change in p_x due to collisions in time dt is

$$d\mathsf{p}_x = -\mathsf{p}_x \frac{dt}{\bar{t}} \tag{3-32}$$

[10]Equations (3-30) and (3-31) are typical of events dominated by random processes, and the forms of these equations occur often in many branches of physics and engineering. For example, in the radioactive decay of unstable nuclear isotopes, N_0 nuclides decay exponentially with a mean lifetime $\bar{t}$. Other examples will be found in this text, including the absorption of light in a semiconductor and the recombination of excess EHPs.

The rate of change of p_x due to the decelerating effect of collisions is

$$\left.\frac{d\mathsf{p}_x}{dt}\right|_{\text{collisions}} = -\frac{\mathsf{p}_x}{\bar{t}} \tag{3-33}$$

The sum of acceleration and deceleration effects must be zero for steady state. Taking the sum of Eqs. (3-29) and (3-33), we have

$$-\frac{\mathsf{p}_x}{\bar{t}} - nq\mathscr{E}_x = 0 \tag{3-34}$$

The average momentum per electron is

$$\langle \mathsf{p}_x \rangle = \frac{\mathsf{P}_x}{n} = -q\bar{t}\mathscr{E}_x \tag{3-35}$$

where the angular brackets indicate an average over the entire group of electrons. As expected for steady state, Eq. (3-35) indicates that the electrons have *on the average* a constant net velocity in the negative x-direction:

$$\langle \mathsf{v}_x \rangle = \frac{\langle \mathsf{p}_x \rangle}{m_n^*} = -\frac{q\bar{t}}{m_n^*}\mathscr{E}_x \tag{3-36}$$

Actually, the individual electrons move in many directions by thermal motion during a given time period, but Eq. (3-36) tells us the *net drift* of an average electron in response to the electric field. The drift speed described by Eq. (3-36) is usually much smaller than the random speed due to the thermal motion v_{th}.

The current density resulting from this net drift is just the number of electrons crossing a unit area per unit time ($n\langle \mathsf{v}_x \rangle$) multiplied by the charge on the electron ($-q$):

$$\boxed{\begin{gathered} J_x = -qn\langle \mathsf{v}_x \rangle \\ \frac{\text{ampere}}{\text{cm}^2} = \frac{\text{coulomb}}{\text{electron}} \cdot \frac{\text{electrons}}{\text{cm}^3} \cdot \frac{\text{cm}}{\text{s}} \end{gathered}} \tag{3-37}$$

Using Eq. (3-36) for the average velocity, we obtain

$$J_x = \frac{nq^2\bar{t}}{m_n^*}\mathscr{E}_x \tag{3-38}$$

Thus the current density is proportional to the electric field, as we expect from Ohm's law:

$$J_x = \sigma\mathscr{E}_x, \quad \text{where } \sigma = \frac{nq^2\bar{t}}{m_n^*} \tag{3-39}$$

The conductivity $\sigma(\Omega\text{-cm})^{-1}$ can be written

$$\sigma = qn\mu_n, \quad \text{where } \mu_n = \frac{q\bar{t}}{m_n^*} \tag{3-40a}$$

The quantity μ_n, called the *electron mobility,* describes the ease with which electrons drift in the material. Mobility is a very important quantity in characterizing semiconductor materials and in device development.

Here m_n^* is the conductivity effective mass for electrons, different from the density-of-states effective mass mentioned in Eq. (3-16b). While we use the density-of-states effective mass to count the number of carriers in bands, we must use the conductivity effective mass for charge transport problems. To illustrate how it is obtained from the band curvature effective masses mentioned in Section 3.2.2, once again let us consider the 6 equivalent conduction band minima along the X-directions for Si, with the band curvature longitudinal effective mass, m_l, along the major axis of the ellipsoid, and the transverse effective mass, m_t, along the two minor axes (Fig. 3-10b). Since we have $1/m_n^*$ in the mobility expression Eq. (3-40a), by using dimensional equivalence, we can write the conductivity effective mass as the harmonic mean of the band curvature effective masses.

$$\frac{1}{m_n^*} = \frac{1}{3}\left(\frac{1}{m_l} + \frac{2}{m_t}\right) \tag{3-40b}$$

EXAMPLE 3-6

Calculate the conductivity effective mass of electrons in Si.

SOLUTION

For Si, $m_l = 0.98\, m_0$; $m_t = 0.19\, m_0$ (Appendix III).
There are 6 equivalent X valleys in the conduction band.

$$1/m_n^* = 1/3(1/m_x + 1/m_y + 1/m_z) = 1/3(1/m_l + 2/m_t)$$

$$1/m_n^* = \frac{1}{3}\left(\frac{1}{0.98\, m_0} + \frac{2}{0.19\, m_0}\right)$$

$$m_n^* = 0.26\, m_0$$

Note: For GaAs, the conduction band equi-energy surfaces are spherical. So there is only one band curvature effective mass. (The density of states effective mass and the conductivity effective mass are both $0.067\, m_0$.)

The mobility defined in Eq. (3-40a) can be expressed as the average particle drift velocity per unit electric field. Comparing Eqs. (3-36) and (3-40a), we have

$$\mu_n = -\frac{\langle v_x \rangle}{\mathscr{E}_x} \tag{3-41}$$

The units of mobility are (cm/s)/(V/cm) = cm^2/V-s, as Eq. (3-41) suggests. The minus sign in the definition results in a positive value of mobility, since electrons drift opposite to the field.

The current density can be written in terms of mobility as

$$J_x = qn\mu_n \mathscr{E}_x \tag{3-42}$$

This derivation has been based on the assumption that the current is carried primarily by electrons. For hole conduction we change n to p, $-q$ to $+q$, and μ_n to μ_p, where $\mu_p = +\langle v_x \rangle / \mathscr{E}_x$ is the mobility for holes. If both electrons and holes participate, we must modify Eq. (3-42) to

$$\boxed{J_x = q(n\mu_n + p\mu_p)\mathscr{E}_x = \sigma \mathscr{E}_x} \tag{3-43}$$

Values of μ_n and μ_p are given for many of the common semiconductor materials in Appendix III. According to Eq. (3-40), the parameters determining mobility are m^* and mean free time τ. Effective mass is a property of the material's band structure, as described by Eq. (3-3). Thus we expect m_n^* to be small in the strongly curved Γ minimum of the GaAs conduction band (Fig. 3-6), with the result that μ_n is very high. In a more gradually curved band, a larger m^* in the denominator of Eq. (3-40) leads to a smaller value of mobility. It is reasonable to expect that lighter particles are more mobile than heavier particles (which is satisfying, since the common-sense value of effective mass is not always apparent). The other parameter determining mobility is the mean time between scattering events, τ. In Section 3.4.3 we shall see that this is determined primarily by temperature and impurity concentration in the semiconductor.

3.4.2 Drift and Resistance

Let us look more closely at the drift of electrons and holes. If the semiconductor bar of Fig. 3-21 contains both types of carrier, Eq. (3-43) gives the conductivity of the material. The resistance of the bar is then

$$R = \frac{\rho L}{wt} = \frac{L}{wt}\frac{1}{\sigma} \tag{3-44}$$

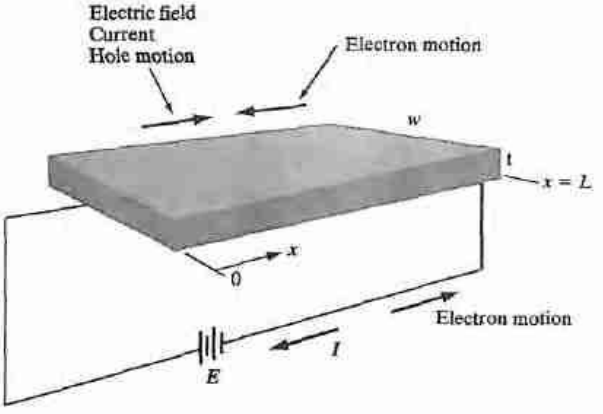

Figure 3-21 Drift of electrons and holes in a semiconductor bar.

where ρ is the resistivity (Ω-cm). The physical mechanism of carrier drift requires that the holes in the bar move as a group in the direction of the electric field and that the electrons move as a group in the opposite direction. Both the electron and the hole components of current are in the direction of the $\mathscr{E}$ field, since conventional current is positive in the direction of hole flow and opposite to the direction of electron flow. The drift current described by Eq. (3-43) is constant throughout the bar. A valid question arises, therefore, concerning the nature of the electron and hole flow at the contacts and in the external circuit. We should specify that the contacts to the bar of Fig. 3-21 are *ohmic*, meaning that they are perfect sources and sinks of both carrier types and have no special tendency to inject or collect either electrons or holes.

If we consider that current is carried around the external circuit by electrons, there is no problem in visualizing electrons flowing into the bar at one end and out at the other (always opposite to I). Thus for every electron leaving the left end ($x = 0$) of the bar in Fig. 3-21, there is a corresponding electron entering at $x = L$, so that the electron concentration in the bar remains constant at n. But what happens to the holes at the contacts? As a hole reaches the ohmic contact at $x = L$, it recombines with an electron, which must be supplied through the external circuit. As this hole disappears, a corresponding hole must appear at $x = 0$ to maintain space charge neutrality. It is reasonable to consider the source of this hole as the generation of an EHP at $x = 0$, with the hole flowing into the bar and the electron flowing into the external circuit.

3.4.3 Effects of Temperature and Doping on Mobility

The two basic types of scattering mechanisms that influence electron and hole mobility are *lattice scattering* and *impurity scattering*. In lattice scattering a carrier moving through the crystal is scattered by a vibration of the lattice, resulting from the temperature.[11] The frequency of such scattering events increases as the temperature increases, since the thermal agitation of the lattice becomes greater. Therefore, we should expect the mobility to decrease as the sample is heated (Fig. 3-22). On the other hand, scattering from crystal defects such as ionized impurities becomes the dominant mechanism at low temperatures. Since the atoms of the cooler lattice are less agitated, lattice scattering is less important; however, the thermal motion of the carriers is also slower. Since a slowly moving carrier is likely to be scattered more strongly by an interaction with a charged ion than is a carrier with greater momentum, impurity scattering events cause a decrease in mobility with decreasing temperature. As Fig. 3-22 indicates, the approximate temperature dependencies are $T^{-3/2}$ for lattice scattering and $T^{3/2}$ for impurity scattering. Since the scattering probability of Eq. (3-32) is inversely proportional to the

[11]Collective vibrations of atoms in the crystal are called *phonons*. Thus lattice scattering is also known as *phonon scattering*.

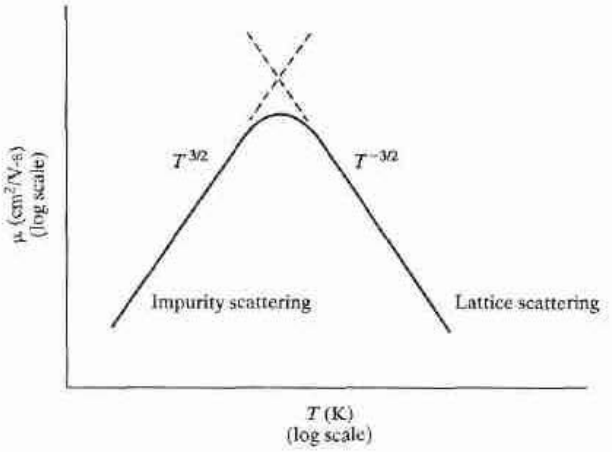

Figure 3–22 Approximate temperature dependence of mobility with both lattice and impurity scattering.

mean free time and therefore to mobility, the mobilities due to two or more scattering mechanisms add inversely:

$$\frac{1}{\mu} = \frac{1}{\mu_1} + \frac{1}{\mu_2} + \ldots \tag{3-45}$$

As a result, the mechanism causing the lowest mobility value dominates, as shown in Fig. 3–22.

As the concentration of impurities increases, the effects of impurity scattering are felt at higher temperatures. For example, the electron mobility μ_n of intrinsic silicon at 300 K is 1350 cm²/(V-s). With a donor doping concentration of 10^{17} cm^{-3}, however, μ_n is 700 cm²/(V-s). Thus, the presence of the 10^{17} ionized donors/cm³ introduces a significant amount of impurity scattering. This effect is illustrated in Fig. 3-23, which shows the variation of mobility with doping concentration at room temperature.

EXAMPLE 3–7 A Si bar 0.1 cm long and 100 μm² in cross-sectional area is doped with 10^{17} cm^{-3} phosphorus. Find the current at 300 K with 10 V applied.

SOLUTION For this applied voltage, we see that the electric field is low enough that we are in the ohmic regime. From Fig. 3-23, for this doping, the $\mu_n = 700$ cm²/V-s.

$$\sigma = q\mu_n n_0 = 1.6 \times 10^{-19} \times 700 \times 10^{17} = 11.2(\Omega \cdot \text{cm})^{-1} = \rho^{-1}$$

$$\rho = 0.0893\ \Omega \cdot \text{cm}$$

$$R = \rho L/A = 0.0893 \times 0.1/10^{-6} = 8.93 \times 10^3 \Omega$$

$$I = V/R = 10/(8.93 \times 10^3) = \mathbf{1.12\ mA}$$

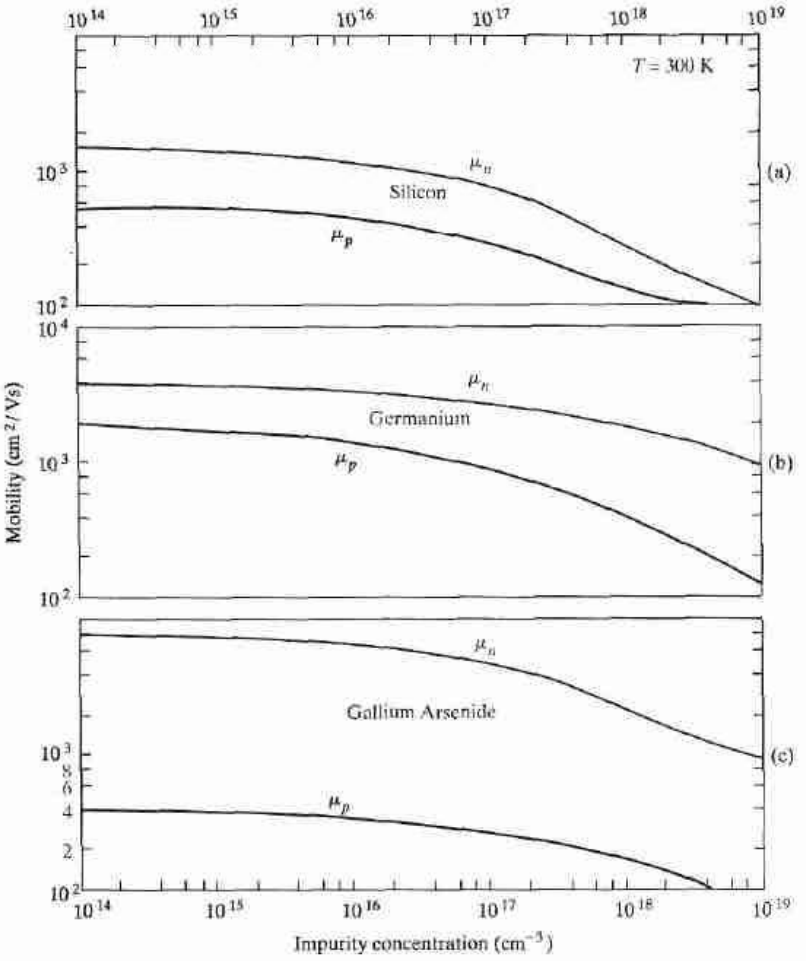

Figure 3–23
Variation of mobility with total doping impurity concentration ($N_a + N_d$) for Ge, Si, and GaAs at 300 K.

3.4.4 High-Field Effects

One assumption implied in the derivation of Eq. (3-39) was that Ohm's law is valid in the carrier drift processes. That is, it was assumed that the drift current is proportional to the electric field and that the proportionality constant (σ) is not a function of field $\mathscr{E}$. This assumption is valid over a wide range of $\mathscr{E}$. However, large electric fields ($> 10^3$V/cm) can cause the drift velocity and therefore the current $J = -qnv_d$ to exhibit a sublinear dependence on the

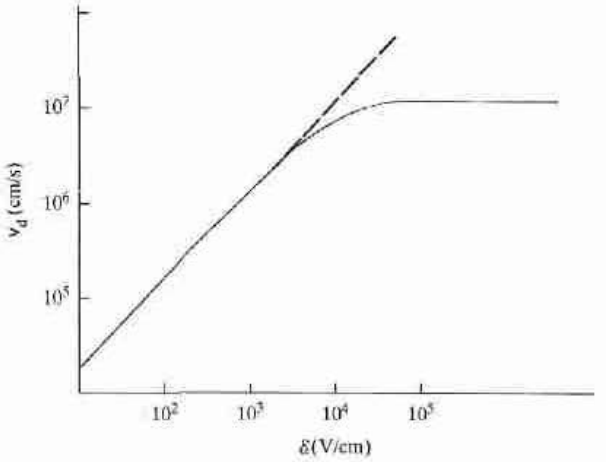

Figure 3–24 Saturation of electron drift velocity at high electric fields for Si.

electric field. This dependence of σ upon $\mathscr{E}$ is an example of a *hot carrier* effect, which implies that the carrier drift velocity v_d is comparable to the thermal velocity v_{th}.

In many cases an upper limit is reached for the carrier drift velocity in a high field (Fig. 3–24). This limit occurs near the mean thermal velocity ($= 10^7$ cm/s) and represents the point at which added energy imparted by the field is transferred to the lattice rather than increasing the carrier velocity. The result of this *scattering limited velocity* is a fairly constant current at high field. This behavior is typical of Si, Ge, and some other semiconductors. However, there are other important effects in some materials; for example, in Chapter 10 we shall discuss a *decrease* in electron velocity at high fields for GaAs and certain other materials, which results in negative conductivity and current instabilities in the sample. Another important high-field effect is avalanche multiplication, which we shall discuss in Section 5.4.2.

3.4.5 The Hall Effect

If a magnetic field is applied perpendicular to the direction in which holes drift in a p-type bar, the path of the holes tends to be deflected (Fig. 3–25). Using vector notation, the total force on a single hole due to the electric and magnetic fields is

$$\mathbf{F} = q(\mathscr{E} + \mathbf{v} \times \mathscr{B}) \tag{3-46}$$

In the y-direction the force is

$$F_y = q(\mathscr{E}_y - v_x \mathscr{B}_z) \tag{3-47}$$

The important result of Eq. (3–47) is that unless an electric field $\mathscr{E}_y$ is established along the width of the bar, each hole will experience a net force

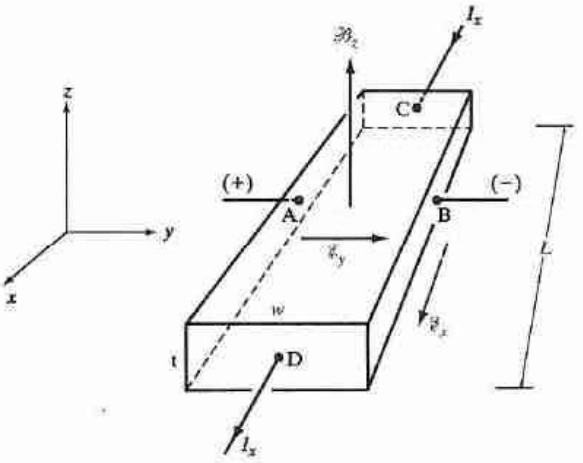

Figure 3–25
The Hall effect.

(and therefore an acceleration) in the $-y$-direction due to the $qv_x\mathcal{B}_z$ product. Therefore, to maintain a steady state flow of holes down the length of the bar, the electric field $\mathscr{E}_y$ must just balance the product $v_x\mathcal{B}_z$:

$$\mathscr{E}_y = v_x\mathcal{B}_z \tag{3-48}$$

so that the net force F_y is zero. Physically, this electric field is set up when the magnetic field shifts the hole distribution slightly in the $-y$-direction. Once the electric field $\mathscr{E}_y$ becomes as large as $v_x\mathcal{B}_z$, no net lateral force is experienced by the holes as they drift along the bar. The establishment of the electric field $\mathscr{E}_y$ is known as the *Hall effect*, and the resulting voltage $V_{AB} = \mathscr{E}_y w$ is called the *Hall voltage*. If we use the expression derived in Eq. (3-37) for the drift velocity (using $+q$ and p_0 for holes), the field $\mathscr{E}_y$ becomes

$$\mathscr{E}_y = \frac{J_x}{qp_0}\mathcal{B}_z = R_H J_x \mathcal{B}_z, \quad R_H \equiv \frac{1}{qp_0} \tag{3-49}$$

Thus the Hall field is proportional to the product of the current density and the magnetic flux density. The proportionality constant $R_H = (qp_0)^{-1}$ is called the *Hall coefficient*. A measurement of the Hall voltage for a known current and magnetic field yields a value for the hole concentration p_0

$$p_0 = \frac{1}{qR_H} = \frac{J_x\mathcal{B}_z}{q\mathscr{E}_y} = \frac{(I_x/wt)\mathcal{B}_z}{q(V_{AB}/w)} = \frac{I_x\mathcal{B}_z}{qtV_{AB}} \tag{3-50}$$

Since all of the quantities in the right-hand side of Eq. (3-50) can be measured, the Hall effect can be used to give quite accurate values for carrier concentration.

If a measurement of resistance R is made, the sample resistivity ρ can be calculated:

$$\rho(\Omega\text{-cm}) = \frac{Rwt}{L} = \frac{V_{CD}/I_x}{L/wt} \tag{3-51}$$

Since the conductivity $\sigma = 1/\rho$ is given by $q\mu_p p_0$, the mobility is simply the ratio of the Hall coefficient and the resistivity:

$$\mu_p = \frac{\sigma}{qp_0} = \frac{1/\rho}{q(1/qR_H)} = \frac{R_H}{\rho} \tag{3-52}$$

Measurements of the Hall coefficient and the resistivity over a range of temperatures yield plots of majority carrier concentration and mobility vs. temperature. Such measurements are extremely useful in the analysis of semiconductor materials. Although the discussion here has been related to p-type material, similar results are obtained for n-type material. A negative value of q is used for electrons, and the Hall voltage V_{AB} and Hall coefficient R_H are negative. In fact, measurement of the sign of the Hall voltage is a common technique for determining if an unknown sample is p-type or n-type.

EXAMPLE 3-8 Referring to Fig. 3-25, consider a semiconductor bar with $w = 0.1$ mm, $t = 10$ μm, and $L = 5$ mm. For $\mathcal{B} = 10$ kg in the direction shown (1 kG = 10^{-5} Wb/cm^2) and a current of 1 mA, we have $V_{AB} = -2$ mV, $V_{CD} = 100$ mV. Find the type, concentration, and mobility of the majority carrier.

SOLUTION $\mathcal{B}_z = 10^{-4}$ Wb/cm^2

From the sign of V_{AB}, we can see that the majority carriers are electrons:

$$n_0 = \frac{I_x\mathcal{B}_z}{qt(-V_{AB})} = \frac{(10^{-3})(10^{-4})}{1.6 \times 10^{-19}(10^{-3})(2 \times 10^{-3})} = 3.125 \times 10^{17}\ \text{cm}^{-3}$$

$$\rho = \frac{R}{L/wt} = \frac{V_{CD}/I_x}{L/wt} = \frac{0.1/10^{-3}}{0.5/0.01 \times 10^{-3}} = 0.002\ \Omega \cdot \text{cm}$$

$$\mu_n = \frac{1}{\rho q n_0} = \frac{1}{(0.002)(1.6 \times 10^{-19})(3.125 \times 10^{17})} = \mathbf{10{,}000\ cm^2(V \cdot s)^{-1}}$$

3.5 INVARIANCE OF THE FERMI LEVEL AT EQUILIBRIUM

In this chapter we have discussed homogeneous semiconductors, without variations in doping and without junctions between dissimilar materials. In the following chapters we will be considering cases in which nonuniform doping occurs in a given semiconductor, or junctions occur between different semiconductors or a semiconductor and a metal. These cases are crucial

to the various types of electronic and optoelectronic devices made in semiconductors. In anticipation of those discussions, an important concept should be established here regarding the demands of equilibrium. That concept can be summarized by noting that *no discontinuity or gradient can arise in the equilibrium Fermi level* E_F.

To demonstrate this assertion, let us consider two materials in intimate contact such that electrons can move between the two (Fig. 3-26). These may be, for example, dissimilar semiconductors, n- and p-type regions, a metal and a semiconductor, or simply two adjacent regions of a nonuniformly doped semiconductor. Each material is described by a Fermi-Dirac distribution function and some distribution of available energy states that electrons can occupy.

There is no current, and therefore no net charge transport, at thermal equilibrium. There is also no net transfer of energy. Therefore, for each energy E in Fig. 3-26 any transfer of electrons from material 1 to material 2 must be exactly balanced by the opposite transfer of electrons from 2 to 1. We will let the density of states at energy E in material 1 be called $N_1(E)$ and in material 2 we will call it $N_2(E)$. At energy E the rate of transfer of electrons from 1 to 2 is proportional to the number of filled states at E in material 1 times the number of empty states at E in material 2:

$$\text{rate from 1 to 2} \propto N_1(E)f_1(E) \cdot N_2(E)[1 - f_2(E)] \qquad (3\text{-}53)$$

where $f(E)$ is the probability of a state being filled at E in each material, i.e., the Fermi-Dirac distribution function given by Eq. (3-10). Similarly,

$$\text{rate from 2 to 1} \propto N_2(E)f_2(E) \cdot N_1(E)[1 - f_1(E)] \qquad (3\text{-}54)$$

At equilibrium these must be equal:

$$N_1(E)f_1(E) \cdot N_2(E)[1 - f_2(E)] = N_2(E)f_2(E) \cdot N_1(E)[1 - f_1(E)] \qquad (3\text{-}55)$$

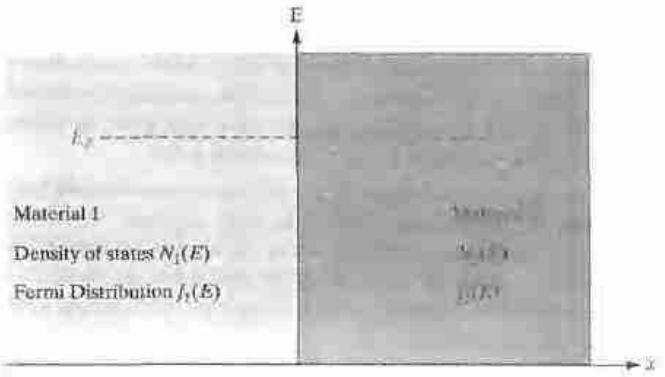

Figure 3-26
Two materials in intimate contact at equilibrium. Since the net motion of electrons is zero, the equilibrium Fermi level must be constant throughout.

Rearranging terms, we have, at energy E,

$$N_1 f_1 N_2 - N_1 f_1 N_2 f_2 = N_2 f_2 N_1 - N_2 f_2 N_1 f_1 \tag{3-56}$$

which results in

$$f_1(E) = f_2(E), \quad \text{that is,} \quad [1 + e^{(E - E_{F1})/kT}]^{-1} = [1 + e^{(E - E_{F2})/kT}]^{-1} \tag{3-57}$$

Therefore, we conclude that $E_{F1} = E_{F2}$. That is, there is no discontinuity in the equilibrium Fermi level. More generally, we can state that the Fermi level at equilibrium must be constant throughout materials in intimate contact. One way of stating this is that no gradient exists in the Fermi level at equilibrium:

$$\boxed{\frac{dE_F}{dx} = 0} \tag{3-58}$$

We will make considerable use of this result in the chapters to follow.

SUMMARY

3.1 In a diamond lattice, each Si atom (with four valence electrons) is surrounded by four Si atoms that form four *covalent* bonds consisting of shared electron pairs, thereby forming an *octet* of electrons in the valence shell. In zinc blende structures such as GaAs, electrons are partly shared (covalent bonding) and partly transferred from Ga to As (*ionic* bonding).

3.2 In crystals, electronic *wave functions overlap* to give various linear combinations of atomic orbitals (LCAO). Bonding or symmetric combinations of the wave functions of valence-shell electrons form (*almost*) *continuous allowed bands* of energies in the (*almost*) *filled valence* band, separated by an energy gap from higher energy states in an (*almost*) *empty conduction* band that correspond to the antibonding or antisymmetric LCAOs. Empty electronic states in the valence band can be considered to be positively charged carriers (*holes*), while filled states in the conduction band are negatively charged (*conduction*) *electrons*.

3.3 If the band gaps are large, we get insulators; if they are small (~1 eV), we get semiconductors; and if they are zero, we get conductors (metals).

3.4 *Simplified* band diagrams plot *electron energy* in the conduction band (*increasing upwards*) as a function of position. The *band edge* corresponds to *potential* energy, and the distance from the band edge gives the *kinetic* energy. *Hole energies increase downward* in the valence band.

3.5 Carrier energies can also be plotted as a function of wave vector **k** (proportional to velocity or momentum) to give $(E, \mathbf{k})$ *band structures*, which can be direct (conduction band minimum directly above valence band maximum) or indirect. The *curvature* of the $(E, \mathbf{k})$ is inversely proportional to the *effective mass* m^* of the carriers. The m^* accounts for the interactions of the carriers with the periodic crystal potential.

3.6 In a pure semiconductor, we have an *intrinsic* concentration of electrons (or holes), n_i, that result from *thermal* generation–recombination between the valence and conduction band (or bond breaking). If we replace some Si atoms (with four valence electrons) with *donor* impurities with five valence electrons, they donate conduction electrons, n ($= N_d^+$); similarly, *acceptors* create holes p.

3.7 The number of electrons, n, is the integral with respect to energy from the bottom to the top of the conduction band of the product of the available *density of states* (DOS) and the *Fermi–Dirac* (FD) distribution function. For parabolic band structures, we get a parabolic DOS. The FD function is the average occupancy of an electronic state. The electron concentration n can also be expressed as the product of an *effective* DOS at the band edge and the FD occupancy at E_c, and similarly for holes p. The np product in equilibrium is constant (n_i^2).

3.8 Electrons in a solid execute *random Brownian* motion with an average kinetic energy related to the thermal energy kT. In an electric field, electrons *drift* (on top of the random motion) with a velocity equal to *mobility* times field in the *ohmic* regime and *saturation velocity* at *high fields*. The drift current is proportional to carrier concentration times drift velocity. Negatively charged electrons drift opposite to the electric field, and the current is opposite to the motion. Positively charged holes drift in the direction of the electric field, and the current goes in the same direction as the hole flow.

3.9 Carrier mobility is determined by *scattering*, caused by *deviations* from a periodic lattice potential, such as lattice vibrations (phonons) or ionized impurities. Carrier mobility and concentration can be obtained by the Hall effect and resistivity measurements.

PROBLEMS

3.1 Calculate the approximate donor binding energy for GaAs ($\epsilon_r = 13.2$, $m_n^* = 0.067\ m_0$).

3.2 Calculate values for the Fermi function $f(C)$ at 300 K and plot vs. energy in eV as in Fig. 3–14. Choose $E_F = 1$ eV and make the calculated points closer together near the Fermi level to obtain a smooth curve. Notice that $f(E)$ varies quite rapidly within a few kT of E_F. Show that the probability that a state ΔE above E_F is occupied is the same as the probability that the state ΔE below E_F is empty.

3.3 An unknown semiconductor has $E_g = 1.1$ eV and $N_c = N_v$. It is doped with 10^{15} cm^{-3} donors, where the donor level is 0.2 eV below E_c. Given that E_F is 0.25 eV below E_c, calculate n_i and the concentration of electrons and holes in the semiconductor at 300 K.

3.4 At room temperature, an unknown indirect band gap, intrinsic, cubic semiconductor has the following band structure: There are 6 X minima along the $\langle 100 \rangle$ directions. If $m_n^*(\Gamma) = 0.065 m_0$, $m_n^*(X) = 0.30\ m_0$ (for each of the X minima) and $m_p^* = 0.47 m_0$, at what temperature is the number of electrons in the Γ minima and the X minima equal if the Γ to X energy separation is 0.35 eV, and the bandgap is 1.7 eV (m_0 = free electron mass)?

3.5 Since the effective mass of electrons in a conduction band decreases with increasing curvature of the band according to Eq. (3-3), comment on the electron effective mass in the Γ valley of GaAs compared with the indirect X or L valleys. (See Fig. 3-10.) How is this effective mass difference reflected in the electron mobility for GaAs and GaP shown in Appendix III? From Fig. 3-10, what would you expect to happen to the conductivity of GaAs if Γ-valley electrons drifting in an electric field were suddenly promoted to the L valley?

3.6 Calculate the band gap of Si from Eq. (3-23) and the plot of n_i vs. $1000/T$ (Fig. 3-17). *Hint:* The slope cannot be measured directly from a semilogarithmic plot; read the values from two points on the plot and take the natural logarithm as needed for the solution.

3.7 (a) A Si sample is doped with 10^{16} cm^{-3} boron atoms and a certain number of shallow donors. The Fermi level is 0.36 eV above E_i at 300 K. What is the donor concentration N_d?

(b) A Si sample contains 10^{16} cm^{-3} In acceptor atoms and a certain number of shallow donors. The In acceptor level is 0.16 eV above E_v, and E_F is 0.26 eV above E_v at 300 K. How many (cm^{-3}) In atoms are un-ionized (i.e., neutral)?

3.8 Show that Eq. (3-25) results from Eqs. (3-15) and (3-19). If $n_0 = 10^{16}$ cm^{-3}, where is the Fermi level relative to E_i in Si at 300 K?

3.9 Derive an expression relating the intrinsic level E_i to the center of the band gap $E_g/2$. Calculate the displacement of E_i from $E_g/2$ for Si at 300 K, assuming the effective mass values for electrons and holes are $1.1m_0$ and $0.56m_0$, respectively.

3.10 A semiconductor device requires n-type material; it is to be operated at 400 K. Would Si doped with 10^{15} atoms/cm^3 of arsenic be useful in this application? Could Ge doped with 10^{15} cm^{-3} antimony be used?

3.11 A new semiconductor has $N_c = 10^{19}$ cm^{-3}, $N_v = 5 \times 10^{18}$ cm^{-3}, and $E_g = 2$ eV. If it is doped with 10^{17} donors (fully ionized), calculate the electron, hole, and intrinsic carrier concentrations at 627°C. Sketch the simplified band diagram, showing the position of E_F.

3.12 (a) Show that the minimum conductivity of a semiconductor sample occurs when $n_0 = n_i\sqrt{\mu_p/\mu_n}$. *Hint:* begin with Eq. (3-43) and apply Eq. (3-24).

(b) What is the expression for the minimum conductivity σ_{min}?

(c) Calculate σ_{min} for Si at 300 K and compare with the intrinsic conductivity.

3.13 (a) A Si bar 0.1 μm long and 100 μm^2 in cross-sectional area is doped with 10^{17} cm^{-3} phosphorus. Find the current at 300 K with 10 V applied. Repeat for a Si bar 1 μm long.

(b) How long does it take an average electron to drift 1 μm in pure Si at an electric field of 100 V/cm? Repeat for 10^5 V/cm.

3.14. (a) A Si sample is doped with 10^{17} boron atoms/cm^3. What is the electron concentration n_0 at 300 K? What is the resistivity?

(b) A Ge sample is doped with 3×10^{13} Sb atoms/cm^3. Using the requirements of space charge neutrality, calculate the electron concentration n_0 at 300 K.

3.15 For a Si conductor of length 5 μm, doped n-type at 10^{15} cm^{-3}, calculate the current density for an applied voltage of 2.5 V across its length. How about for a voltage of 2500 V? The electron and hole mobilities are 1500 cm^2/V-s and 500 cm^2/V-s, respectively, in the ohmic region for electric fields below 10^4 V/cm. For higher fields, electrons and holes have a saturation velocity of 10^7 cm/s.

3.16 In a long semiconductor bar ($E_G = 2$ eV), conduction band electrons come in from the left in the positive x direction with a kinetic energy of 3 eV. They move from location A to B to C to D. Between A and B, the electric field is zero; between locations B and C, there is a linearly varying voltage increase of 4 V; between C and D, the field is again zero. Assuming no scattering, sketch a *simplified* band diagram describing the motion of these electrons. Assuming that these electrons can be described as plane waves, with a free-electron mass, write down the wave function of the electrons at D. Leave your result in terms of an arbitrary normalization constant.

3.17 Assume that a conduction electron in Si (μ_n = 1350 cm^2/V-s) has a thermal energy of kT, related to its mean thermal velocity by $E_{th} = (m_0 v_{th}^2)/2$. This electron is placed in an electric field of 100 V/cm. Show that the drift velocity of the electron in this case is small compared with its thermal velocity. Repeat for a field of 10^4 V/cm, using the same value of μ_n. Comment on the actual mobility effects at this higher value of the field.

3.18 Use Eq. (3-45) to calculate and plot the mobility vs. temperature $\mu(T)$ from 10 K to 500 K for Si doped with $N_d = 10^{14}$, 10^{16}, and 10^{18} donors cm^{-3}. Consider the mobility to be determined by impurity and phonon (lattice) scattering. Impurity scattering limited mobility can be described by

$$\mu_I = 3.29 \times 10^{15} \frac{\epsilon_r^2 T^{3/2}}{N_d^+ (m_n^*/m_0)^{1/2} \left[\ln(1 + z) - \dfrac{z}{1 + z} \right]}$$

where

$$z = 1.3 \times 10^{13} \epsilon_r T^2 (m_n^*/m_0)(N_d^+)^{-1}$$

Assume that the ionized impurity concentration N_d^+ is equal to N_d at all temperatures.

The conductivity effective mass m_n^* for Si is 0.26 m_0. Acoustic phonon (lattice) scattering limited mobility can be described by

$$\mu_{AC} = 1.18 \times 10^{-5} c_1 (m_n^*/m_0)^{-5/2} T^{-3/2} (E_{AC})^{-2}$$

where the stiffness (c_1) is given by

$$c_1 = 1.9 \times 10^{12} \text{ dyne cm}^{-2} \text{ for Si}$$

and the conduction band acoustic deformation potential (E_{AC}) is

$$E_{AC} = 9.5 \text{ eV for Si}$$

3.19 Rework Prob. 3.18 considering carrier freeze-out onto donors at low T. That is, consider

$$N_d^+ = \frac{N_d}{1 + \exp(E_d/kT)}$$

as the ionized impurity concentration. Consider the donor ionization energy (E_d) to be 45 meV for Si.

3.20 Hall measurements are made on a p-type semiconductor bar 500 μm wide and 20 μm thick. The Hall contacts A and B are displaced 2 μm with respect to each other in the direction of current flow of 3 mA. The voltage between A and B with a magnetic field of 10 kG (1kG = 10^{-5} Wb/cm^2) pointing out of the plane of the sample is 3.2 mV. When the magnetic field direction is reversed the voltage changes to −2.8 mV. What is the hole concentration and mobility?

3.21 In soldering wires to a sample such as that shown in Fig. 3–25, it is difficult to align the Hall probes A and B precisely. If B is displaced slightly down the length of the bar from A, an erroneous Hall voltage results. Show that the true Hall voltage V_H can be obtained from two measurements of V_{AB}, with the magnetic field first in the $+z$-direction and then in the $-z$-direction.

3.22 A sample of Si is doped with 10^{17} phosphorus atoms/cm^3. What would you expect to measure for its resistivity? What Hall voltage would you expect in a sample 100 μm thick if I_x = 1 mA and B_z = 1 kG = 10^{-5} Wb/cm^2?

READING LIST

Blakemore, J. S. *Semiconductor Statistics*. New York: Dover Publications, 1987.

Hess, K. *Advanced Theory of Semiconductor Devices*, 2d ed. New York: IEEE Press, 2000.

Kittel, C. *Introduction to Solid State Physics*, 7th ed. New York: Wiley, 1996.

Neamen, D. A. *Semiconductor Physics and Devices: Basic Principles*. Homewood, IL: Irwin, 2003.

Pierret, R. F. *Semiconductor Device Fundamentals*. Reading, MA: Addison-Wesley, 1996.

Schubert, E. F. *Doping in III–V Semiconductors*. Cambridge: Cambridge University Press, 1993.

Singh, J. *Semiconductor Devices*. New York: McGraw-Hill, 1994.

Wang, S. *Fundamentals of Semiconductor Theory and Device Physics*. Englewood Cliffs, NJ: Prentice Hall, 1989.

Wolfe, C. M., G. E. Stillman, and N. Holonyak, Jr. *Physical Properties of Semiconductors*. Englewood Cliffs, NJ: Prentice Hall, 1989.

SELF QUIZ

Question 1

(a) The following three diagrams show three different energy bands of some hypothetical crystalline materials (energy varies vertically). The only difference between the three materials is the assumed Fermi level energy E_F. Characterize each material as a ***metal***, an ***insulator***, or a ***semiconductor***.

(b) Assuming you can see through one and only one of the materials of part (a) above, which one would it most likely be? ***Material 1 / Material 2 / Material 3***

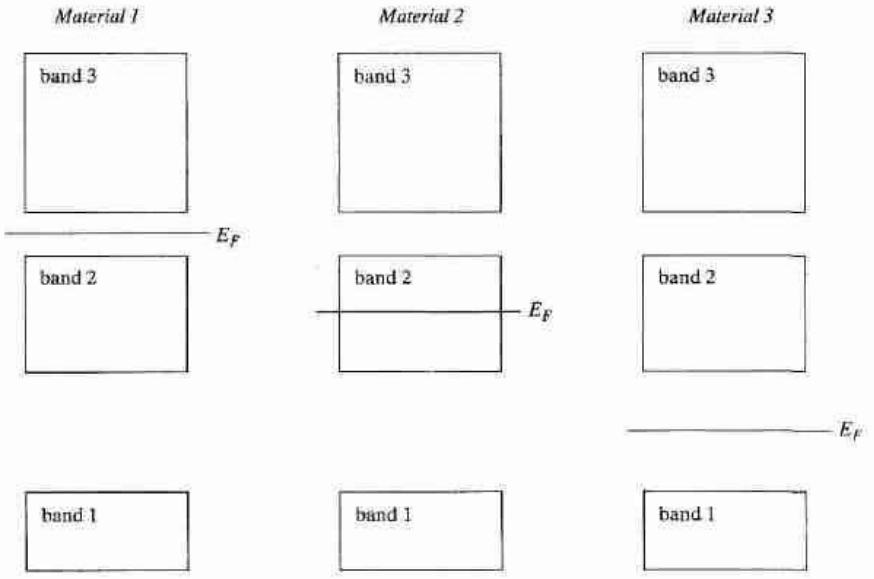

Question 2

Consider the following conduction band energy E vs. wave vector k_x dispersion relation.

(a) Which energy valley has the greater effective mass in the x-direction m_x (circle one)? **Γ-valley / X-valley**

(b) Consider two electrons, one each located at the positions of the heavy crosses. Which has the greater velocity magnitude (circle one)? **The one in the Γ-valley / The one in the X-valley**

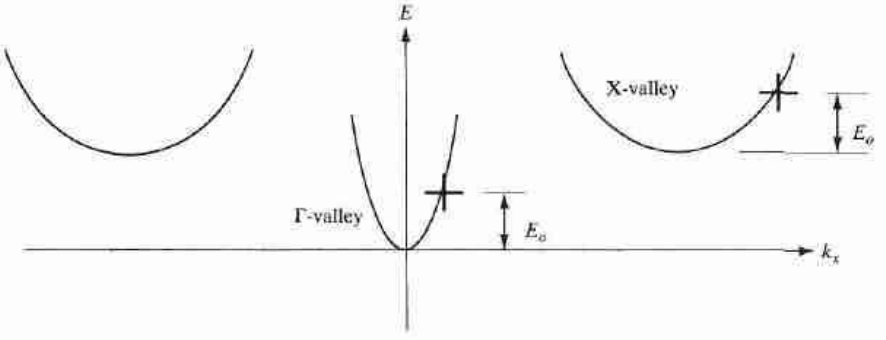

Question 3

These questions refer to the band structures of Si and GaAs shown in Fig. 3–10.

(a) Which material appears to have the *lowest* (conduction band) electron effective mass, Si or GaAs?

(b) Which of these would you expect to produce photons (light) more efficiently through electron–hole recombination?

(c) Consistent with your answer to part (b) and making use of Appendix III, what would you expect the energy of the emitted photons to be? What would be their wavelength in μm? Would these be visible, infrared, or ultraviolet?

(d) How many equivalent conduction band minima do we have for Si? GaAs?

Question 4

Refer to Fig. 3–10, which shows the E vs. $\mathbf{k}$ dispersion relations for gallium arsenide (GaAs) and for silicon (Si) along the [111] and [100] directions, showing both valence and conduction bands.

(a) Neglecting differences in electron scattering rates in the two materials, would you expect Si or GaAs to have the greatest electron mobility μ_n?

(b) If a constant force were applied in the [100] direction for a short period of time on an electron initially located at the conduction band minimum of each semiconductor and if scattering were neglected, would the magnitude of change in $\mathbf{k}$ in Si be greater, equal to, or smaller than the magnitude of the change in $\mathbf{k}$ in GaAs for the same force $\mathbf{F}$?

greater/equal/smaller

Question 5

(a) The equilibrium band diagram for a doped direct gap semiconductor is shown below. Is it n-type, p-type, or unknown? Circle one below.

n-type/p-type/not enough information provide

(b) Based on the band diagram opposite (E_i is in the middle of the gap), would you expect that the conduction band density-of-states effective mass is greater than, equal to, or smaller than the valence band effective mass? Circle one:

Greater than/equal/smaller than

(c) What, if any, of the following conditions by themselves could lead to the above band diagram? Circle each correct answer.

(a) very high temperature

(b) very high acceptor doping

(c) very low acceptor doping

Question 6

A hypothetical semiconductor has an intrinsic carrier concentration of $1.0 \times 10^{10}/\text{cm}^3$ at 300 K, it has conduction and valence band effective densities of states N_c and N_v, both equal to $10^{19}/\text{cm}^3$.

(a) What is the band gap E_g?

(b) If the semiconductor is doped with $N_d = 1 \times 10^{16}$ donors/cm^3, what are the equilibrium electron and hole concentrations at 300K?

(c) If the same piece of semiconductor, already having $N_d = 1 \times 10^{16}$ donors/cm^3, is also doped with $N_a = 2 \times 10^{16}$ acceptors/cm^3, what are the new equilibrium electron and hole concentrations at 300 K?

(d) Consistent with your answer to part (c), what is the Fermi level position with respect to the intrinsic Fermi level, $E_F - E_i$?

Question 7

What is the difference between density of states and *effective* density of states, and why is the latter such a useful concept?

Question 8

(a) Does mobility have any meaning at very high field? Why?

(b) How do you measure mobility and carrier concentration?